NUMERICAL MODELING AND EXPERIMENTAL VERIFICATION OF TIME-DEPENDENT PHASE CHANGE IN FOODSTUFF

by

Çağrı Kocatürk

B.S., Mechanical Engineering, Yıldız Technical University, 2017

Submitted to the Institute for Graduate Studies in
Science and Engineering in partial fulfillment of
the requirements for the degree of
Master of Science

Graduate Program in Mechanical Engineering
Boğaziçi University

2021

ACKNOWLEDGEMENTS

I would first like to thank my thesis advisor Assoc. Prof. Hasan Bedir of the Mechanical Engineering Department at Boğaziçi University for his valuable guidance and continuous support throughout the course of this work.

I would also like to thank Arçelik Central R&D Center and Fluid Dynamics Department for this great opportunity enabling me to exploit its facilities. Moreover, I would like to thank our R&D Director Mr. Dr. Emre Oğuz, Fluid Dynamics Technology Team Leader Mr. Vasi Kadir Ertiş, Senior Specialist Mrs. Beria Işık Koç, Senior Specialist Mr. Aydın Çelik, Senior Specialist Mr. Ünsal Kaya, lab technician Mr. Cafer Özyurd and lab technician Mr. İlyas Aydın.

I must express my sincere gratitude to my parents and Miss. Şeyda Özdemir for their eternal support and considerable encouragement throughout all my life. Without you, I would have never been able to accomplish anything. Thank you for everything!

ABSTRACT

NUMERICAL MODELING AND EXPERIMENTAL VERIFICATION OF TIME-DEPENDENT PHASE CHANGE IN FOODSTUFF

Time-dependent phase change in beef is modeled numerically and the results are verified experimentally. The thermal properties of beef significantly change with temperature and unlike for a pure material, the phase change occurs in a certain temperature range. Therefore, they are expressed as a function of temperature. The apparent heat capacity method is used as the phase-change model. The specific heat and the thermal conductivity of beef are measured with differential scanning calorimetry and heat flow meter, respectively. People typically cover beef with a stretch film before they put it in a freezer compartment. Hence to simulate user behavior, and also to reduce complexity mass transfer between cooling air and the beef is neglected. Since cooling air considerably impacts the freezing, it is included in the simulations. A refrigerator is utilized in both the simulations and the experiments. Its cooling system is updated so as to determine the effect of air velocity, circulation system and shelf design on the phase change process of beef. The influence of three different fan speed, two alternative blowing methods and three discrete shelf designs are investigated. A comparison of results of simulations and experiments in terms of temperature distribution and freezing time, shows that the numerical results are in agreement with the experimental measurements. As it is expected, the freezing time of beef decreases, while the fan speed is increased. The results show that more optimum freezing process could be obtained by increasing conduction heat transfer rate with the shelf design even if air flow rate is not increased. Moreover, it is observed that the top blowing method leads to a more uniform temperature gradient in beef during the freezing process.

ÖZET

GIDALARDA ZAMANA BAĞLI FAZ DEĞİŞİMİNİN SAYISAL MODELLENMESİ VE DENEYSEL DOĞRULAMASI

Bu çalışmada sığır etinde zamana bağlı faz değişimi sayısal olarak modellenir ve sonuçlar deneysel olarak doğrulanır. Sığır etinin ısıl özellikleri sıcaklıkla önemli ölçüde değişir ve saf bir malzemeden farklı olarak, faz değişimi belirli bir sıcaklık aralığında gerçekleşir. Bu nedenle, yoğunluk hariç, sıcaklığın bir fonksiyonu olarak ifade edilir. Görünür ısı kapasitesi yöntemi, faz değişim modeli olarak kullanılır. Sığır etinin özgül ısısı ve ısıl iletkenliği, sırasıyla diferansiyel taramalı kalorimetri ve ısı akış ölçer ile ölçülür. İnsanlar genellikle sığır etini dondurucu bölmesine koymadan önce streç filmle kaplarlar. Bu nedenle, kullanıcı davranışını simüle etmek ve karmaşıklığı azaltmak için soğutma havası ile sığır eti arasındaki kütle geçişi ihmal edilir. Soğutma havası donmayı önemli ölçüde etkilediği için simülasyonlara dahil edilir. Hem simülasyonlarda hem de deneylerde buzdolabı kullanıllır. Soğutma sistemi, hava hızı, sirkülasyon sistemi ve raf tasarımının dana etinin faz değişim sürecine etkisini belirleyecek şekilde güncellenmiştir. Üç farklı fan hızının, iki alternatif üfleme yönteminin ve üç ayrı raf tasarımının etkisi derinlemesine incelenir. Sıcaklık dağılımı ve donma süresi açısından simülasyon ve deney sonuçlarının karşılaştırılması, sayısal sonuçların deneysel ölçümlerle uyum içinde olduğunu gösterir. Beklendiği gibi dana etinin donma süresi azalırken fan hızı da yükselir. Raf tasarımının sığır etinin dondurulmasına etkisi değerlendirilir. Sonuçlar, hava debisi artırılmasa bile raf tasarımı ile iletimle ısı transfer hızının artırılarak daha optimum dondurma işleminin elde edilebileceğini gösterir. Ayrıca üstten üfleme yönteminin, dondurma işlemi sırasında sığır etinde daha homojen bir sıcaklık değişimine yol açtığı görülür.

TABLE OF CONTENTS

LIST OF FIGURES

LIST OF TABLES

LIST OF SYMBOLS

c_{app}	Apparent specific heat
c_{eff}	Effective specific heat
C_f	Skin-friction coefficient
c_p	Specific heat
f_i	Body force per unit volume in i direction
G_b	Production of turbulent kinetic energy due to buoyancy
G_k	Production of turbulent kinetic energy due to mean velocity gradients
$\widetilde{H}$	Instantaneous total enthalpy
$\overline{H}$	Time-averaged total enthalpy
H	Fluctuating total enthalpy
$\widetilde{h}$	Instantaneous specific enthalpy
$\overline{h}$	Time-averaged specific enthalpy
h	Fluctuating specific enthalpy
k	Thermal conductivity
K	Turbulence kinetic energy
L	Latent heat per unit mass
l	Characteristic length
$\widetilde{p}$	Instantaneous pressure
$\overline{P}$	Time-averaged pressure
p	Fluctuating pressure
Pr_t	Turbulent Prandtl number
r	Position vector
Re	Reynolds number
S	Source term for momentum
S_T	Source term for enthalpy
$\widetilde{T}$	Instantaneous temperature
$\overline{T}$	Time-averaged temperature

T	Fluctuating temperature
t	Time
U^*	Friction velocity
$\widetilde{u_i}$	Instantaneous (or Laminar) velocity in x_i-direction
$\overline{U_i}$	Time-averaged velocity in x_i-direction
u_i	Fluctuating velocity x_i-direction
U_∞	Free stream velocity
V	Volume
x_i	Cartesian coordinates in i direction
y^+	A dimensionless wall distance
δ_{ij}	Kronecker delta function
β	Liquid fraction
Γ_t	Turbulent diffusion coefficient
ε	Dissipation of turbulence kinetic energy
μ	Dynamic viscosity
μ_t	Turbulence (Eddy) viscosity
ν	Kinematic viscosity
ρ	Density
τ_{wall}	Wall shear stress
ϕ	Energy dissipation term
ω	Angular velocity

LIST OF ACRONYMS/ABBREVIATIONS

AMCA	The Air Movement and Control Association International
app	Apparent
AHCM	Apparent Heat Capacity Method
ASHRAE	American Society of Heating Refrigerating and Air Conditioning Engineers
CFD	Computational Fluid Dynamics
DNS	Direct Numerical Simulation
DSC	Differential Scanning Calorimetry
eff	Effective
EHCM	Effective Heat Capacity Method
EM	Enthalpy Method
f	Final
FDM	Finite Differences Method
FEM	Finite Element Method
FVM	Finite Volume Method
HTC	Heat Transfer Coefficient
IFP	Initial Freezing Point
i	Initial
l	Liquid
LES	Large Eddy Simulation
MAE	Mean Absolute Error
MAPE	Mean Absolute Percentage Error
MRF	Moving Reference Frame
mush	Mushy Zone
PCM	Phase Change Material
PE	Percentage Error
PU	Polyurethane
PWM	Pulse-width Modulation

r	Relative
R&D	Research and Development
ref	Reference
RANS	Reynolds-Averaged Navier-Stokes
RH	Relative Humidity
RMSE	Root Mean Squared Error
RPM	Rotate Per Minute
s	Solid
SIMPLE	Semi-Implicit Method for Pressure linked Equations
sl	Solid-Liquid
t	Turbulence
UDAQ	Arçelik Universal Data Acquisition & Network
UPS	Uninterruptible Power Supply

1. INTRODUCTION

1.1. Research Background

Food preservation is undoubtedly one of the most significant issue which has been dealt with by scientist for a long time in order to reduce the rate of death due to starvation, to overcome the illnesses caused by malnutrition and to create a sustainable environment by decreasing nutrient waste. A United Nations (UN)' report [2] reveals that almost nine percent of people in the planet did not have sufficient food in 2019 and it forecasts that this number might reach to 10 in 2030 if no global action is taken. Another UN's report [3] predicts that people in the world are able to consume only 66.66 percent of nutrient every year. Although the best solution for starvation is to enable all people to access to sufficient supplies and not to waste food, preservation of food could be shown as one of satisfactory solutions of this problem even in case the former is not able to be achieved.

The scientists have conducted a large number of researches to protect food from spoilage and putrefaction and to keep food as fresh as much for a long time. As a result of these scientific investigations, extensive knowledge about preservation technologies in food has been gained and published on scientific journals. When preservation methods for food are evaluated in detail, refrigeration of the food is considered as one of the most widespread protection methods of food. Because microbiological activities and rate of chemical reactions are directly proportional to temperature. Those who are interested in preservation of food utilize the effect of temperature on food to slow metabolic activities by decreasing temperature of food, therefore. Refrigeration applications for safekeeping of food are generally divided into three groups which are chilling, freezing and super-chilling by scientists in literature [4]. Since this study mainly focuses on preservation of meat, especially beef, these refrigeration methods will be explained based on the characteristics of meat after this. Chilling and freezing method basically are applied at the temperature which is above and below the freezing point of meat,

respectively. When chilling and freezing application in literature and industry are investigated, the temperature of the former ranges from 273.15K to 281.15K, while the temperature of the latter is generally accepted at 255.15K or less. The third one is a relatively novel method and Le Danois expressed it firstly without using any industrial or marketing name like super-chilling or soft freezing [4]. In this refrigeration method, meat is kept at the environment whose temperature is 1-2 degree below the initial freezing point (INF) of it [5]. As that is easily realized from the differences among the methods, there are two fundamental issues which should be considered and evaluated. The first one is whether an application includes phase-change phenomenon in meat or not and as a result of this, how a cooling system should be designed efficiently, how its operating condition should be determined properly and how the effectiveness of it should be measured. To answer these questions, a person working on cooling system design should know the cooling process of a material basically. Since cooling of a material without any phase change is a fundamental subject coming from heat transfer due to temperature difference, it is intentionally left to a reader if s/he would like to remember it. To construct a solid basis for phase-change phenomenon and then turn it into a complex structure, the most logical way is to start with the simplest physical event.

A good start is to deal with phase-transition of a pure material such as water since the characteristic of a pure material differs from an impure material and water exists in nature and meat excessively. When a cylindrical body of water with initial temperature (T_i) which is surrounded with cold environment is considered, its temperature will change as a function of time and space. This process is schematically illustrated on Figure 1.1. Under atmospheric condition, solidification or melting of pure water naturally occurs at 273.15K. When the first example is evaluated, surface temperature of the body sharply goes down, while its center temperature decreases slowly even though its initial temperature (T_i) is uniform. This temperature difference between center and surface occurs due to thermal resistance of the body to heat transfer; so, temperature equality is not achieved until steady-state which is the final temperature on Figure 1.1 (T_f). Consequently, thermal conductivity and diffusivity,

have a great impact on heat transfer rate. The phase-transition takes place at a constant temperature as it is observed from the solid line at the center of the body on Figure 1.1. Therefore, temperature at center of the body remains until phase-change is completed and then, it sharply starts to decrease. Another phenomenon is nucleation at phase-transition process. It should be stated that the nucleation is observed at most experiments, while it is not observed at few experiments, as Kah-Chye Tan et. all [6] and Gholaminejad and Hosseini [7] reports that supercooling was sensitive to cooling rate, ambient temperature and initial temperature of the material. Since it is a really complicated occurrence to explain theoretically and to model numerically, nucleation is not included in this study.

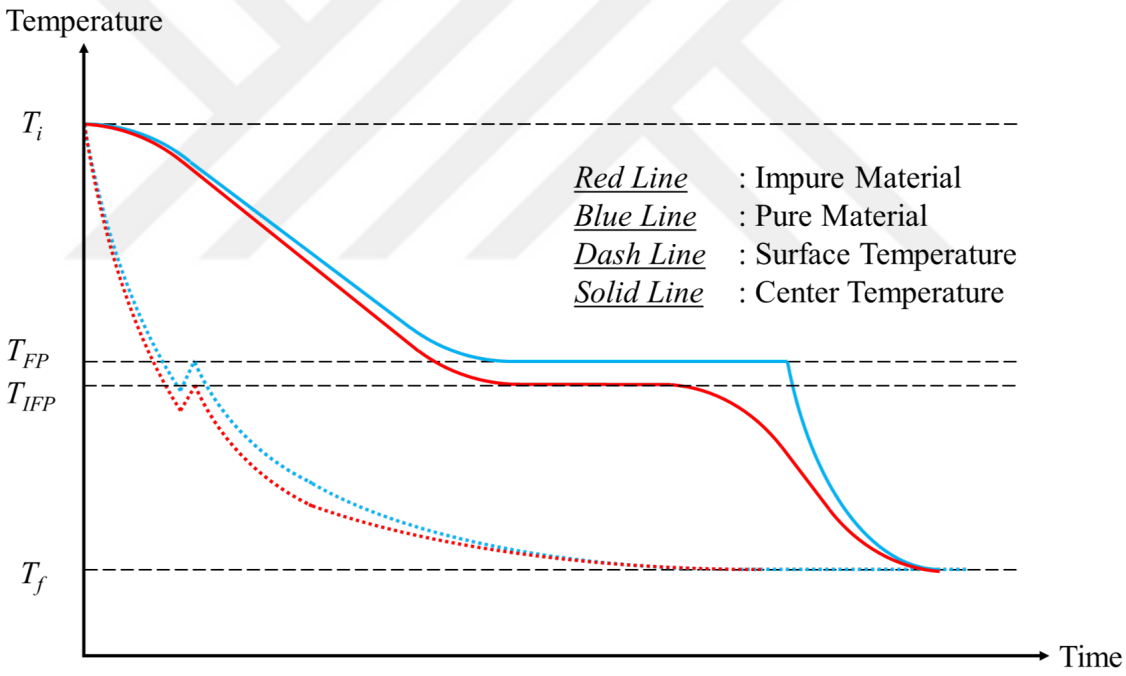

Figure 1.1. The freezing process of a pure and an impure material.

A more complex phase change event certainly happens in food since it is composed of more than one compounds. In other words, solidification or thawing process of food differs from a pure material's because protein, carbonhydrate, fat, mineral, salt, sugar and water that constitute food affect the process directly. Some of these substances such as salt, mineral, vitamins are dissolvable in water, while the others such as fat,

muscle are not soluble in water. Since freezing occurs in the liquid part of food, the content of this mixture has a great importance for phase change. When the phase transition of a mixture is considered the temperature at which freezing first begins is known as the initial freezing point. After the first nucleation, the percentage of the dis-solvable material in the mixture increases because some amount of water has been frozen and the amount of liquid water has been decreased. As a result of this, the phase change occurs at a temperature below the initial freezing point after the first freezing and this repeats itself until phase change is completed. Therefore, phase change of food happens in a temperature range. However, the core temperature of the food equals to the IFP of it until the phase transition process starts here. After the freezing around the center begins or outer layer of the center is frozen, the temperature in the core goes down slowly unlike pure material as it could be observed from red dash line on Figure 1.1.

After a general briefing about phase transition phenomenon, a few important term about freezing process of foodstuff should be known basically in order to compare different freezing processes with each other and generate common results. The first important thing is freezing time. Even though it looks like a basic term, there are more than one definition for freezing time [8]. It could be defined as:

- The time interval from the beginning of the freezing process until the end of the freezing process.
- The time interval from the beginning of the freezing process until center temperature reaches 263.15 K or 255.15 K.
- The time interval from the initial freezing point until the center temperature is 10 K below the initial freezing point temperature.
- The time interval in which the center temperature drops from 272.15 K to 268.15 K.

The second significant thing is freezing rate. It is described in different ways, as it is in freezing time [8]. Freezing rate could be expressed as:

- The ratio of thickness or half thickness of slab foodstuff to freezing time for one side cooling or two side cooling, respectively. If this ratio is smaller than 1, between 1 and 5, and higher than 5, freezing rate is accepted slow, moderate and fast, respectively.
- If the time interval in which the center temperature drops from 272.15 K to 268.15 K is not higher than 30 minutes, freezing rate is accepted as quick.
- The ratio of the half thickness of foodstuff to the time interval from the surface temperature of foodstuff is 273.15 K until the center temperature of foodstuff is 258.15 K [9].
- The ratio of the temperature difference between initial and final temperature of foodstuff to time from the beginning of the freezing process to the end of the freezing process [9].
- The ratio of the distance between surface and center to the time interval from the surface temperature of foodstuff is 273.15 K until the center temperature of foodstuff is 5 K below the initial freezing point temperature [8].
- The ratio of the minimum distance between surface and center to the time interval from the surface temperature of foodstuff is 273.15 K until the center temperature of foodstuff is 10 K below the initial freezing point temperature [10]. If this ratio is 0.2-0.5, 0.5-3, 5-10 and 10-100, freezing rate is accepted slow, quick, rapid and ultra freezing, respectively [11].

Even tough researchers try to create common criteria for evaluation of a freezing process, there is no exact definition and calculation instruction unfortunately.

1.2. Problem Overview

In this study, phase change in food which is placed in a domestic refrigerator cabinet is modeled numerically and the results are verified experimentally. The freezing process is evaluated for different cases in terms of the freeing time and temperature change in the food. The cases are compared with each other in terms of energy efficiency, freezing time and freezing quality to determine most appropriate freezing

conditions.

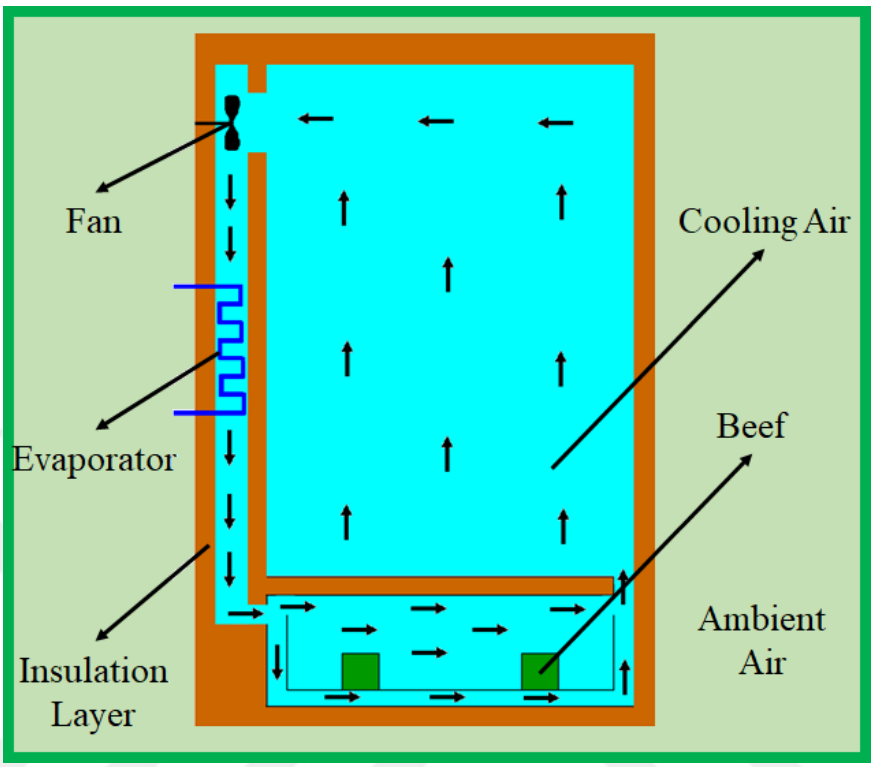

Figure 1.2. Schematic illustration of the numerical and experimental model.

The system studied is mainly composed of inside air, a cabin, a fan, an evaporator, a shelf, beef and ambient air as it can be observed on Figure 1.2. The fan is responsible for air circulation, the evaporator is utilized for cooling, the cabin surrounded with insulation material Polyurethane (PU) protects inside air from heating, the shelf is used to put beef and ambient air is the warm or hot environment.

When the boundary conditions of the system are considered, it is a completely closed domain since infiltration due to gasket is neglected. Inside air is surrounded by solid surfaces which are defined no-slip boundary condition and coupled boundary condition for fluid- flow and heat transfer, respectively. To create air flow inside the refrigerator, a pulse-width modulation (PWM) fan is employed. Rotational speed of a PWM fan can be controlled robustly and therefore it is possible to adjust the air velocity to a desired value. In the CFD analysis, fan geometry is kept originally, and fan rotation

is provided with Moving Reference Frame (MRF) method [12]. A fin-type evaporator is used in not only experimental studies but also in numerical calculations since this type evaporator has higher cooling capacity than a tube type evaporator. No simplifications such as porous model for evaporator is not utilized in order not to be faced with extra error due to these simplifying assumptions. It is defined as time-dependent surface temperature thanks to the results of experimental studies. The cabinet is defined as a solid body with its own thermal properties such thermal conductivity, specific heat and density and some layers next to the cabinet such as the outer metal sheet and the inner plastic sheet are not included in model since their thicknesses are very small. The exterior surfaces are defined as a convection boundary condition which is specified with a free stream temperature and a convective heat transfer coefficient. Values of both are obtained from the results of the experiments. In the experiments, the refrigerator is placed in a temperature and humidity-controlled environment. The temperature and relative humidity (RH) are controlled to be kept at 298.15±1.5K and 50±15 %, respectively.

The parameters having a significant effect on phase-transition or freezing time are air velocity, drawer design or material and blowing type. Since air velocity or in more general terms fluid velocity affects convective heat transfer rate directly, its impact on freezing or cooling time is investigated both numerically and experimentally in this study. As it is expressed above, the change in air velocity or air flow rate could be provided simply with a PWM fan.

The second important parameter is definitely the drawer design and/or material because the bottom surface of a food product is in direct contact with the drawer. Therefore, the influence of the drawer on heat transfer is evaluated. To determine this effect, three different types of shelf are used in experiments and also in numerical calculations. These three models are demonstrated schematically in Figure 1.3. In CFD calculations the drawer is defined as a solid body like the cabinet geometry with its own thermal properties.

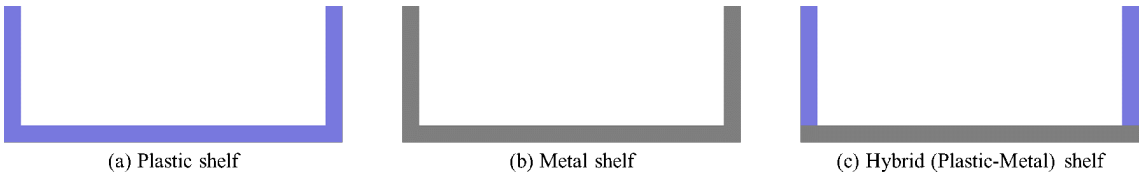

Figure 1.3. Schematic illustration of different shelf designs (a) plastic shelf design, (b) metal shelf design and (c) hybrid (plastic-metal) shelf design.

The last parameter subject to this study is the blowing type. In other words, how homogeneous and heterogeneous blowing styles affect phase-change of food is investigated in terms of freezing time and temperature gradient distribution. The influence of two alternative blowing methods which are shown on Figure 1.3 is analyzed in this thesis. In the first blowing method, air coming from evaporator region exits from an air duct and enters the drawer region. The drawer region is described as a partition surrounded with insulation material and it has a drawer, product(s), air inlet(s), air paths and air outlets. Upon entrance the air flow is divided into two parts. In the first blowing method one part of the air flows into the drawer, spreads inside the drawer and exits from the end of the front wall of drawer, while the other part first goes down, and then passes the bottom of drawer and leaves this partition by going up. In the second blowing method, air comes to inlet under the same conditions as in the first one. Yet, it moves into a channel which has a lot of small openings, and air naturally falls like a shower. It is aimed to have a homogeneous air distribution in the drawer. In this design, air velocity between drawer and cabinet is relatively less than the first design.

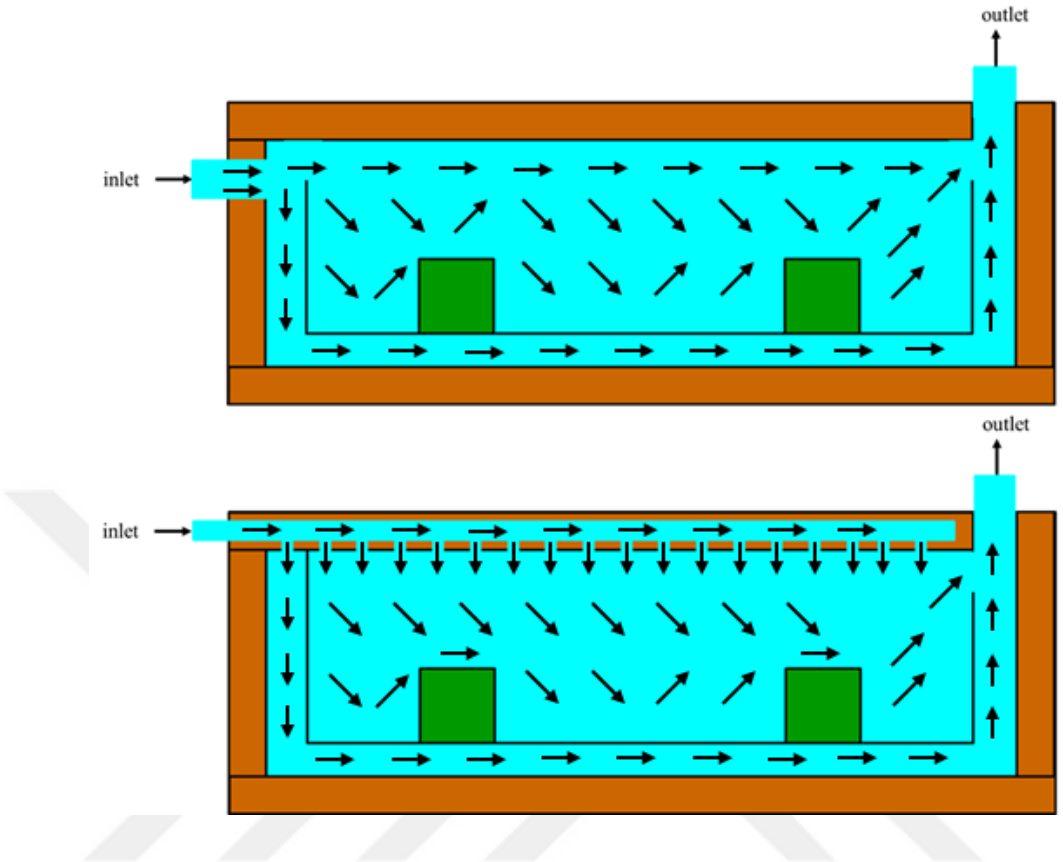

Figure 1.4. Schematic illustration of the blowing types.

The last significant statement is related to properties and definitions of food without doubt in this study. As the phase-change phenomenon in food is clearly explained in the previous section, it takes place in a temperature range instead of a constant temperature value. Thermal properties such as the thermal conductivity, specific heat and density of the food change in a non-linear manner depending on the temperature. In addition, ingredients of the food have an important effect on its thermal properties. The properties of almost of all type of foods are available in "Refrigeration" handbook [13] published by the American Society of Heating Refrigerating and Air Conditioning Engineers (ASHRAE). However, the thermal properties such specific heat and conductivity are measured experimentally in this study.

A differential scanning calorimetry (DSC) method is utilized to obtain specific heat and a hot-plate method is used to measure the thermal conductivity. The thermal

expansion of the product is neglected in this study, and the density of it is taken as constant. In order to make many experiments without exploiting any nutrition and to get rid of any error stems from use of different specimens, a test package which simulates the beef is used. The test package is composed of 76.4% water, 23.0% ethyl methyl cellulose, 0.5% sodium chloride and 0.08% 6-chloro-m-cresol.

1.3. The Objectives of The Present Study

The main aims of this study are to model the phase-change process in beef and to predict freezing time of beef and to verify the numerical model with experimental results. The numerical model takes into account the variable thermal properties because they drastically vary especially in the range of phase-change temperature. In addition, the author model not only phase transition process in beef but also its environment since ambient condition is not the same on the every every surface or every time during.

The first purpose is to model the phase change of food inside a domestic refrigerator numerically and to obtain a basic knowledge about the food freezing. In other words, this work is expected to help designing a cooling system of a new domestic refrigerator. The model will supply data on the selection of air flow rate, air circulation system and a special shelf design.

The second goal is to reveal the freezing process parameters such air flow rate, blowing position, drawer design and material and to divulge which parameter has how much impact on the freezing process especially on the freezing time.

The third objective is to increase the confidence in numerical methods for phase-transition by verifying the numerical results with the experimental results since there is still an apparent lack of trust in numerical methods or models in academia or industry.

2. THE MATHEMATICAL MODELS

2.1. Introduction

Phase transition in foods is one the most widespread issues in literature since the beginning of the 1970s. A review of the studies about solidification of food in literature reveals that this phenomenon is considered according to the freezing time of food. In other words, scientists have usually worked on calculating the time which is necessary for a complete freezing of food. There are many methods for determining freezing time and simulating the phase change of food in literature. They are simply sorted analytical, approximate, empirical and numerical. It should be stated that the mathematical phase change models suitable for numerical solutions will be evaluated in this thesis.

When the phase change process of a material is considered, two fundamental physical events should be evaluated. The first is the effect of the latent heat due to solidification or thawing, while the second one is the impact of the fluid flow due to liquid parts of material. Therefore, fluid flow and heat transfer mechanisms should be taken into account for a phase change problem basically. If heat transfer mechanism is considered, a phase transition problem may include two fundamental heat flow mechanisms, which are conduction and convection heat transfer, as Henry Hu et al. [14], José et al. [15] and Andreas et al. [16] review in their studies. In this point, the type of foodstuff plays an important role which mechanism(s) has a great effect on this process. For example, some food items contain significant amount of liquid, while others have low moisture content, relatively. As a result of this, convective heat transfer is equally important as conductive heat transfer in the former, while convective effects could be neglected in the latter. Naturally, the effect of the fluid flow on the phase change process is shaped according to this. Depending on the content of the material, the influence of the fluid flow is included or not in mathematical models. In literature, apparent specific heat capacity, effective heat capacity, heat source and enthalpy

methods are developed for latent modeling, while source term and variable viscosity methods are introduced for fluid flow modeling.

In addition to phase transition phenomenon, the author is interested in fluid flow and heat transfer inside a domestic refrigerator in this study since convective heat transfer coefficient (HTC) on the surface of a material under phase-change has a great impact on the calculation of the solidification/melting time. Although almost all researchers take the average HTC value in their simulation in order to reduce the complexity of model and to save computational time, a fatal error in the estimation of the freezing time comes from this assumption [17–23]. Hoang et al. [20, 24] does not give any information about the surface heat transfer coefficient in detail. Only Moraga et al. [19, 22, 23] show the change of HTC along the surface of foodstuff explicitly. Yet, they simulate this process by reducing the problem to 2D under natural convection cooling [19] and they model the freezing of food with 3D model under natural convection [23]. Even they focus on the forced convection cooling [22], they are not interested in turbulence modelling. Therefore, the author tries to simulate not only phase change of beef but also cooling air or refrigerator cabin with a 3D model, under forced convection cooling air and including turbulence effect in this study. This simulation model differentiates the present work from the others.

2.2. Governing Equations

The mathematical models for both phase change and fluid flow which are going to be clarified in below are expressed with the governing equations for incompressible flow.

2.2.1. Continuity Equation

The general form of continuity equation is given by:

$$\frac{\partial \widetilde{u_i}}{\partial x_i} = 0 \tag{2.1}$$

where $\widetilde{u_i}$ and x_i represent the velocity components and the directions, respectively. Also, i is used to show each component of velocity vector and coordinate axis by taking it 1,2 and 3.

2.2.2. Momentum Equation

The general form of momentum equation is written as:

$$\rho\left(\frac{\partial\widetilde{u_i}}{\partial t}+\widetilde{u_j}\frac{\partial\widetilde{u_i}}{\partial x_j}\right)=-\frac{\partial\widetilde{p}}{\partial x_i}+\frac{\partial}{\partial x_j}\left(\mu\frac{\partial\widetilde{u_i}}{\partial x_j}\right)+f_i+S_i \tag{2.2}$$

where ρ is density, t is time, $\widetilde{p}$ is pressure, μ dynamic viscosity, f body force and S_i source term.

2.2.3. Energy Equation

The general form of energy equation except for radiation effect is expressed by:

$$\rho\left(\frac{\partial\widetilde{h}}{\partial t}+\widetilde{u_i}\frac{\partial\widetilde{h}}{\partial x_i}\right)=\left(\frac{\partial}{\partial x_i}\left[k\frac{\partial\widetilde{T}}{\partial x_i}\right]\right)+\phi+S_T \tag{2.3}$$

where $\widetilde{h}$ is enthalpy per unit mass, ρ is density, $\widetilde{T}$ is temperature, k is thermal conductivity, ϕ is dissipation term and S_T is source term. The enthalpy and dissipation terms are expressed by:

$$\widetilde{h}=c_p\widetilde{T} \tag{2.4}$$

$$\phi=2\nu\left[\left(\frac{\partial\widetilde{u}}{\partial x}\right)^2+\left(\frac{\partial\widetilde{v}}{\partial y}\right)^2+\left(\frac{\partial\widetilde{w}}{\partial z}\right)^2+\frac{1}{2}\left(\frac{\partial\widetilde{v}}{\partial x}+\frac{\partial\widetilde{u}}{\partial y}\right)^2+\frac{1}{2}\left(\frac{\partial\widetilde{w}}{\partial y}+\frac{\partial\widetilde{v}}{\partial z}\right)^2+\frac{1}{2}\left(\frac{\partial\widetilde{u}}{\partial z}+\frac{\partial\widetilde{w}}{\partial x}\right)^2\right]. \tag{2.5}$$

2.2.4. Turbulence Equation

Turbulence is one of the most important issues which are massively studied by not only academic people but also engineers at industry since it has a great impact on fluid flow and heat transfer. However, turbulence modeling is a very difficult topic, as it is known from those who spend effort on this subject know very well. Since turbulence modeling is a comprehensive subject, it is simply touched upon in this study.

In literature, turbulence modeling is expressed with RANS equations or LES method, while it is solved with DNS. In fact, the solution of turbulence is done instead of modeling as the method goes from RANS to DNS. Since the main point of this study is not turbulence modeling, each method is not explained in detail and only general comparison is made to show the advantage and disadvantage of them. The physical event is resolved in DNS completely and in LES partially, while it is modeled with RANS equations. The results of the DNS and LES comply with real events entirely and almost entirely, respectively. However, they require high computational time and high-performance computer. On the other hand, the models based on RANS equations are able to give usable results even if they are not as accurate and detail as the result of DNS and LES.

The turbulence modeling based upon RANS equations mainly comes from the decomposition of a variable into a mean and a fluctuating part. According to that, velocity components and the other scalars such pressure and temperature are written respectively as:

$$\widetilde{u_i} = \overline{U_i} + u_i \tag{2.6}$$

$$\widetilde{p_i} = \overline{P_i} + p_i \tag{2.7}$$

$$\widetilde{T_i} = \overline{T_i} + T_i \tag{2.8}$$

where the overbar and the normal character on the right-hand-side express the mean and the fluctuating part of a quantity, respectively. After these are substituted into the governing equations and some algebraic arrangements are made, they are written as:

$$\frac{\partial \overline{U_i}}{\partial x_i} = 0 \tag{2.9}$$

$$\rho\left(\frac{\partial \overline{U_i}}{\partial t} + \overline{U_j}\frac{\partial \overline{U_i}}{\partial x_j}\right) = -\frac{\partial \overline{P}}{\partial x_i} + \frac{\partial}{\partial x_j}\left(\mu\frac{\partial \overline{U_i}}{\partial x_j} - \overline{u_i u_j}\right) + f_i + S_i \tag{2.10}$$

$$\rho c_p\left(\frac{\partial \overline{T}}{\partial t} + \overline{U_j}\frac{\partial \overline{T}}{\partial x_j}\right) = \left(\frac{\partial}{\partial x_j}\left[k\frac{\partial \overline{T}}{\partial x_j}\right]\right) + \frac{\partial}{\partial x_j}\left(\overline{u_i T}\right) + \phi + S_T \tag{2.11}$$

where μ_t is turbulence or eddy viscosity and K is turbulence kinetic energy.

As it can be noticed, a new term appears on the right-hand side of the momentum equations due to the fluctuation part of the velocity components. This is called as Reynolds stress term in the literature and it needs to be defined properly in order to model turbulence. To achieve that, Boussinesq hypothesis is widely utilized for RANS models. After some rearrangements, the Reynolds stress term is written with Boussinesq hypothesis as:

$$-\rho\overline{u_i u_j} = \mu_t\left(\frac{\partial \overline{u_i}}{\partial x_j} + \frac{\partial \overline{u_j}}{\partial x_i}\right) - \frac{2}{3}\left(\rho K + \mu_t\frac{\partial \overline{u_k}}{\partial x_k}\right)\delta_{ij} \tag{2.12}$$

where μ_t is turbulence or eddy viscosity and K is turbulence kinetic energy. The turbulence viscosity is written as:

$$\mu_t = \rho C_\mu \frac{k^2}{\varepsilon} \tag{2.13}$$

where C_μ is expressed by:

$$C_\mu = \frac{1}{A_0 + A_s \frac{kU^*}{\varepsilon}} \tag{2.14}$$

where U^* is:

$$U^* \equiv \sqrt{S_{ij}S_{ij} + \widetilde{\Omega_{ij}}\widetilde{\Omega_{ij}}} \tag{2.15}$$

and

$$\widetilde{\Omega_{ij}} = \Omega_{ij} - 2\varepsilon_{ijk}\omega_k \tag{2.16}$$

$$\Omega_{ij} = \overline{\Omega}_{ij} - \varepsilon_{ijk}\omega_k \tag{2.17}$$

where Ω_{ij} is the rate-of-rotation tensor and ω_k is angular velocity. The model constants are written as:

$$A_0 = 4.04 \tag{2.18}$$

$$A_s = \sqrt{6}\cos\varphi \tag{2.19}$$

where φ is:

$$\phi = \frac{1}{3}\cos^{-1}\left(\sqrt{6}\frac{S_{ij}S_{jk}S_{ki}}{\left(\sqrt{S_{ij}S_{ij}}\right)^3}\right) \tag{2.20}$$

$$-\rho\overline{u_i T} = \Gamma_t \frac{\partial \overline{T}}{\partial x_i} \tag{2.21}$$

where Γ_t is turbulence diffusion coefficient which is given by:

$$Pr_t = \frac{\mu_t}{\Gamma_t}. \tag{2.22}$$

2.3. The Mathematical Models for Phase Change

In this section, the mathematical models for phase transition are summarized explicitly. When the phase change process is considered, the two fundamental physical events should be evaluated. One of them is the effect of the latent heat due to solidification or melting, while the second one is the impact of the fluid flow due to liquid parts of material. Therefore, apparent heat capacity, effective heat capacity, heat source and enthalpy methods are explained for modeling latent heat and source term and variable viscosity methods are used for modeling fluid flow. However, it should not be forgotten that this phenomenon takes place at very small velocity values, so the turbulence part of the governing equations which are illustrated at the previous section is ignored for phase-change modeling methods.

2.3.1. Apparent Heat Capacity Method

The approach was firstly recommended in 1967 [25]. It is based on combining latent heat capacity with sensible heat capacity as a function of temperature. According to this, the new specific heat capacity is expressed by:

$$c_{app} = \begin{cases} c_{p,s}, & T < T_s \\ c_{p,sl}, & T_s < T < T_l \\ c_{p,l}, & T > T_l \end{cases} \tag{2.23}$$

where

$$c_{p,sl} = \frac{\int_{T_s}^{T_l} c_p\,(T)\,dT + L}{(T_l - T_s)} \tag{2.24}$$

c_p is specific heat of the material due to sensible heat and energy equation is expressed as

$$\rho c_{app}\left(\frac{\partial \widetilde{T}}{\partial t}+\widetilde{u}_i\frac{\partial \widetilde{T}}{\partial x_i}\right)=\left(\frac{\partial}{\partial x_i}\left[k\frac{\partial \widetilde{T}}{\partial x_i}\right]\right)+\phi+S_T. \tag{2.25}$$

Though this approach looks like a simple method to apply, it has two drawbacks. The first disadvantage is that it could be implemented numerically if phase transition occurs in a temperature range. The second disadvantage is that in the implementation it requires very small time-steps in order to catch phase change region properly. Nevertheless, this method gives good and reasonably accurate results to researcher [19–24, 26–32] and is easily applicable. If some studies used the apparent heat capacity method for latent heat modeling are evaluated mainly, they could be summarized as below.

Dima et al. [26] are interested in the freezing of marine products. They model phase transition of Patagonian marine crab numerically and validate numerical results with experimental measurements. To simulate this process, they prefer to use finite element method to solve energy equation with their own MATLAB code. The apparent specific heat of marine product is determined by using differential scanning calorimetry and then, it is expressed with special mathematical functions. They model only foodstuff by using constant HTC in their simulation as a boundary condition.

Hoang et al. [20, 24] spend effort to simulate the freezing of bulk foodstuff and to validate their calculations with experiments in their two publications. They take packed poultry products, which are whole chickens and drumsticks in the first and second publications, respectively. As distinct from the previous study, they consider the effect of the ambient air and air voids inside the whole chicken on the freezing process of the food stuff. Therefore, they model ambient air instead of using average HTC and calculate natural convection in the chicken. To achieve that, they utilize CT scanner to generate geometric model of the specimen for numerical analysis. However,

they do not explain the importance of the modelling ambient air by showing the change in time-dependent and space-dependent surface HTC. Both numerical calculation and experimental measurement are done in industrial freezing tunnel with constant cooling temperature. The authors take thermal properties such as specific heat and thermal conductivity as a function of temperature. To calculate them, they utilize two reference publications. The first one provides the composition of chicken for them, while the second one enables them to calculate the thermal properties.

Santos et al. [28] work on freezing of bakery product. They try to model phase change of food numerically and verify it experimentally. They define thermal properties such as thermal conductivity and specific heat as a function of temperature. The specific heat of bakery product is measured by DSC, while its thermal conductivity is taken from literature. They write their own finite element code to solve governing equations numerically. Though they model freezing of foodstuff without ambient air and use constant surface HTC as a boundary condition, they pay attention to the impact on the surface HTC.

Tocci and Mascheroni [29] model the freezing process of spherical food products by considering heat and mass transfer. They generate their own FDM code to solve governing equations. In this study, ambient air is not included in the model. Instead, its effect is provided by defining as a boundary condition. Heat transfer and mass transfer coefficient are defined as constant during the numerical calculation. In this study, temperature-dependent specific heat and conductivity are also used.

Moraga at al. [19, 30] carry out sequential studies about modelling of foodstuff with ambient air. They model only heat flow during the phase change of the foodstuff in the first study, while they simulate both heat and mass transfer in the second study. Temperature-dependent thermal properties such as thermal conductivity and specific heat of foodstuff are obtained from literature. They pay attention to the importance of the local HTC on the foodstuff surfaces. However, they model freezing of foodstuff with a 2D model under natural convection cooling in both studies. On the other hand,

Moraga and Salinas [21] work on the freezing of salmon meat under forced convection with a 2D model. But they do not give any information about the change of the surface HTC. In addition to them, Moraga and Medina [22] focus on the surface HTC of the food under forced convection freezing process. However, they reduce their problem to a 2D model and they do not include the turbulence effect in their numerical calculation. In the final pre-proofed study, Moraga and Rivera [23] model the freezing of food in domestic freezer with a 3D model and turbulence effects but they investigate the impact of the turbulence and 3D model under natural convection cooling process.

Huan et al. [31] work on the modeling of the freezing of a test package without including cooling air. They investigate the influence of the some parameters such as freezing air, freezing air velocity, food shape and size on freezing process numerically. However, the numerical result of only one case is verified experimentally. They use temperature-dependent thermal properties such as specific heat and thermal conductivity in numerical studies. For numerical calculation, FEM is utilized.

2.3.2. Effective Heat Capacity Method

The technique was initially suggested in 1988 [33]. This approach was offered to enhance the previous method and to obtain more accurate and reliable results. It is given by:

$$c_{eff} = \frac{\int c_{app} dV}{V} \tag{2.26}$$

where V is the control volume. As it could be understood from the formula, specific heat value is effectively calculated through the control volume, or in other words, inside the control volume by integration. This enables use of larger time-steps in integration of the energy equation, thus eliminates one drawback of the apparent specific heat method. Yet, effective heat capacity method still requires too high computational time since a volume integration should be calculated at each time step [14, 33–35] and it is not still proper for isothermal phase change problem like the apparent heat capacity. In

addition to that, this method needs more effort than the previous one since it requires a change of the CFD code.

2.3.3. Heat Source Method

Voller and Swaminathan [36] put forward this method in 1991, which is also known as fictitious method in literature. It is different from the previous approaches in that specific heat in this method is not composed of the total of the sensible and the latent heats. The latter due to phase transition is considered separately as a heat source for melting and a heat sink for solidification. According to this model, the source term in the energy conservation (2.10) is taken as:

$$S_T = -\frac{\partial(\rho L \beta)}{\partial t} \tag{2.27}$$

where ρ, L, and β represent density, latent heat and fraction of liquid, respectively. β equals to zero and one for solid and liquid states, respectively, and it is generally expressed with solidus and liquidous temperature.

Since the implementation of heat source or heat sink to numerical solver is effortless, it is one of the most widely used methods for phase change problem [37]. Yet, it may give accurate results for non-isothermal solidification/melting problems such as food freezing since latent heat could be distinguished successfully from specific heat in temperature range. On the other hand, it may give oscillatory results for isothermal problem since latent heat could not be differentiated easily from this specific heat at constant temperature.

2.3.4. Enthalpy Method

Enthalpy method is different from the others in terms of the way the energy equation is expressed, and the latent heat is examined. In the articles on phase-change problems this method is exploited excessively [38–48] together with commercial

software such as Ansys Fluent, Star CCM+, COMSOL etc. This approach tries to create a connection between temperature and enthalpy in order to express the influence of latent heat. Though it looks like the apparent specific heat methods, enthalpy method differs from them in that the former does not combine sensible and latent heat. Instead, they are expressed separately and their effects on the phase change are included by using a fraction function which is shown by β and is generally expressed as a function of solidus (T_s) and liquidus (T_l) temperature. The energy equation is given by:

$$\frac{\partial \widetilde{H}}{\partial t} + \widetilde{u_i}\frac{\partial \widetilde{H}}{\partial x_i} = \left(\frac{\partial}{\partial x_i}\left[k\frac{\partial \widetilde{T}}{\partial x_i}\right]\right) + \phi + S_T. \tag{2.28}$$

One of the most known form of enthalpy was suggested by Swaminathan and Voller [35].

$$\widetilde{H} = (1-\beta)\int_{T_ref}^{T} \rho c_{p,s} dT + \beta \int_{T_ref}^{T} \rho c_{p,l} dT + \beta \rho L \tag{2.29}$$

where $\widetilde{H}$ is total enthalpy, β is fraction of liquid, T_{ref} is reference temperature and ρ is density.

Scheerlinck et al. [38] model the test package with the temperature-dependent specific heat and thermal conductivity by writing their own FEM code. To reduce the effect of the surface HTC on freezing process, they cover their specimen with a copper container. To prevent the numerical calculation from any quick jump in thermal conductivity and missing point in specific heat due to improper numerical procedure such as high time step or coarse grid structure, they propose using volumetric specific enthalpy instead of apparent specific heat for latent heat modeling and Kirchhoff function, which is a transformation method to integrate the thermal conductivity, instead of thermal conductivity. To do that, they write their own numerical code in MATLAB. In addition to that, they model the same problem with the apparent heat capacity method and only enthalpy method in order to compare them with each other in terms of accuracy, applicability and computational cost. They conclude that the apparent heat

capacity method requires the most computation time, while their approach requires the least computation time. They say that the surface temperature value obtained with apparent heat capacity method is different from the value obtained with their own code. However, it should not be forgotten that the former is sensitive to time step size. Therefore, it cannot give accurate results in case of insufficient time step. Therefore, it does not catch the same results in which temperature changes rapidly. Lastly, their method requires extra coding to implement this improvement to a problem.

Camila et al. [39] try to simulate the freezing of green bean in their study by using the same method as the previous study. The utilize the volumetric specific enthalpy and Kirchhoff transformation. Since they are aware of the importance of the convective heat transfer among food surfaces and its ambient, they conduct their experimental and numerical studies at different convective conditions. Yet, they do not model ambient like the previous work.

Zilio et al. [40] work on the phase transition of poultry products. They firstly review the freezing time calculation methods for foodstuff and secondly spend time to investigate the capability of the Star CCM+ for a solidification problem. They use chicken breast in their study as a sample and work numerically and experimentally. They utilize the enthalpy method for their numerical calculation with temperature dependent thermal properties such as specific heat and thermal conductivity. Since they prefer to use Star CCM+ as a CFD solver, they have to use finite volume method to solve partial differential equations. As they mention in their publication, they use VOF model for phase change process and define the sample as solid domain in software. Yet, they do not give information about which governing equations (which is continuity, momentum and energy) are solved and how VOF model is implemented to only solid domain. They use special scanning system, which is Near Infrared Spectrometer, to determine the composition of the foodstuff and then, they calculate thermal properties of the material thanks to this composition data according to ASHRAE handbook. Like the Dima's study, they use average HTC in their simulation as a boundary condition of finite cylinder specimen and also, they express that their preliminary test results

show that HTC should be calibrated when the numerical calculations are compared to experiments.

Kiani et al. [47] are interested in the modeling of the freezing process of potato under ultrasound environment. They develop a program in OpenFOAM software, which is a open source CFD solver and based on FVM. They prefer to use enthalpy method for the latent heat modeling and they calculate volumetric specific enthalpy and time-dependent thermal conductivity of the potato by using some approaches based on the composition of the material in the literature. Tough this study is relatively similar to others until this point, it differs from them in that the modeling of the impact of the ultrasound. To simulate the influence of the ultrasound, they utilize the source term. Therefore, this study includes both heat source method and enthalpy method.

Iten et al. [49] work on solidification and melting process of a PCM. They try to both compare EM and EHCM numerically and to validate their simulation results with experimental measurements. They utilize ANSYS Fluent as a CFD solver based on FVM for both methods. For non-isothermal phase transition process, they suggest the EHCM when it is compared with EM since the percentage error of the former is %2.6 for melting, while it is %5.7 in the latter.

Up to now, the energy equation has been examined in different ways for the phase change problems. The dissipation terms due to viscous effect may be neglected since they have too small impact on results for low speed incompressible flows. Moreover, if the phase change takes place in solid form material such as beef, the components of the velocity vector on left-hand side of energy equation could be taken as zero by assuming that conduction is more dominant than convection.

Since the impact of the latent heat on phase change is dominant, the methods explained so far focus intensely on how latent heat is expressed. However, for aqueous foods, the convective term on left hand side of the energy equation should be added to calculation since convective heat transfer plays a significant role at least as much as

conduction heat transfer is. Therefore, the momentum equation should be included to calculation. The next two methods are frequently preferred in the literature for these kind of problem are explained briefly.

2.3.5. Source Term Method for Momentum Equation

The main objective of this method is to calculate the momentum equation for liquid region by separating liquid region from solid region thanks to source term on right hand side of momentum equation. When a liquid material under solidification process reaches to solid state, the velocity value of this region is decreased by increase in source term and so, momentum equation for solid frozen region is not solved since its value will be negligible. Voller and Prakash [50] recommended one of the famous source term methods in 1987. According to this method which is utilized in both commercial package programs such as Fluent, CFX, etc. and some in-house codes, the source term is expressed thanks to Darcy's law. S is defined as:

$$S_i = \frac{(1-\beta)^2}{(\beta^3 - e)} A_{mush} \left(\widetilde{u}_i\right) \tag{2.30}$$

where β is fraction of liquid, e is a small number (e=0.001) to not make source term infinite, A_{mush} is the constant for mushy zone and $\widetilde{u}_i$ is the velocity vector components in x, y, z direction, respectively.

2.3.6. Variable Viscosity Method

Variable viscosity approach is actually a straightforward method when it is compared with the previous one since it calculates momentum equation by using variable viscosity instead of any source terms. In this method, the impact of source term is provided directly with increased viscosity for solid state calculation. To apply this method, the scientists have published several viscosity functions some of which are expressed as a function of temperature, while the others are given as a ratio of solid and fluid state constitutes [15].

2.4. The Mathematical Models for Refrigerator

As it is mentioned before, modeling the fluid flow and heat transfer inside the domestic refrigerator is one of the topics of this research. When the physical events occurring inside the fridge are considered, it may be said that there is air movement due to a turbomachinery unit and heat transfer due to temperature differences between different surfaces. The modeling of fluid flow and heat transfer inside the refrigerator will be evaluated in the following subsections.

2.4.1. Moving Reference Frame (MRF) Method

Moving reference frame is an approximation exploited in industry in order to model the problems that include rotating parts such as turbomachinery, moving walls and etc. Since MRF is one of the easiest and the most reliable methods for modeling a fan application, it is preferred in this thesis. As it is realized from the name of this approximation, two different reference frames shown on Figure 2.1 are defined to solve the governing equations for both a stationary zone and a moving zone.

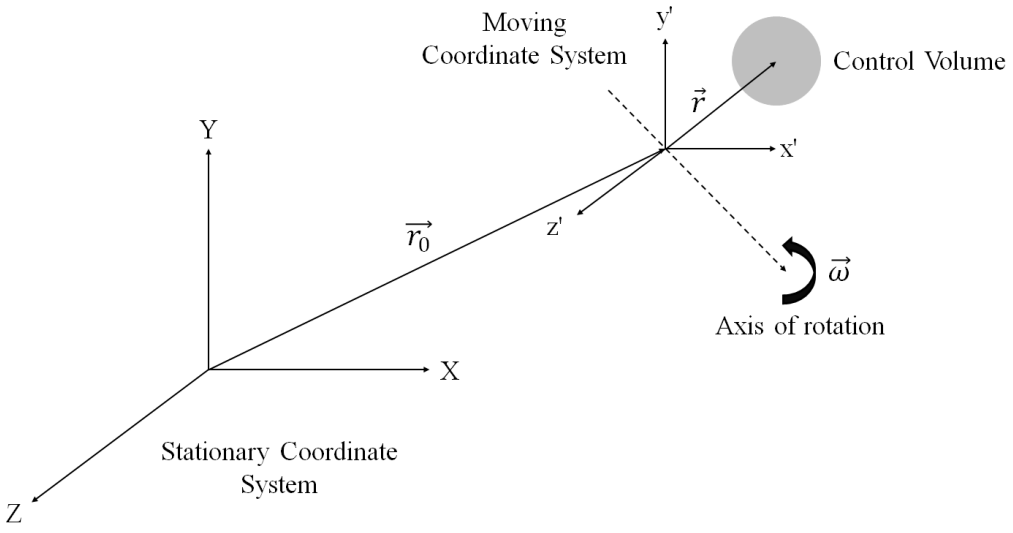

Figure 2.1. Stationary and Moving Reference Frames.

While there is no change in solution of the equations for inertial part, the calcu-

lation for non-inertial part requires updating mathematical expressions. According to this, the governing equations for moving zone with absolute velocity formulation are written as:

$$\frac{\partial \widetilde{u_i}}{\partial x_i} = 0 \tag{2.31}$$

$$\rho\left(\frac{\partial \widetilde{u_i}}{\partial t} + \left(\widetilde{u_j}\right)_r \frac{\partial \widetilde{u_i}}{\partial x_j}\right) = -\frac{\partial \widetilde{p}}{\partial x_i} + \frac{\partial}{\partial x_j}\left(\mu \frac{\partial \widetilde{u_i}}{\partial x_j}\right) - \omega \times \widetilde{u_i} + S_i \tag{2.32}$$

where $\left(\widetilde{u_j}\right)_r$ is relative velocity and is defined as:

$$\left(\widetilde{u_j}\right)_r = \left(\widetilde{u_j}\right) - \omega \times r \tag{2.33}$$

where $\widetilde{u_j}$ is absolute velocity, ω is angular velocity and r is position vector.

2.4.2. Turbulence Modeling

In this study, it is preferred to use the realizable k-ε model with the standard wall function, which is a two-equation turbulence model based on RANS equation, since it requires less computational time, gives acceptable results and is one of the most common methods in industrial applications. Since the main purpose of this study is not how RANS model is derived in detail, it is not explained explicitly.

For turbulence kinetic energy (K),

$$\rho\left(\frac{\partial K}{\partial t} + \frac{\partial}{\partial x_j}\left(K u_j\right)\right) = \frac{\partial}{\partial x_j}\left[\left(\mu + \frac{\mu_t}{\sigma_k}\right)\frac{\partial K}{\partial x_j}\right] + G_k + G_b - \rho\varepsilon. \tag{2.34}$$

For turbulence dissipation (ε),

$$\rho\left(\frac{\partial \varepsilon}{\partial t} + \frac{\partial}{\partial x_j}\left(\varepsilon u_j\right)\right) = \frac{\partial}{\partial x_j}\left[\left(\mu + \frac{\mu_t}{\sigma_\varepsilon}\right)\frac{\partial \varepsilon}{\partial x_j}\right] + \rho C_1 S_\varepsilon - \rho C_2 \frac{\varepsilon^2}{K + \sqrt{\nu\varepsilon}} \tag{2.35}$$

where

$$C_1 = \max\left[0.43, \frac{\eta}{\eta+5}\right] \tag{2.36}$$

$$\eta = S\frac{K}{\varepsilon} \tag{2.37}$$

$$S = \sqrt{2S_{ij}S_{ij}} \tag{2.38}$$

where the constants are σ_k=1.0, σ_ε=1.2, $C_{1\varepsilon}$=1.44, and C_2=1.9, which is proposed by Tsan Hsing et al. [51].

2.4.3. Heat Transfer Modeling

As the problem is explained in the introduction, a refrigerator numerical model with its solid and fluid parts is also expected from the present study, in addition to the modeling of the freezing of beef. As the physical model is illustrated on Figure 1.2, a refrigerator is composed of fluid, the cooling air inside the main body and solid parts like the insulation material, PU, evaporator cover, drawer, shelf glasses. In the model the energy equation should be solved in both solid and fluid zones. When the common surfaces between two neighboring zones are considered, their temperatures should be the same. Therefore, conjugate heat transfer model for two types of zone should be set up. The governing equations are firstly solved for fluid zone and then the energy equation is solved for solid zone by utilizing the solution data of fluid zone on the interface between the solid and fluid zones. The energy equation solved for this numerical calculation is expressed for solid and fluid regions, respectively as:

$$\rho\left(\frac{\partial h}{\partial t} + u_i\frac{\partial h}{\partial x_i}\right) = \left(\frac{\partial}{\partial x_i}\left[k\frac{\partial T}{\partial x_i}\right]\right) \tag{2.39}$$

where

$$h = \int_{T_{ref}}^{T} c_p dT \tag{2.40}$$

$$\rho\left(\frac{\partial h}{\partial t} + u_i \frac{\partial h}{\partial x_i}\right) = \left[\frac{\partial}{\partial x_j}\left[\left(k + \frac{c_p \mu_t}{Pr_t}\right)\frac{\partial T}{\partial x_j} + u_i\left(\tau_{ij}\right)_{eff}\right]\right] \tag{2.41}$$

where

$$\left(\tau_{ij}\right)_{eff} = \mu_{eff}\left(\frac{\partial u_j}{\partial x_i} + \frac{\partial u_i}{\partial x_j}\right) - \frac{2}{3}\mu_{eff}\frac{\partial u_k}{\partial x_k}\delta_{ij}. \tag{2.42}$$

3. THE COMPUTATIONAL MODEL

3.1. Introduction

The numerical models for phase transition problems in literature are basically diverted into two fundamental groups which are fixed and variable grid methods. As it could be realized from their names, the former uses stable grid structure, while the latter utilizes a deforming grid structure.

Variable grid methods solve two set of equations for solid and fluid domains separately and they track interface between solid and fluid region explicitly. To achieve this, either the grid is adjusted and updated dynamically at each step or the time step is changed to match the position of fluid-solid interface with grid points [14]. Both dynamic grid [52, 53] and dynamic time step [54, 55] methods have been applied successfully in different studies by the scientists.

Unlike variable grid methods, fixed grid methods do not follow liquid-solid interface directly and compute continuity, momentum and energy equations for only one domain with volume fraction. Therefore, it is more straightforward, affordable and widespread than variable grid methods. Even though the variable grid methods are more strong solution methods for a phase change problem, the fixed grid methods also give quite accurate results. Therefore, the apparent specific heat method which is one of the most widespread fixed grid approaches for phase-transition issues in literature is preferred in order to reduce complexity and save computational time for phase change of beef in this study. This numerical calculation is applied via ANSYS Fluent 19 R1.

3.2. Finite Volume Method

One of the most preferred numerical methods for fluid mechanics and heat transfer problem is finite volume method (FVM) since it has many advantages when compared

with the others finite element and finite differences methods. Versteeg and Malalasekera [56] simply describe the solution procedure of FVM as follow:

- Firstly, the governing equations in differential form are converted into integral form for a control volume.
- Secondly, they are discretized and transformed to algebraic equations.
- Finally, these algebraic equations are solved with iterative methods.

3.3. Geometry and Boundary Condition

The geometry of the problem with dimensions 1.059x0.594x0.643 m^3 consists of solid domains and fluid domains as it is shown on Figure 3.1. The air inside the refrigerator which is one of the fluid domains is surrounded by solid insulation material which is polyurethane. To generate high quality mesh structure and apply moving reference frame (MRF) method for air circulation, the inside air is split up to three parts: main air domain, air duct domain and fan domain.

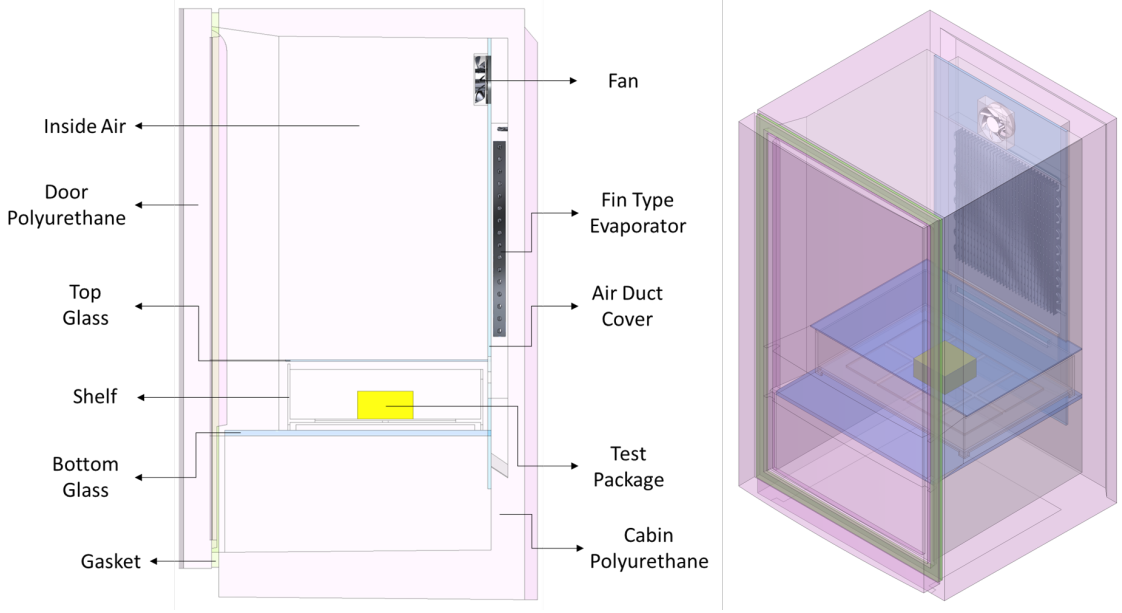

Figure 3.1. The Geometric Model of the problem.

The mesh generation of the geometry which has rear blowing and top blowing is completed via ANSYS Fluent Meshing with 15,157,071 and 20,484,152 poly elements whose maximum aspect ratios are 20 and 15, and the worst skewness' are 0.85 and 0.80, respectively as they are illustrated on Figure 3.2. It should be stated that the thickness of fin geometry is accepted as 1 mm instead of 0.125 mm to generate high quality mesh. In addition to that, boundary layer meshes are generated according to the standard wall function. In other words, the height of the first element of the boundary layer mesh is determined from the flat-plate boundary layer theory [57] so that y^+ value is greater than 30 and less than 300.

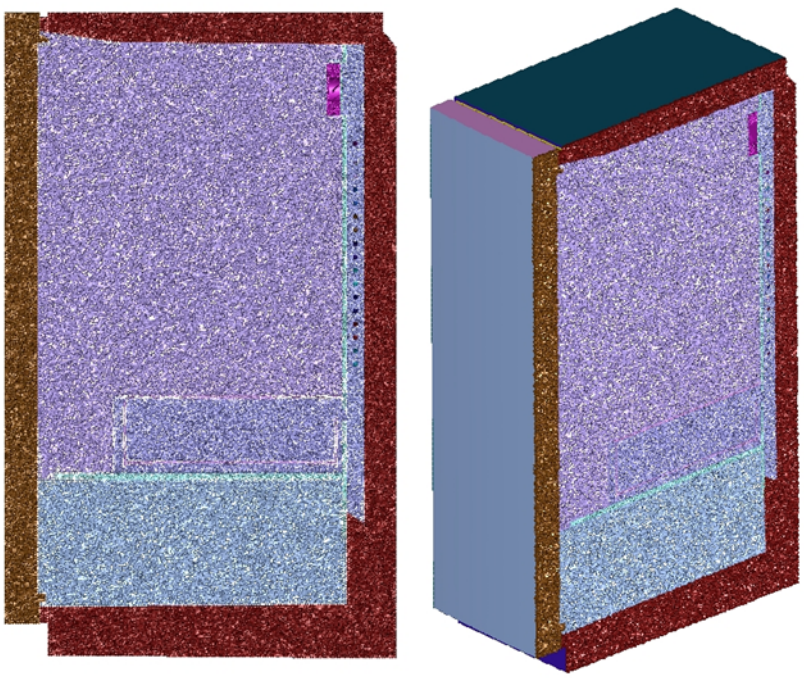

Figure 3.2. The mesh model of the geometry.

According to the flat-plate boundary layer theory, the grid calculation steps can be explained as:

1. The Reynolds number is calculated by:

$$Re = \frac{\rho U_\infty l}{\mu} \tag{3.1}$$

where ρ is free stream density, U_∞ is free stream velocity, l is reference length and μ is dynamic viscosity.

2. The skin-friction coefficient for turbulent flow is found by:

$$C_f = \frac{0.026}{Re_x^{1/7}}. \tag{3.2}$$

3. The wall shear stress is calculated by:

$$\tau_{wall} = \frac{C_f \rho U_\infty^2}{2} \tag{3.3}$$

where C_f is skin-friction coefficient, ρ is free stream density and U_∞ is free stream velocity.

4. The friction velocity is determined by:

$$U^* = \sqrt{\frac{\tau_{wall}}{\rho}} \tag{3.4}$$

where τ_{wall} is wall shear stress and ρ is free stream density.

5. The height of the first cell is expressed by:

$$\Delta s = \frac{y^+ \mu}{U^* \rho} \tag{3.5}$$

where y^+ is a non-dimensional distance, μ is dynamic viscosity, U^* is the friction velocity and ρ is free stream density.

To simulate air circulation, frame motion with the specified rotation axis origin, rotation axis and a rotational velocity is defined to fan domain. In order to generate different air flow rates, the fan rotation speed is defined as 2100, 1818 and 1515

rpm. The other parts which are polyurethane layer, air duct cover, shelf, bottom and top glasses and test package are specified as a solid domain. The surfaces meet each other are defined as interior surfaces. For the other surfaces come into contact with a solid region are defined as a no-slip boundary condition for the momentum and coupled boundary condition for the energy equation, except for fin-type evaporator surfaces. Fin-type evaporator surface thermal boundary condition is defined as time-dependent surface temperature and experimentally measured evaporator surface temperature value is prescribed. All outer shell surfaces such as the outer surfaces of door, cabin and gasket are defined as convection boundary condition with 10 $W/m^2.K$ heat transfer coefficient (HTC) and 298.15 K free stream temperature.

3.4. Thermal Properties of Materials

The thermal properties such density, specific heat and thermal conductivity of the materials which are used in this study are tabulated Table 3.1. It should be stated that dry air used as a simple fluid in this work and its properties are determined accordingly. The properties of test package except for density are defined as a function of temperature and they are described in experimental study section.

Table 3.1. The Thermal Properties of Materials. [1]

Material	**Density (kg/m^3)**	**Specific Heat (J/kg.K)**	**Thermal Conductivity (W/m.K)**
Glass	2,500	792	1.05
Plastic	1,413	1015	0.208
Polyurethane	31	1045	0.022
Tylose	941.4	Figure 4.10	Figure 4.11
Rubber	980	1,200	0.075
Metal Sheet	7,700	480	50

3.5. Numerical Calculation

A simulation of the freezing of beef inside a domestic refrigerator is done with ANSYS Fluent. This commercial CFD software utilizes the finite volume method. Since this problem is considered as an incompressible flow problem, pressure-velocity coupling solver with SIMPLE algorithm is preferred to make the calculation simpler. The momentum, turbulence and energy equations are discretized with a second- order upwind scheme. A fixed time step size of 30 seconds is used in the calculations. Convergence criteria for pressure, momentum, turbulence kinetic energy, turbulence dissipation rate and energy are determined as 10^{-3}, 10^{-3}, 10^{-3}, 10^{-3} and 10^{-8}, respectively. For the different simulation cases the same calculation procedure is followed. Since monitoring the residuals is not considered as a sufficient convergence criterion by the author, air flow rate, suction and blowing temperatures are drawn as a graph for a second verification as well.

4. EXPERIMENTAL STUDY

Experimental studies are conducted to not only verify the numerical results of the freezing process of beef but also obtain temperature profile of evaporator surface in this study. Since the researcher is interested in both phase change of beef and its cooled environment explicitly, the knowledge about environment of beef has a great importance to model this phenomenon accurately.

4.1. Introduction

In this section, what is made as the preparation before starting the experiments, what experiment setup is, how the experiment works, what the properties, abilities and/or error value of devices are and where thermocouples are placed to collect temperature data is explained in detail.

4.1.1. Experiment Setup

To carry out a reliable, scientific and controlled experiment, a domestic refrigerator from the inventory of Arçelik is obtained as it is shown on Figure 4.1. After the properties such as cooling capacity, compressor type, evaporator size, operating temperature range, flow rate, air duct design, and drawer design of the current refrigerator are evaluated thoroughly, it has been decided that some major modifications should be made physically.

Figure 4.1. A domestic refrigerator.

Firstly, since fresh food compartment of the refrigerator is utilized for experiments as a closed insulated partition, the cooling system has been built up from scratch as it is demonstrated on Figure 4.2. To decrease the air temperature to 298.15 K effectively, a new compressor which has higher capacity than the current and larger fin type evaporator instead of only tube evaporator have been preferred. In addition to that, a fixed speed compressor has been used to get rid of complex working algorithm. Coil type condenser with a fan has been implemented for increasing cooling performance instead of a static condenser. Because this cooling system has not been experienced yet, sensitive adjustable expansion valve is assembled in addition to the capillary tube. After a few trials, amount of refrigerant which is isobutane (R600a) has been determined. While the amount of refrigerant and the expansion valve were being adjusted, two things were paid attention. The first one was that refrigerant should be kept at two-phase throughout evaporator in order to reduce temperature difference

among evaporator passes. The second was that refrigerant exiting from evaporator should be completely vapor phase before entering the compressor in order to protect compressor from liquid leakage. These sensitive adjustments have been done manually by controlling temperature data which is obtained from thermocouples fixed on cooling components and comparing them with theoretical cooling calculation for isobutane.

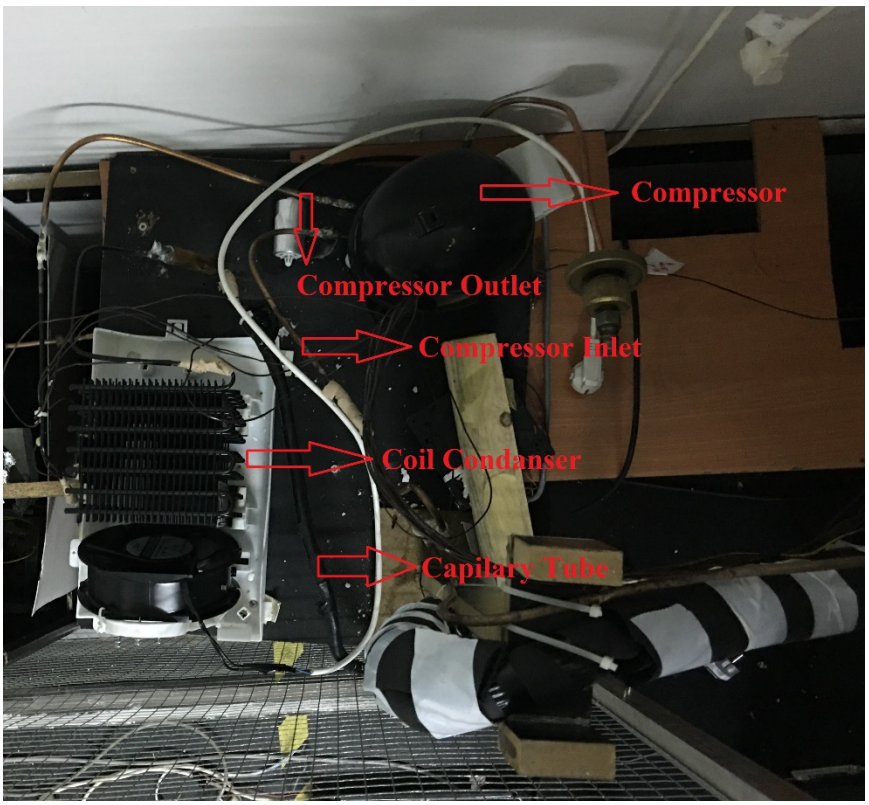

Figure 4.2. Separate cooling system.

Secondly, air duct design which includes blowing and suction openings' size, shape and position, and shelf design which includes its material, size, position and shape have been updated as they are illustrated on Figure 4.3.

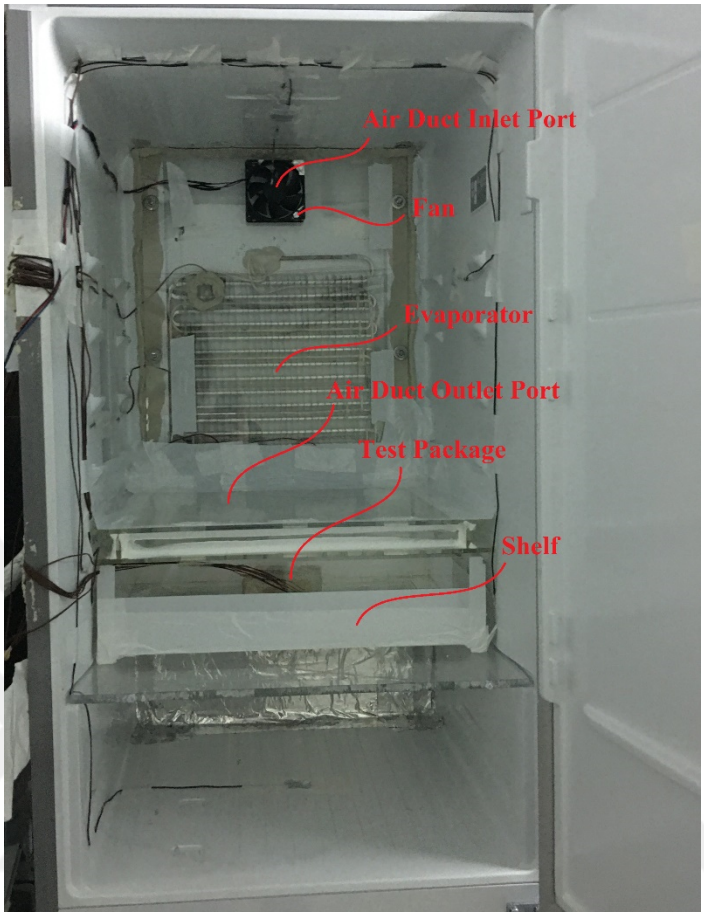

Figure 4.3. The design of the experiment refrigerator.

Since blowing type and air velocity or flow rate are parameters which may have impact on freezing of beef investigated, two different type air channels and PWM fan shown on Figure 4.4 have been produced and assembled. In order to bring fan speed into desired RPM, it is driven with A-UDAQ (Arçelik Universal Data Acquisition & Network) which is a program for administration of an electronic card including PWM algorithm.

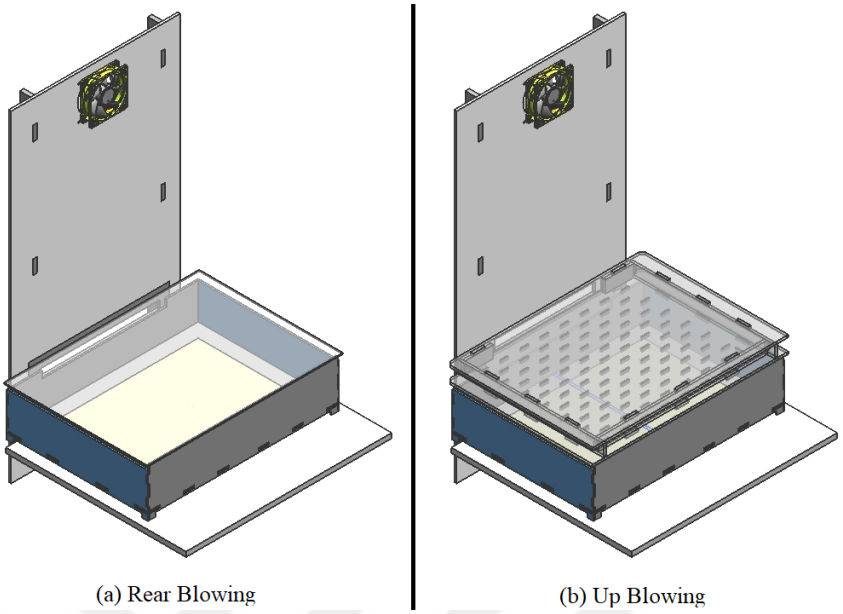

Figure 4.4. Blowing Methods, (a) Rear Blowing and (b) Up Blowing.

Thirdly, the test package that simulates beef has been prepared. It is mainly composed of water, ethyl methyl cellulose and sodium chloride. A standard test package is a rectangular prism, but it has been converted into square prism in order to reduce the time of experiments and simulations. After test package is cut into the desired size (100x100x50 mm), thermocouples have been placed, and it is wrapped with a thin plastic layer to obstruct mass exchange with air inside refrigerator.

In this study, Keysight 34970A Agilent Data Logger has been used to process and collect temperature data. Then, the data are transferred to the test computer through a data cable. To make environment stable in terms of temperature and humidity, the controlled test room in Arçelik RD center has been utilized. The test room temperature fluctuation is ± 1.5K. As a precaution against power failure, cooling and measurement system have been plugged in UPS system like the test room.

4.1.2. Thermocouple Layout

Another subject about experimental study is related to where thermocouples should be for air side, test package and cabin. In the following to generate more readable and understandable graphs, all thermocouple data are not included intentionally. However, all numerical and experimental data of the 1st case is given in Appendix B. In this study, T type thermocouple is used and the measurement uncertainty of it has been obtained from Central R&D calibration center database as ±0.6K. The thermocouples are divided into clusters according to their region and/or duty. These groups are:

I.The thermocouples in test package

II.The thermocouple in inside air

III.The thermocouple in environment air

IV.The thermocouple on cooling system

V.The thermocouple on wall

The first group which is shown on Figure 4.5 has been placed to inside of the test package in order to measure temperature locally and so the impact of parameters such flow rate or air velocity, blowing method and shelf design on phase change could be revealed.

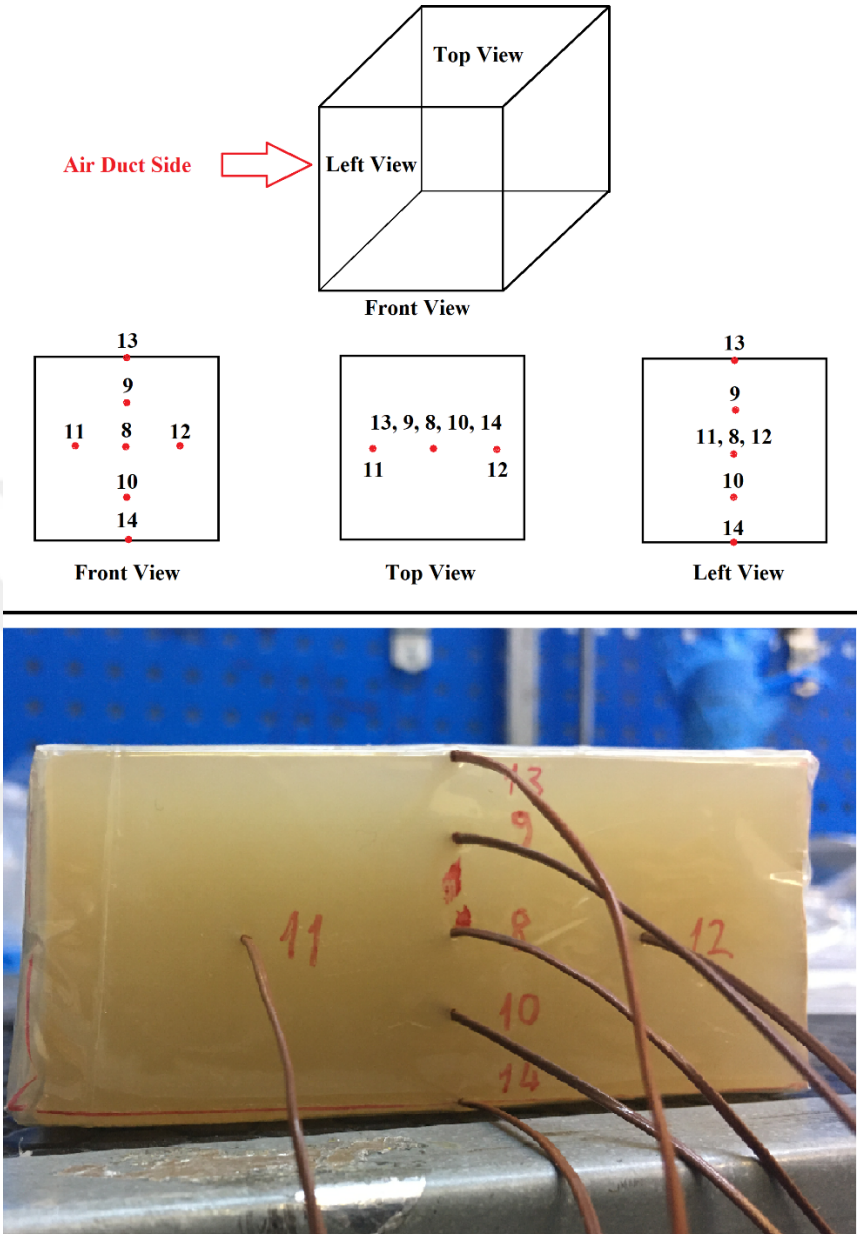

Figure 4.5. Thermocouple Layout Inside Test Package.

The second group which is illustrated on Figure 4.6 has been placed near the suction and blowing ports in order to measure blowing and suction air temperature. Further, these values have been utilized to verify the heat gain calculation from air side by comparing with the second heat gain calculation from cooling system side.

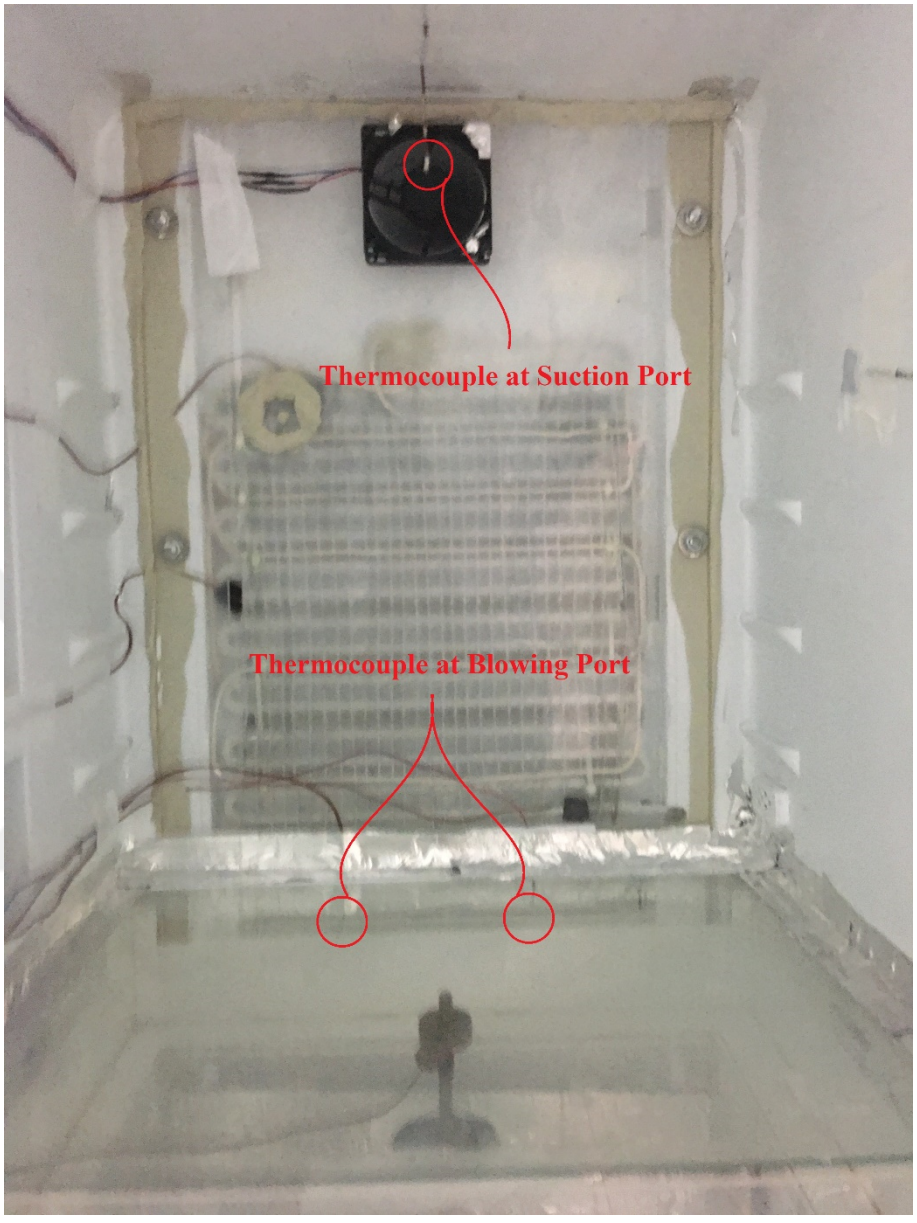

Figure 4.6. Thermocouple Layout Inside Air.

The third group which is demonstrated on Figure 4.7 has been placed in the test room air in order to measure environment temperature.

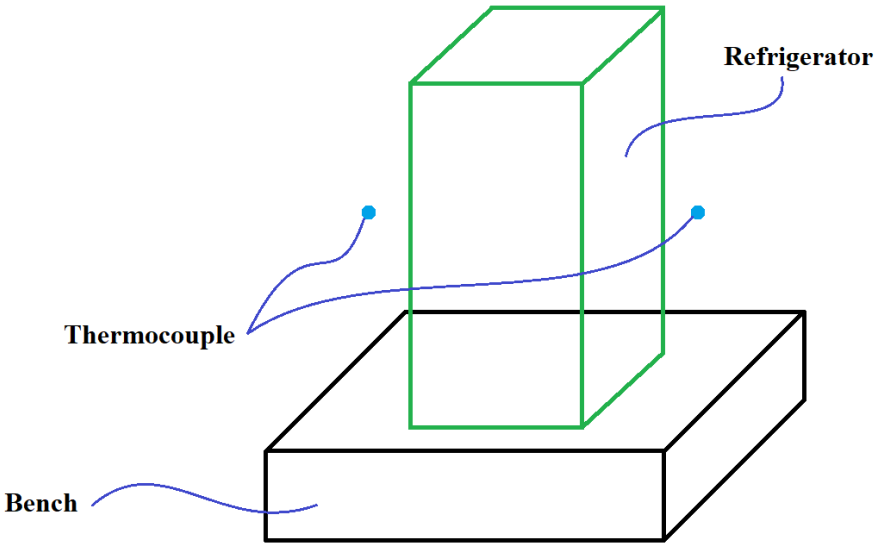

Figure 4.7. Thermocouple Layout Inside Test Room.

The fourth group which is indicated on Figure 4.8 has been placed on cooling system components in order to check whether cooling system works properly or not. Furthermore, transient local temperature data from evaporator surface are used to obtain a time dependent temperature function which is used as the thermal boundary condition on evaporator surface in the calculation.

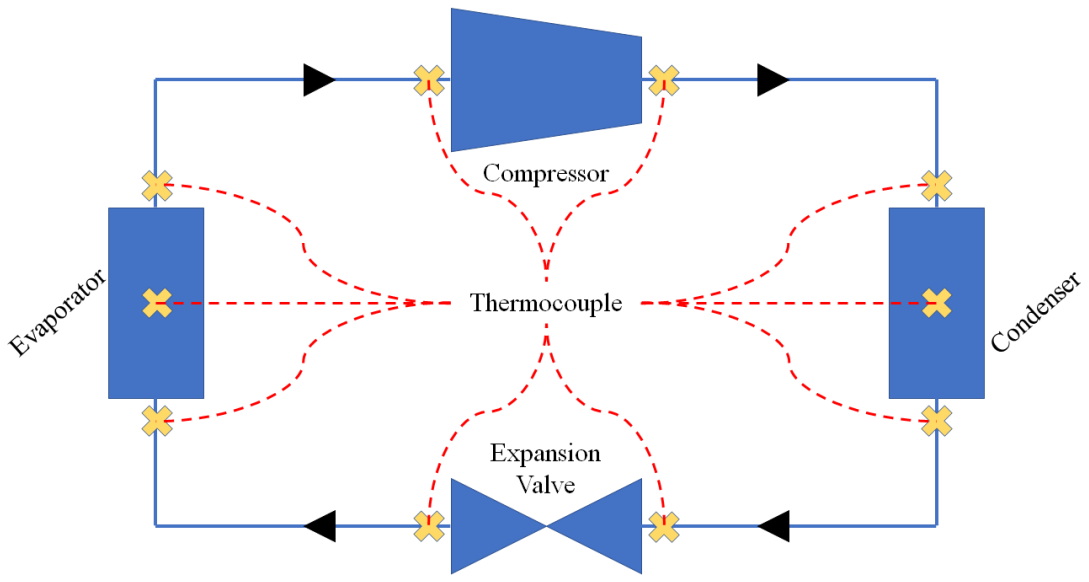

Figure 4.8. Thermocouple Layout on Cooling System.

The fifth group has been placed on the inside and outside walls of refrigerator in order to determine convective heat transfer coefficient which is used to define the boundary condition of outer walls of refrigerator with conservation of heat flux through wall and to provide verification knowledge for heat gain calculation.

4.2. Experiments

In this study, three different types of experiments have been conducted to validate the numerical analysis. These experiment groups are temperature measurement, flow rate measurement and determination of thermal properties of test package, respectively. It should be stated that triple control experiments have been performed to validate whether measurement systems for all experiments are reliable or not before starting the real experiments.

4.2.1. Temperature Measurement Experiments

This group experiments are conducted to obtain the temperature data of specified region. Since the procedure of experiments has been explained at the previous section, only the planned experiments are tabulated in this part as in Table 4.1.

Table 4.1. The Temperature Measurement Experiments List.

Case Number	**Fan Speed (RPM)**	**Blowing Direction**	**Shelf Design**
1	2,100	Rear	Plastic
2	1,818	Rear	Plastic
3	1,515	Rear	Plastic
4	2,100	Rear	Hybrid
5	1,818	Rear	Hybrid
6	1,515	Rear	Hybrid
7	2,100	Rear	Metal
8	1,818	Rear	Metal
9	1,515	Rear	Metal
10	2,100	Up	Plastic
11	1,818	Up	Plastic
12	1,515	Up	Plastic
13	2,100	Up	Hybrid
14	1,818	Up	Hybrid
15	1,515	Up	Hybrid
16	2,100	Up	Metal
17	1,818	Up	Metal
18	1,515	Up	Metal

4.2.2. Flow Rate Measurement

As it can be understood from the heading of this group, these experiments are performed to measure flow rate of the system at different fan speeds. To achieve that, the wind tunnel of Fluid Dynamics Division in Arçelik R&D center, which was constructed according to AMCA 210-15 Standards, has been utilized. The measurement

uncertainty for volumetric flow rate is given in Appendix C. As it is shown on Figure 4.9, these experiments have been completed for both types of blowing design at three different fan RPMs. Therefore, the results of the numerical analysis could be compared with experimental results in terms of flow rate, in addition to thermal comparison. The flow rate measurement experiments are tabulated in Table 4.2.

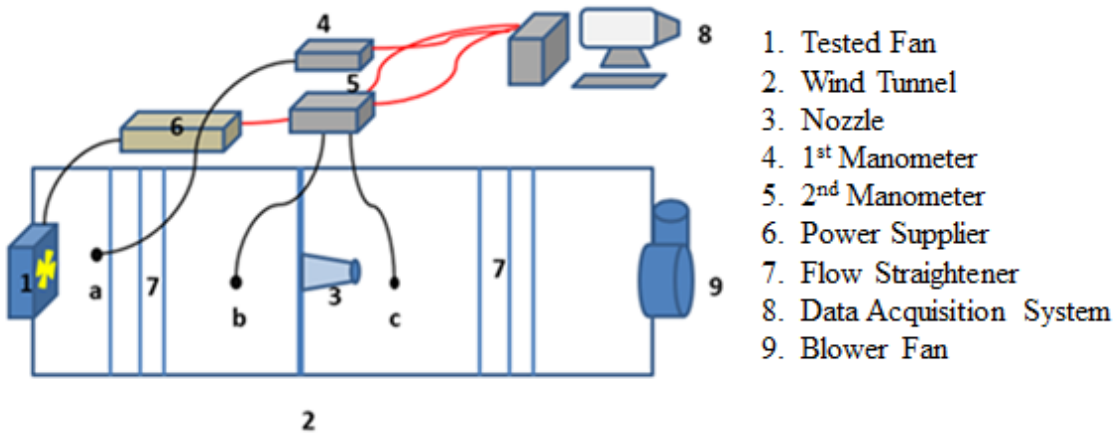

Figure 4.9. Wind Tunnel for Air Flow Rate Measurement.

Table 4.2. The Air Flow Rate Measurement Experiments List.

Case Number	**Fan Speed (RPM)**	**Blowing Direction**	**Air Flow Rate (l/s)**
19	2,100	Rear	7.67
20	1,818	Rear	6.48
21	1,515	Rear	5.34
22	2,100	Up	7.48
23	1,818	Up	6.37
24	1,515	Up	5.19

4.2.3. Determination of The Thermal Properties of Test Package

As it has been stated at the beginning of the thesis, the thermal properties such thermal conductivity and specific heat of the test package which simulates the beef is obtained experimentally in this study. Differential scanning calorimetry (DSC) and hot plate method are used to determine the specific heat and thermal conductivity, respectively.

DSC is a significant method to define the specific heat of a material as a function of temperature. It was built up by E. S. Watson and M. J. O'Neill. Basically, this method calculates the amount of heat which is necessary for raising the temperature of the material according to reference measurement or material system and then, finds the specific heat of the material by processing the collected data. The author has obtained the apparent specific heat of the test package by utilizing Q200 Differential Scanning Calorimeter (DSC) by TA Instruments ($\pm 0.1\%$). The results of measurements are demonstrated in Figure 4.10. A piecewise polynomial fit to data is generated and is used in the numerical simulations. The tabulated data of the apparent specific heat depending as a function temperature of the test package are given in Appendix A.

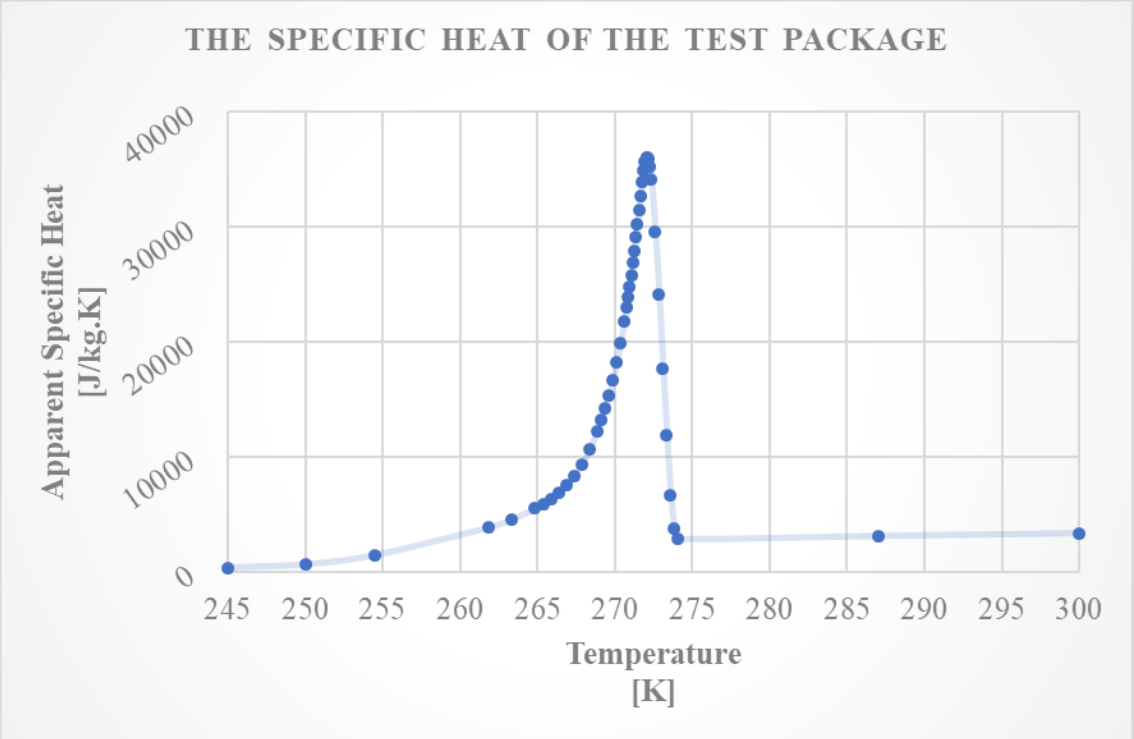

Figure 4.10. The Apparent Specific Heat of The Test Package.

Secondly, hot plate method or heat flux method is a fundamental method to measure the thermal conductivity of a material as a function of temperature. This method is based on heat flux measurements and it calculates the thermal conductivity with measured heat flux and temperature data. In this study, a FOX 314 Heat Flow Meter by TA Instruments ($\pm 1\%$) is utilized, and the thermal conductivity of the test package is determined as it is shown on Figure 4.11. The data is used in the numerical simulations. The tabulated data of the thermal conductivity depending on temperature of the test package are given in Appendix A.

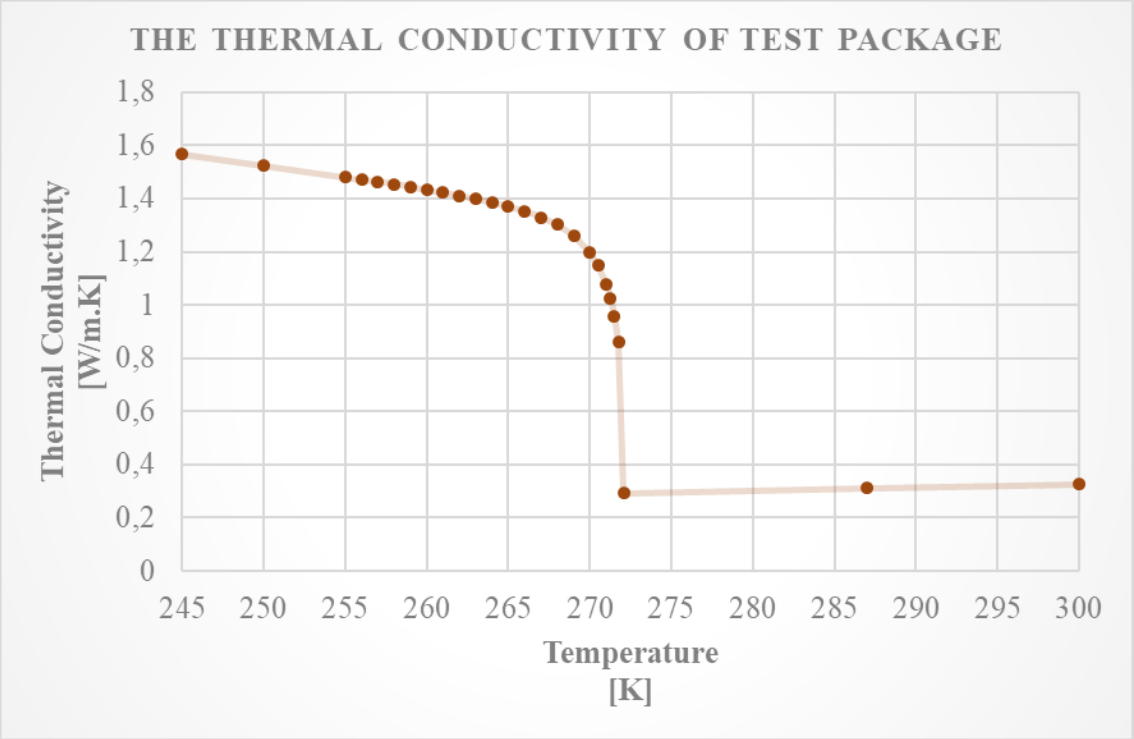

Figure 4.11. The Thermal Conductivity of The Test Package.

5. RESULTS AND DISCUSSION

In this part, numerical results and experimental measurements are shown and discussed in detail. The simulation of phase-change in beef is compared with experimental data and the effect of the parameters on freezing process is evaluated.

5.1. The Evaluation of The Phase Change Process inside Beef

To generate more comprehensive assessment for freezing of beef, different types of comparison are drawn in this part. The cases investigated in this study are interpreted in terms of freezing time. To make a meaningful examination or to normalize all data, freezing process is restricted from 293.15 K to 253.15 K and the time measured experimentally is compared with the time calculated numerically as it is tabulated in Table 5.1. When the Table 5.1 or Figure 5.1 is read in detail, it may be seen that the apparent heat capacity method for freezing of beef inside domestic refrigerator provides reliable results. The percentage error (PE) does not exceed 6.59% and the average of the PE for all cases is 3.47%. When the temperature fluctuation of test room ($\pm$1.5K), and the measurement uncertainty of the thermocouple ($\pm$0.6K) are taken into account, the numerical results are good enough.

Table 5.1. The Comparison Between Numerical Calculation and Experimental Measurement for Freezing Time.

Case	**Experimental Freezing Time (s)**	**Numerical Freezing Time (s)**	**Percentage Error (%)**
1	23,100	22,470	2.73
2	23,970	24,570	2.5
3	24,720	25,380	2.67
4	18,690	19,500	4.33
5	19,110	19,620	2.67
6	19,740	20,280	2.74
7	20,520	19,710	3.95
8	20,940	20,430	2.44
9	21,180	20,940	1.13
10	27,330	25,980	4.94
11	27,990	26,520	5.25
12	29,520	27,900	5.49
13	20,610	20,280	1.6
14	20,760	20,520	1.16
15	21,690	21,990	1.38
16	22,290	20,820	6.59
17	22,110	20,880	5.56
18	22,200	21,000	5.41

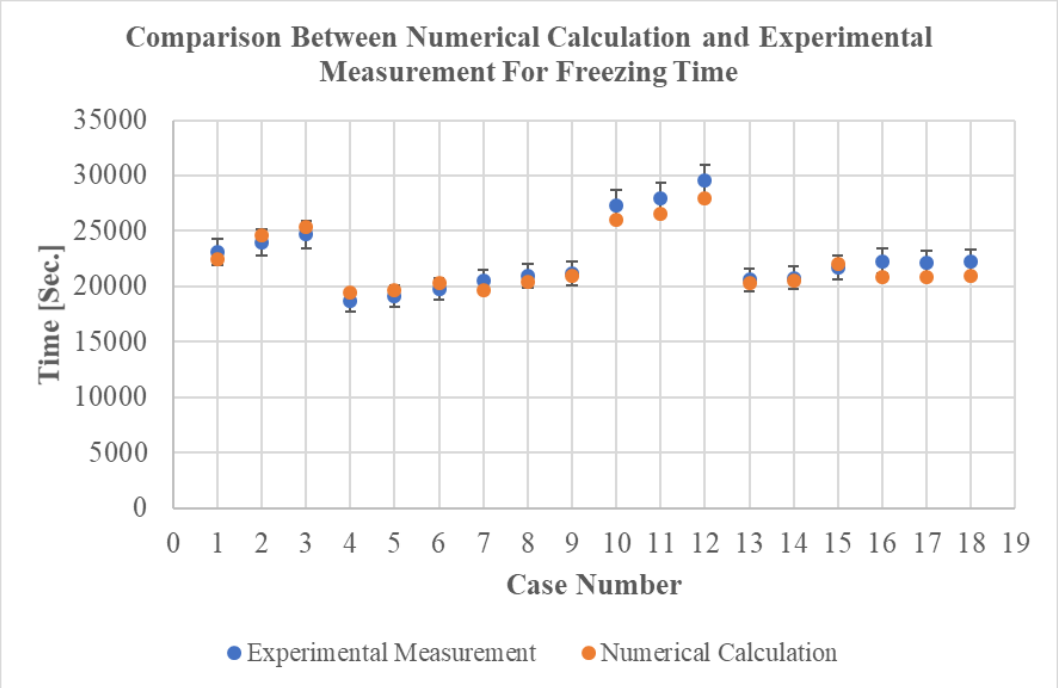

Figure 5.1. Comparison Between Numerical Calculation and Experimental Measurement for Freezing Time (Vertical Line shows the 5% error).

The second detailed assessment is carried out in terms of temperature profile inside the test package. The aim of this comparison is to reveal the capability of numerical analysis, the thermocouple data chosen for evaluation is from the 8th point which is placed at the center of the test package. The temperature trace at the center for the best and worst cases (in terms of PE of freezing time predictions) is illustrated on Figure 5.2 and Figure 5.3, respectively, instead of all cases. The solid line, dash line and vertical bar represent the experimental result, the numerical result and the 1 percentage error (PE), respectively. If these two graphs are examined, numerical results pretty well comply with experimental results for even the worst case of determination of freezing time since numerical results are within 1% error range as seen in Figure 5.2 and 5.3. Therefore, numerical results are quite reliable for assessment of freezing process of food even for the worst case.

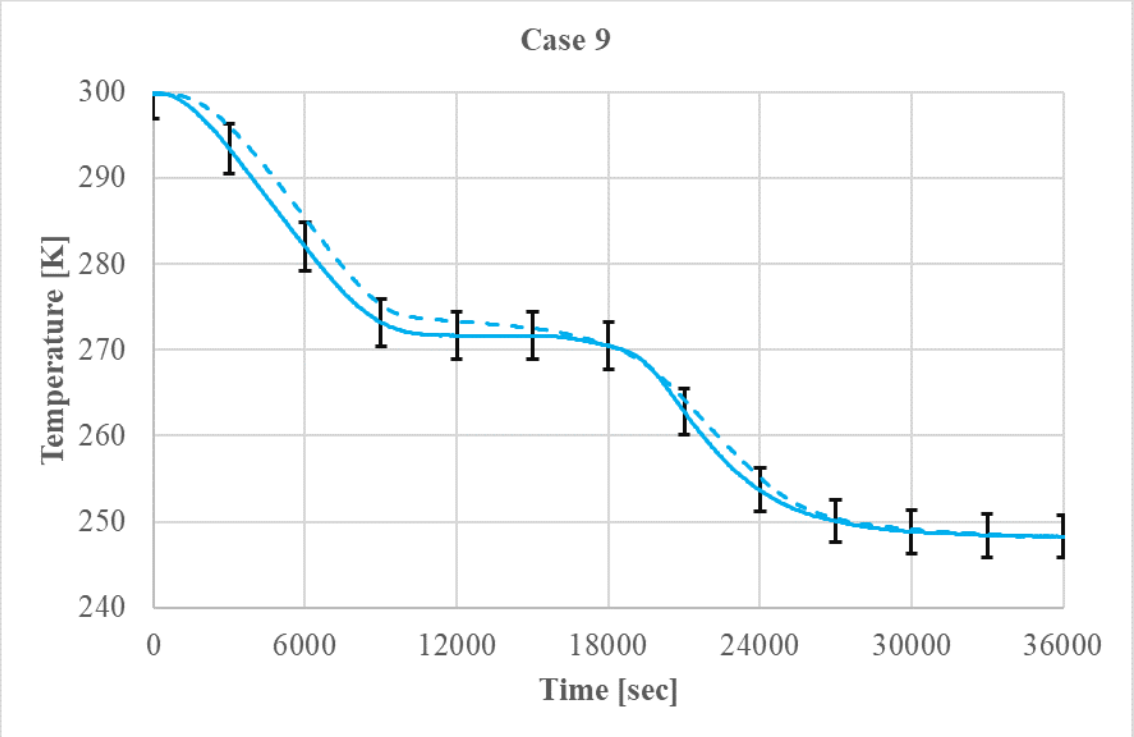

Figure 5.2. The Temperature Profile at The Center of Test Package for The Best Case.

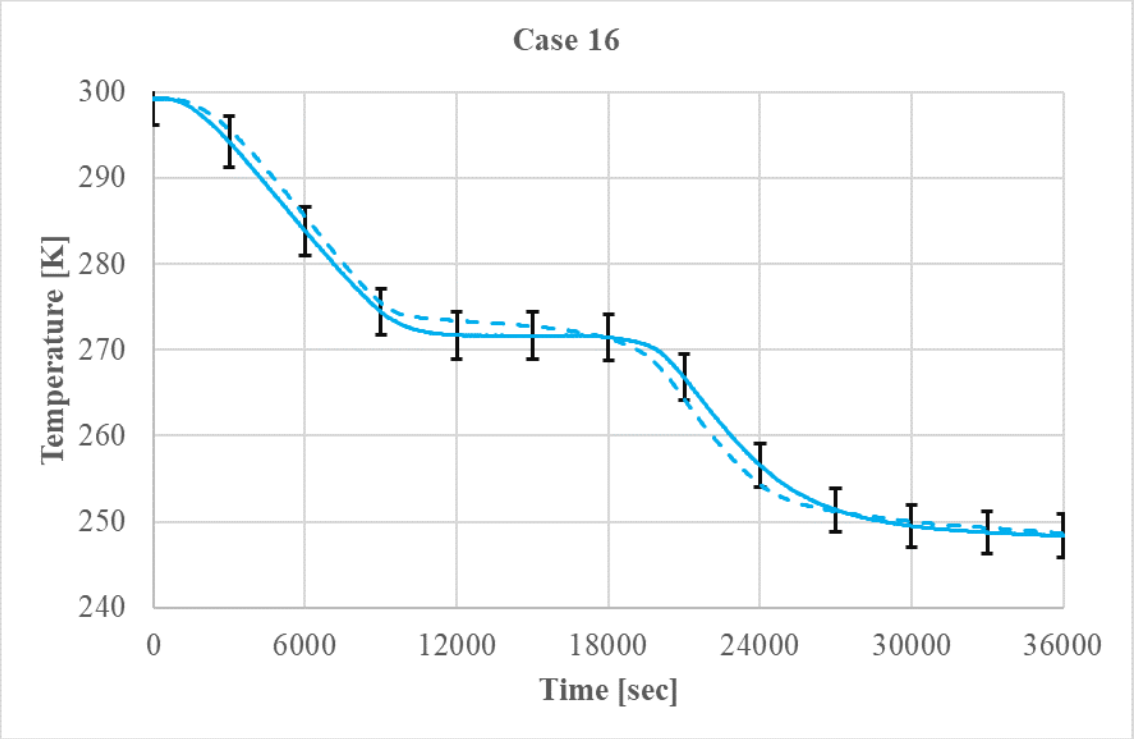

Figure 5.3. The Temperature Profile at The Center of Test Package for The Worst Case.

On the other hand, the comparison and evaluation of the present study with the others published in literature are considered as a double-check chance by the author. Huan et al. [31] reported 8.68% PE maximum error in freezing time predictions. Santos et al. [28] concluded that mean absolute error of temperature prediction is 1.7 K for a published case with good agreement, the lowest and the highest mean absolute error of temperature prediction is equal to 0.41 K and 2.16 K this study, respectively. In addition to those, Dima et al. [26] reported that the root mean squared errors (RMSE) of temperature predictions are between 1.5 K and 2.64 K, respectively. In this study the lowest and the highest RMSE of temperature predictions are 0.62 K and 2.64 K. All the error values for 8^{th} point are given in Table 5.2. These observations validate that the apparent specific heat method is able to produce accurate results.

Table 5.2. The Error Calculation for The Temperature Data of The 8th Point of The Test Package.

Case Number	**Mean Absolute Error (K)**	**Max. Absolute Error (K)**	**Root Mean Squared Error (K)**
1	1.11	1.91	1.23
2	1.16	3.89	1.57
3	2.16	5.82	2.64
4	1.3	3.52	1.64
5	1.9	6.22	2.56
6	1.73	5.07	2.27
7	0.98	2.27	1.18
8	0.9	2.38	1.12
9	1.19	3.41	1.59
10	1.2	2.82	1.43
11	1.17	2.59	1.37
12	0.94	2.18	1.11
13	1.04	2.22	1.18
14	0.41	1.68	0.62
15	1.36	3.91	1.69
16	1.11	2.68	1.32
17	0.99	2.27	1.19
18	0.94	2.03	1.07

5.2. The Evaluation of The Effect of The Air Flow Rate on Phase Change Process

As it is mentioned in the objectives of the present study, a parameter investigated is the air flow rate or the air velocity since the quality of frozen beef directly depends

on it. Though food engineers focus on frozen product quality in detail, mechanical engineers should know the fundamental of this issue to design optimum cooling system. When the studies about the quality of frozen product is looked for in the literature, there are different types of quality measurement for frozen food. Yet, the author considers on only drip loss superficially as a quality attribute. Firstly, this term could be simply defined as the amount of irreversible water thrown away during thawing process [58]. Since not only water but also beneficial material such as vitamins, minerals, etc are lost, drip loss is an important parameter for quality measurement. The studies in the literature show that drip loss is directly proportional to nucleation formation because large and few ice crystal formations mean more drip loss, while small and many ice crystal formations mean less drip loss [9,59]. Since small and multiple crystals could be obtained with high cooling rate, air flow rate has a great role in phase change. It could be concluded that high quality freezing process in terms of drip loss is provided by high flow rate. On the other hand, a user might be satisfied because foodstuff could be frozen in a short time. However, when the energy consumption of the fan is considered for one-year period, it has a great impact on energy label of the refrigerator even if the fan consumes a low amount of energy in comparison to other components such as compressor and defrost heater. As a result, it is an optimization issue between quality and sustainability for an industrial application.

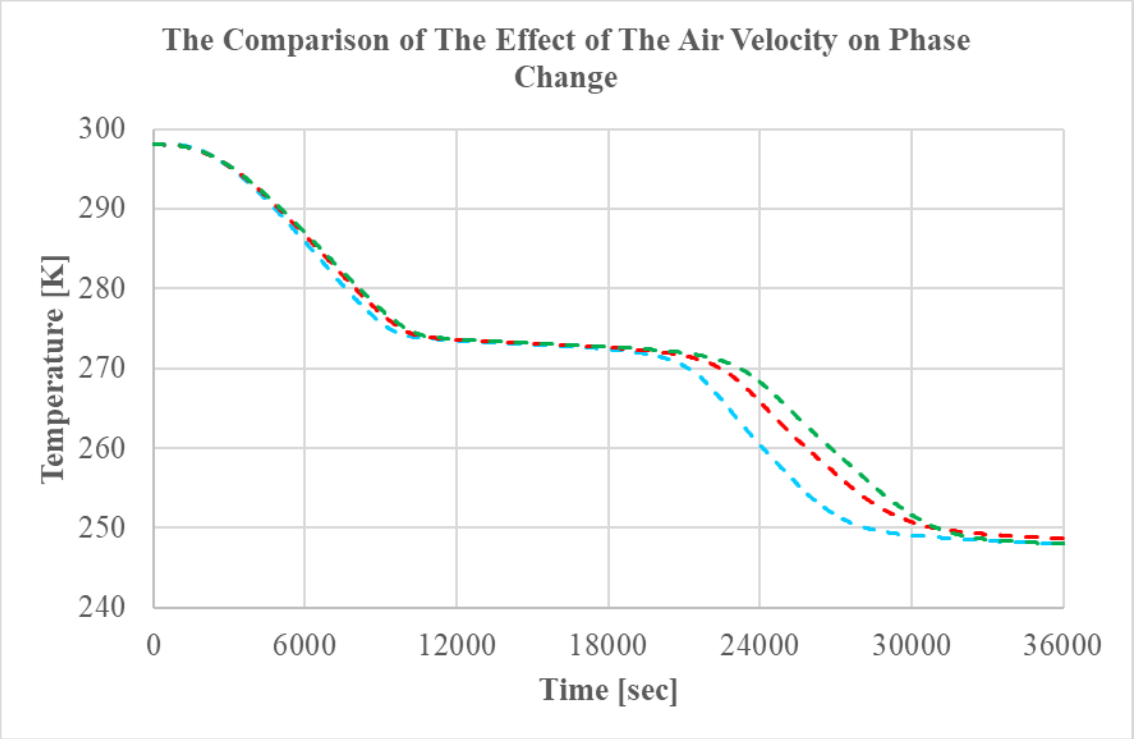

Figure 5.4. The Comparison of The Effect of The Air Velocity on Phase Change.

To demonstrate the influence of the air velocity on the freezing time, the Case 1, 2 and 3 are chosen to be compared with each other. In addition to understanding the effect of the air velocity with this comparison, simulations will again be verified with a cross validation between numerical calculation and experimental measurement one more time. When required time for freezing for case 1, 2 and 3 are read from Table 5.1, it could be easily concluded that the higher air flow rate, the faster the freezing. In the simulations when the fan speed is reduced by 13.43% and 27.86%, freezing times increase 8.90% and 12.95%. In the experiments the freezing time increase are 3.77% and 7.02%. Furthermore, time trace of the temperature in the center (which is 8^{th} point and is illustrated on Figure 4.5) of test package are drawn in Figure 5.4 where the red, blue and green dash lines represent the numerical results of case 1,2 and 3, respectively. Comparison of numerical calculations and experimental measurements of temperature traces at the center of the specimen are given in Figure 5.5, 5.6 and 5.7. The solid lines and vertical bars show the experimental measurement and the 1 percentage error, respectively.

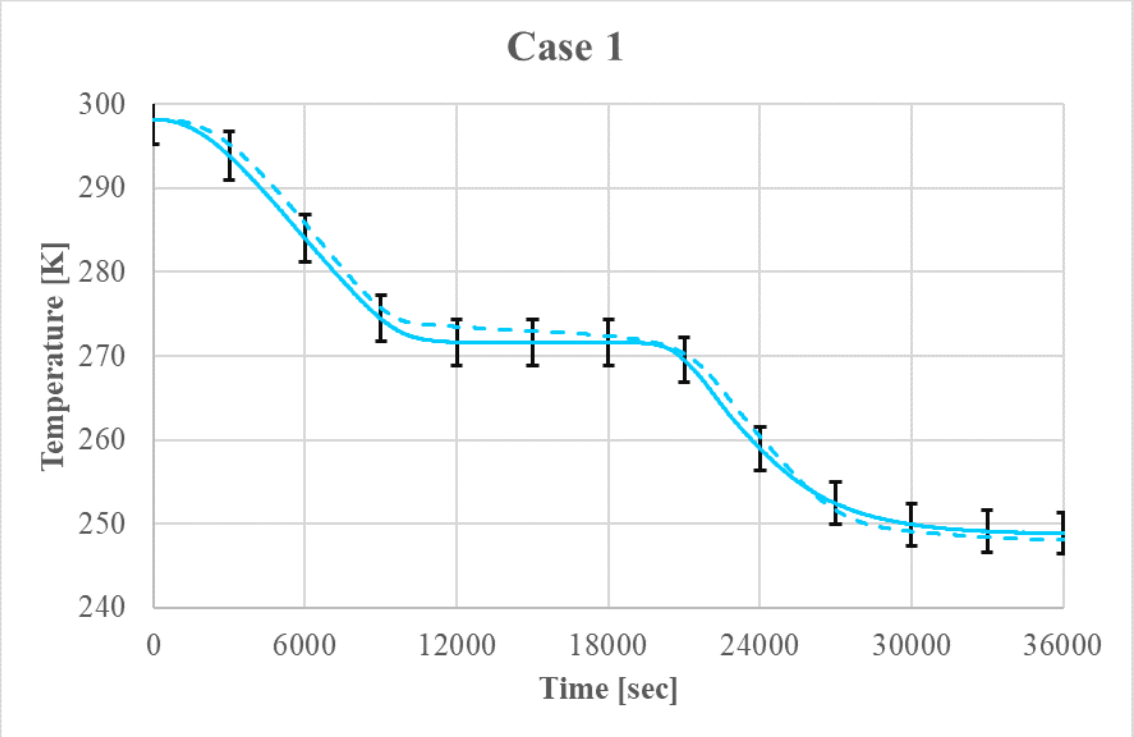

Figure 5.5. The Experimental and Numerical Results for Case 1.

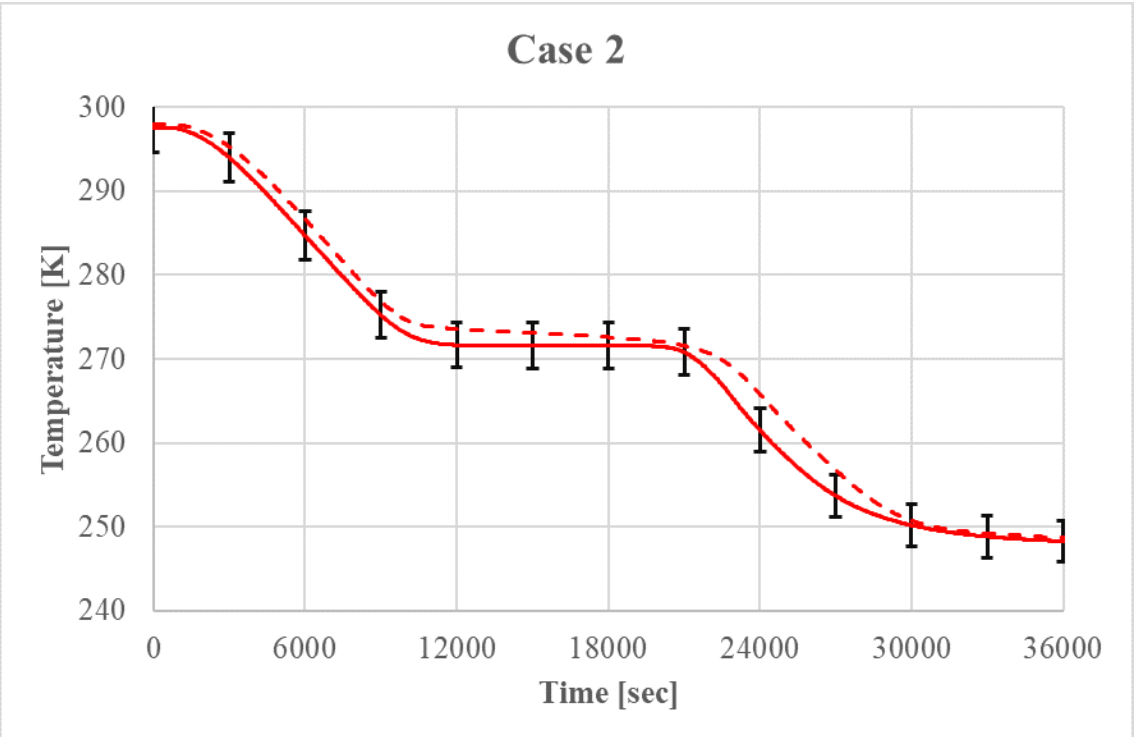

Figure 5.6. The Experimental and Numerical Results for Case 2.

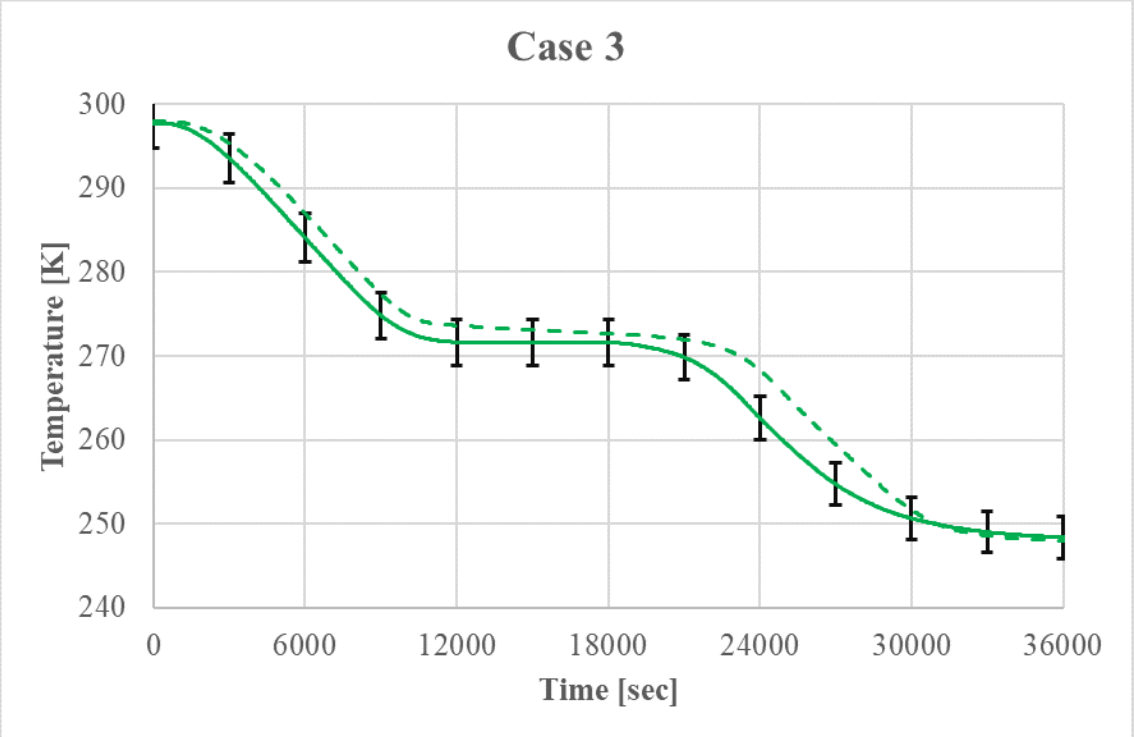

Figure 5.7. The Experimental and Numerical Results for Case 3.

5.3. The Evaluation of The Influence of The Blowing Type on Freezing Process

In this part, the effect of the blowing type is wanted to be revealed explicitly. To analyze that impact thoroughly and consider a different case from the previous cases, 6^{th} and 15^{th} cases are chosen particularly. Yet, data in Table 5.1 show that the blowing method from top side requires more time than the blowing from rear side when the center temperature of the test package is considered. As in the former examinations, the results will be demonstrated experimentally for influence of blowing type and numerically for reliability of CFD.

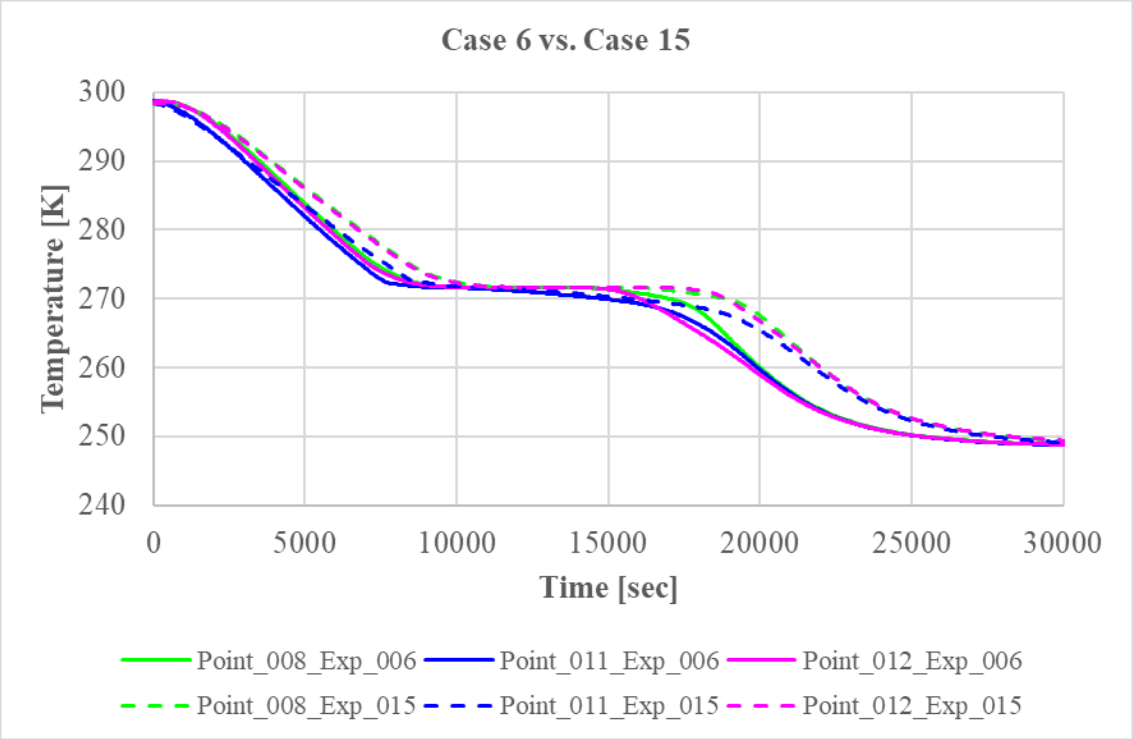

Figure 5.8. The Comparison of The Experimental Results of Case 6 & Case 15.

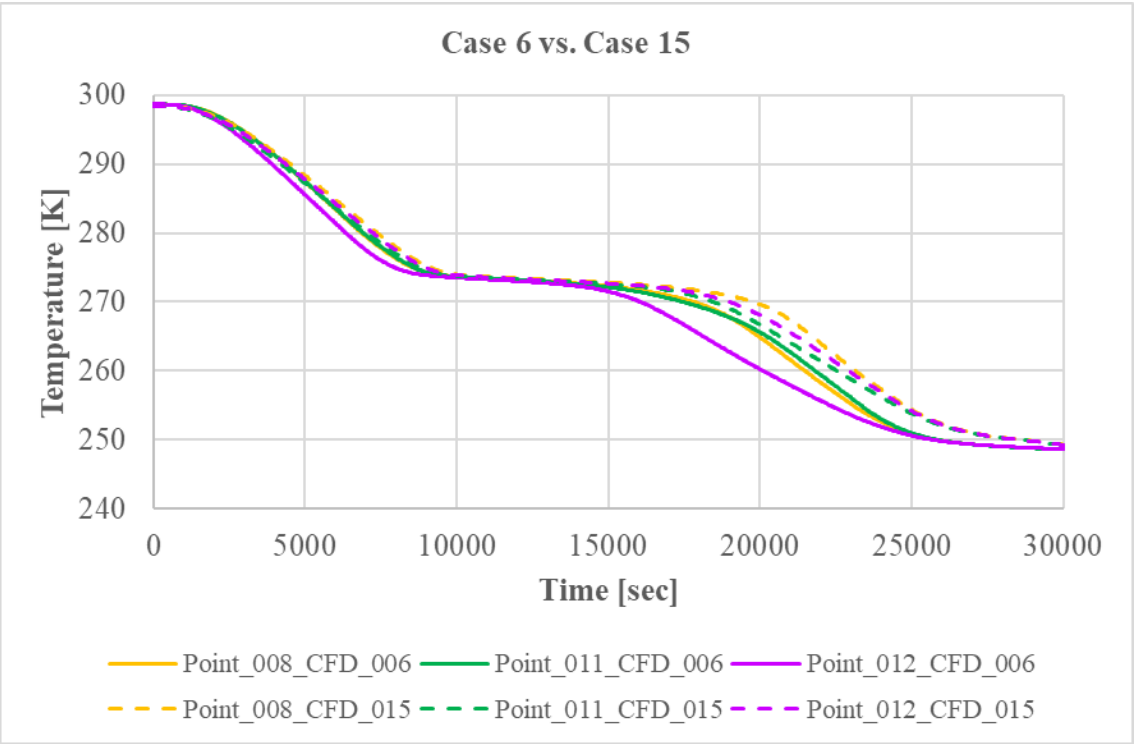

Figure 5.9. The Comparison of The Numerical Results of Case 6 & Case 15.

Since it is believed that the effect of the blowing methods can be observed from 8^{th}, 11^{st} and 12^{nd} thermocouples (where they are placed is shown on Figure 4.5), the curves are drawn accordingly in Figure 5.8 and Figure 5.9. The first thing which could be said that rear blowing method requires less time for freezing. Secondly, the trace of the temperature of the 12^{nd} point for 15^{th} case is smoother than the trace of the temperature of the 12^{nd} point for 6^{th} since the air is excessively not piled into the front of the shelf for the former, which is shown on Figure 5.10 and 5.11. In other words, the homogeneous temperature gradient inside the test package is provided by the top blowing method, while faster freezing is obtained with the rear blowing method.

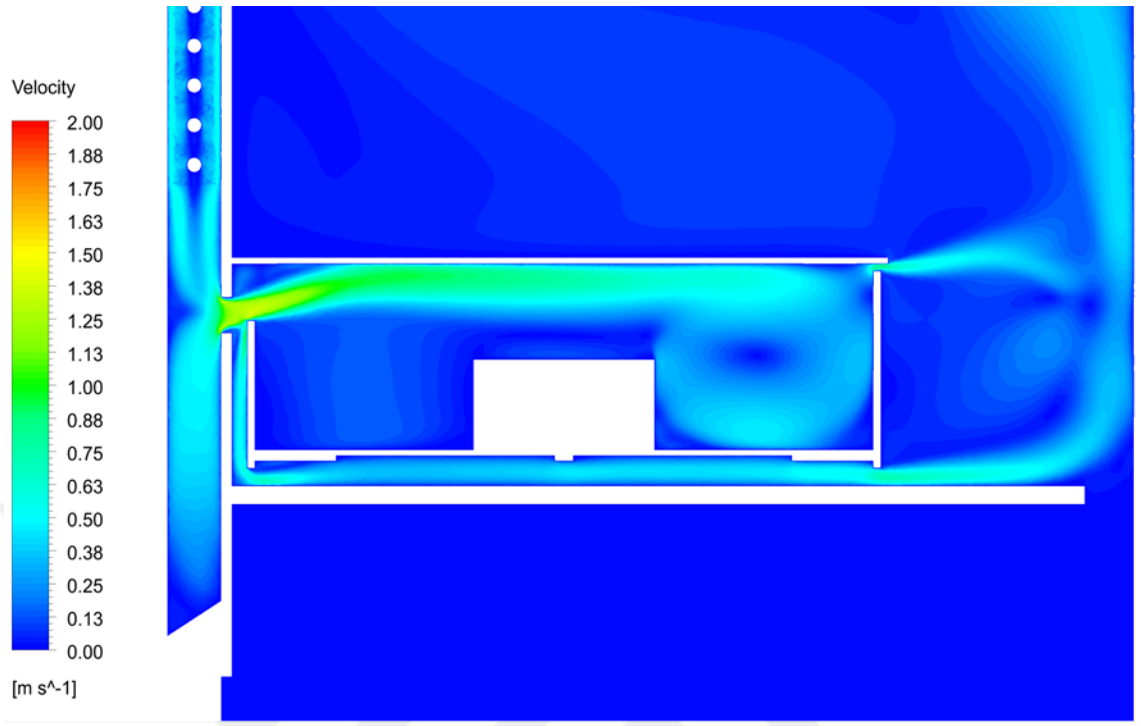

(a) Case 6

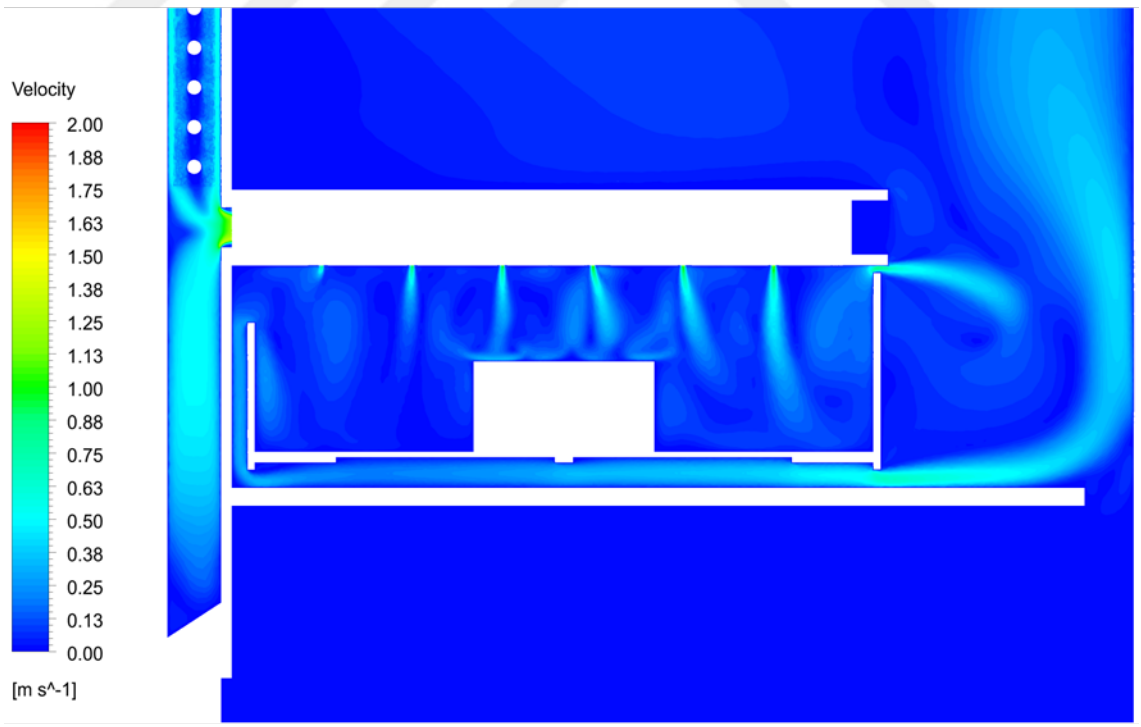

(b) Case 15

Figure 5.10. The Comparison of The Numerical Results of Case 6 & Case 15.

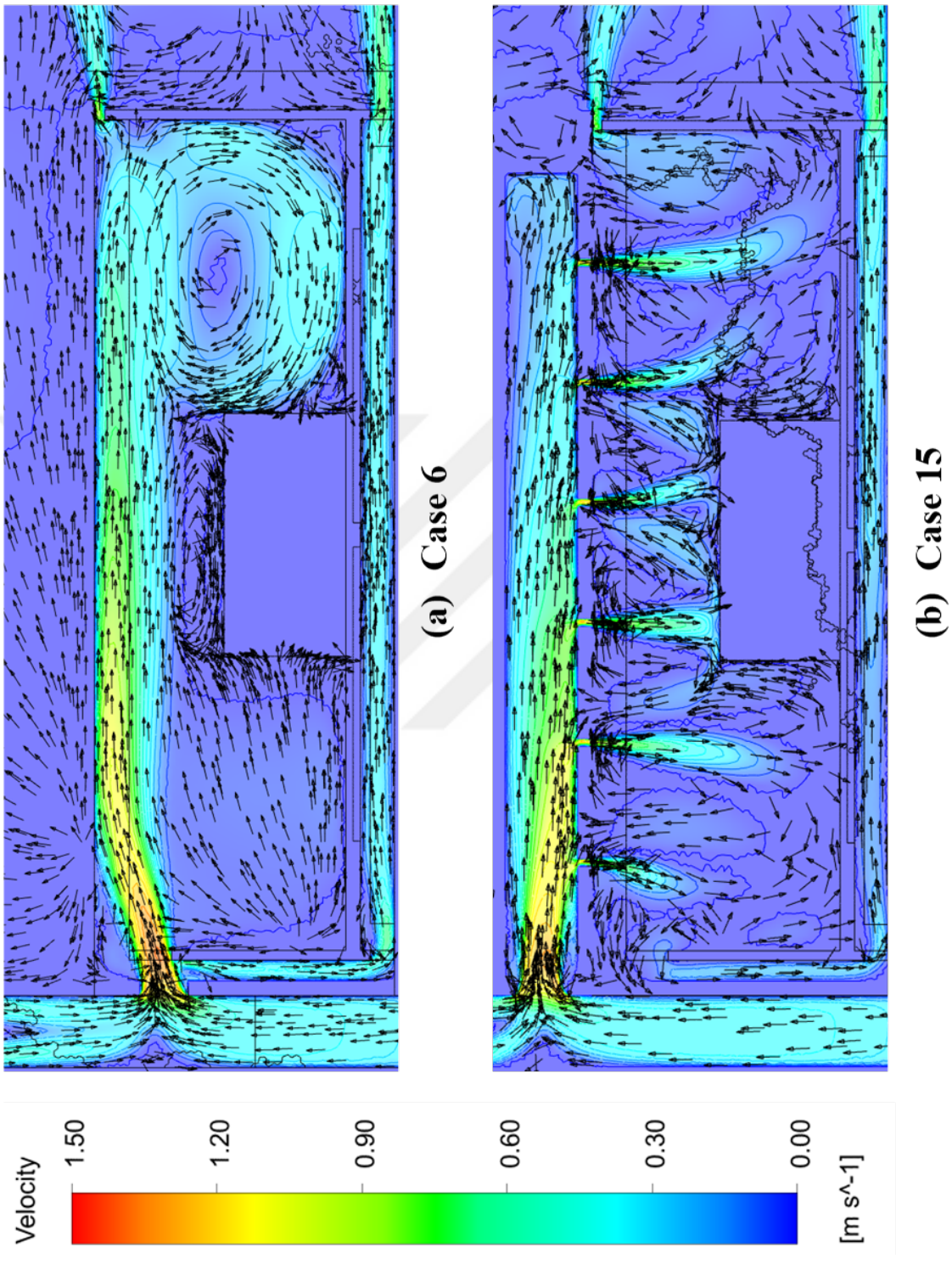

Figure 5.11. The Velocity Contour and Vector of Case 6 (a) & Case 15 (b).

5.4. The Evaluation of The Impact of The Shelf Design on Phase Transition

In this section, the effects of the shelf design and shelf material are examined in detail. To show shelf effect and the reliability of CFD calculations, different cases are reviewed. Further the comparison of conduction and convection heat transfer is also possible. The first evaluation is made according to freezing time from Table 5.1. When the freezing time of 10^{th}, 13^{rd} and 16^{th} cases are read from the Table 5.1, freezing process for plastic shelf takes the most time numerically and experimentally. The bottom wall of the shelf, which is located between the bottom surface of test package and the cooling air going from under shelf, behaves like a resistance due to low thermal conductivity of the plastic material. Therefore, it should be concluded that using more conductive material like metal for shelf decreases the freezing time of the test package since conduction heat transfer rate from the bottom surface of the test package to the bottom surface of the shelf will be increased, which could be observed from the temperature change of 8^{th} point in the test package as it is shown on Figure 5.12 and Figure 5.13, experimentally and numerically. In addition to that, when temperature gradient on the middle plane of the test package is assessed from Figure 5.14, the effect of the conduction heat transfer could be recognized easily (Besides, the temperature distribution in test package is given with partial scale in Appendix D to show it in detail). On the other hand, considering the amount of heat that needs to be transferred to freeze the test package is the same for all the cases studied, the summation of the conduction heat transfer from the test package to shelf via its bottom surface and the convection heat transfer from the test package to air via its other surfaces must be constant. According to this, if there is no change in the properties of air such as velocity and temperature but, the freezing time of the test package is shortened, it could be explained by the fact that the amount of heat transferred by conduction increases, while the amount of heat transferred by convection decreases to preserve the total amount of heat.

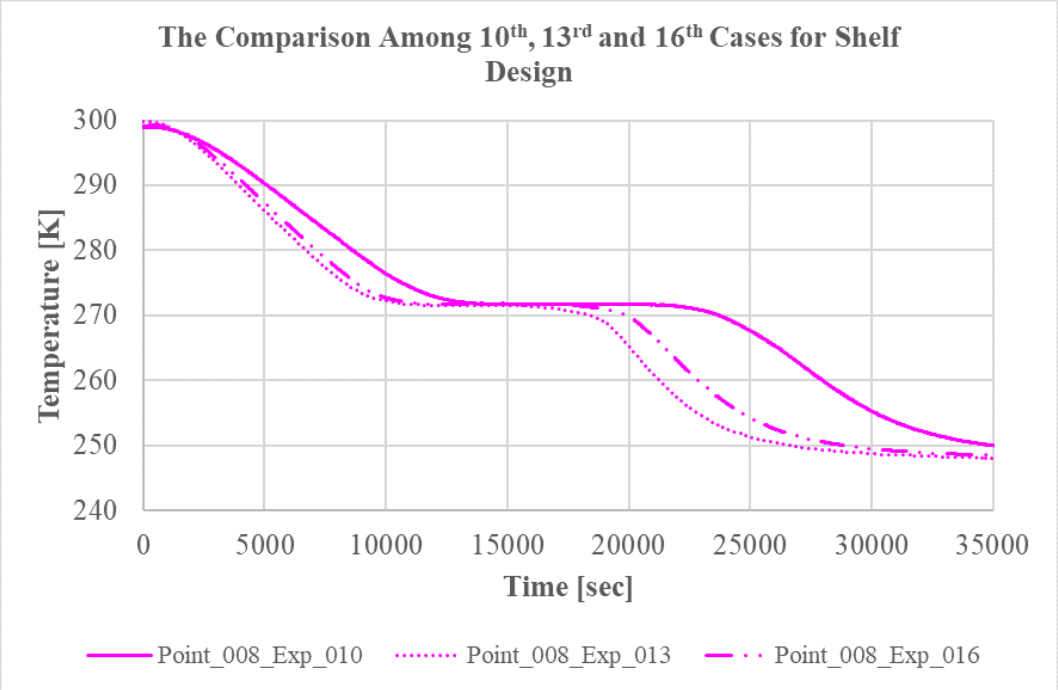

Figure 5.12. The Comparison Among 10th, 13rd and 16th Cases for Shelf Design with Experimental Data.

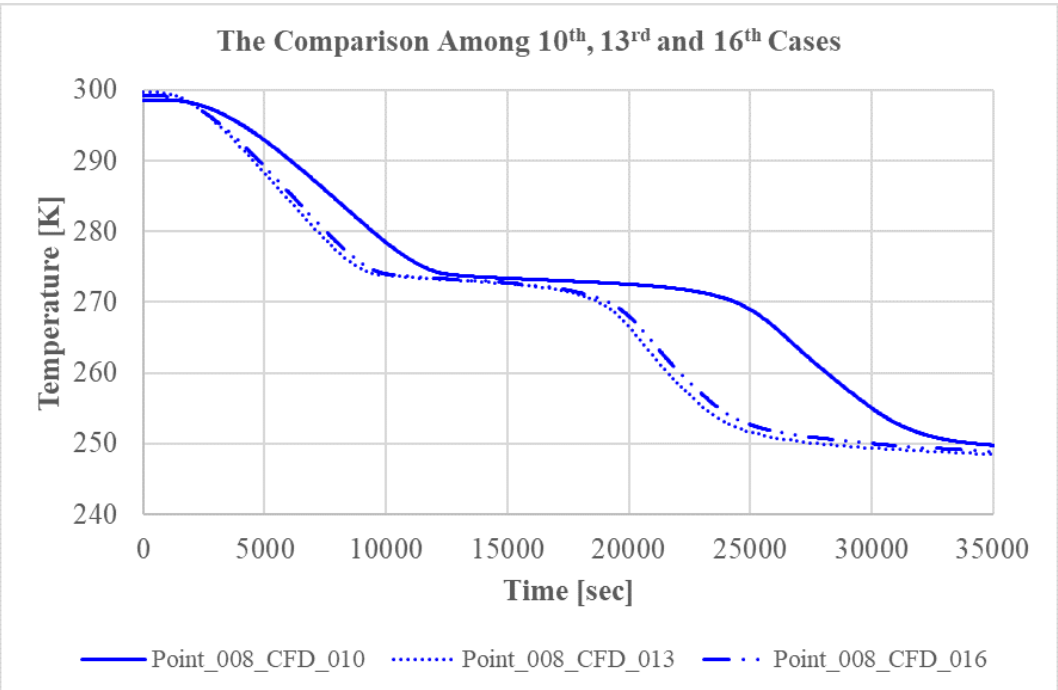

Figure 5.13. The Comparison Among 10th, 13rd and 16th Cases for Shelf Design with Numerical Data.

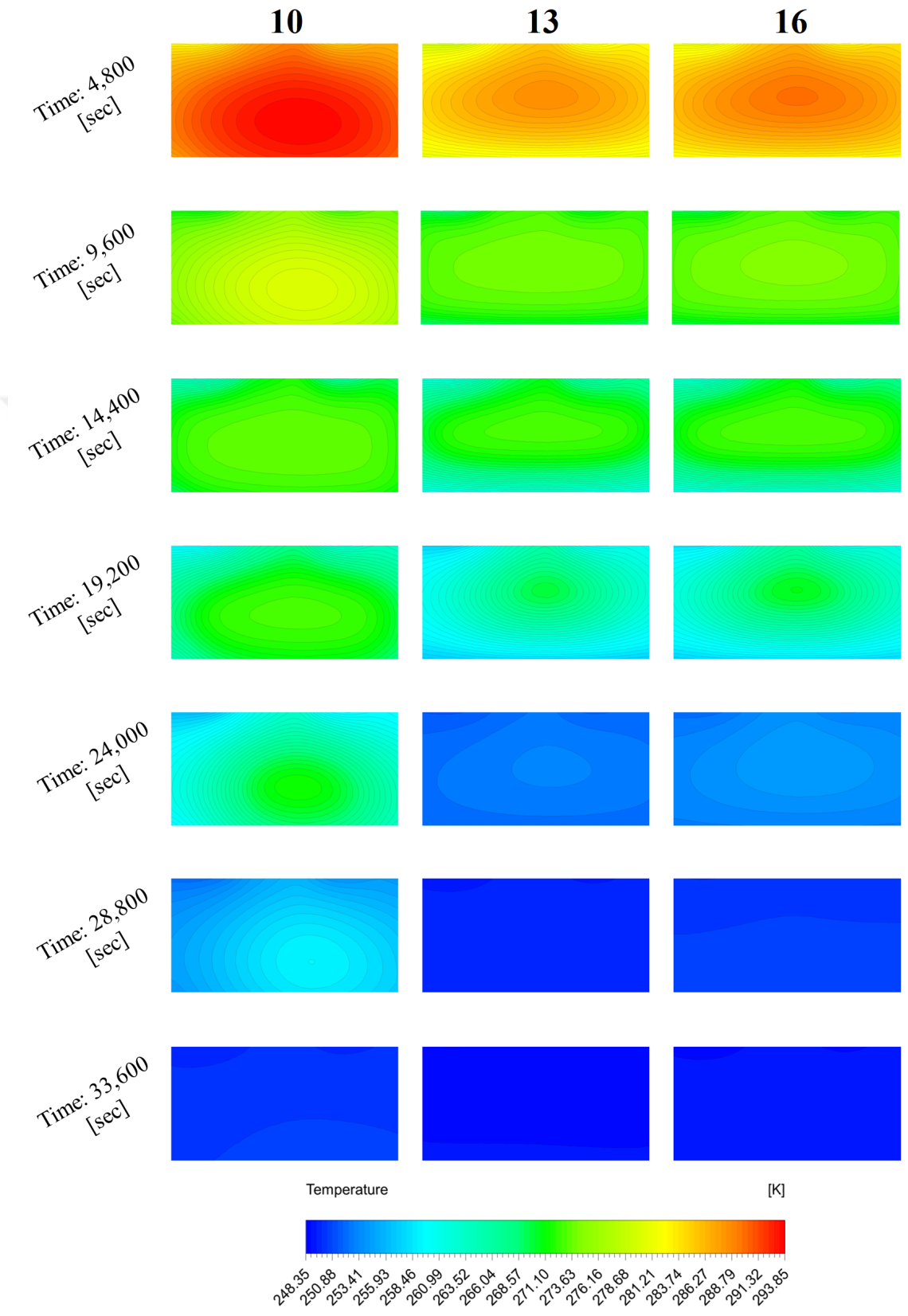

Figure 5.14. The Time-dependent Temperature Gradient in The Mid-section of The Test Package for 10^{th}, 13^{rd} and 16^{th} Cases.

In addition, this conclusion is simply made by evaluating the heat flux value via convection and conduction. Before this assessment is carried out, it should be explained schematically where convection and conduction heat transfer take place in order to make this evaluation more understandable. As they are illustrated on Figure 5.15, the conduction and convection heat transfer occur the bottom surface and the other surfaces of the test package, respectively. When the time-dependent heat flux change or heat transfer rate is examined from on the Figure 5.16 or Figure 5.17, respectively, the amount of the heat flux or heat transfer rate by conduction for the both 13^{rd} and 16^{th} cases is much higher than 10^{th} cases. These graphs show that using hybrid or metal shelf reduces the freezing time of the test package since it enhances the conduction heat transfer rate. However, it should be stated that the freezing time of the test package for the 16^{th} case (metal shelf) is little higher than the 13^{rd}'s freezing time since the heat capacity (or thermal inertia) of the metal shelf is more than the hybrid shelf's.

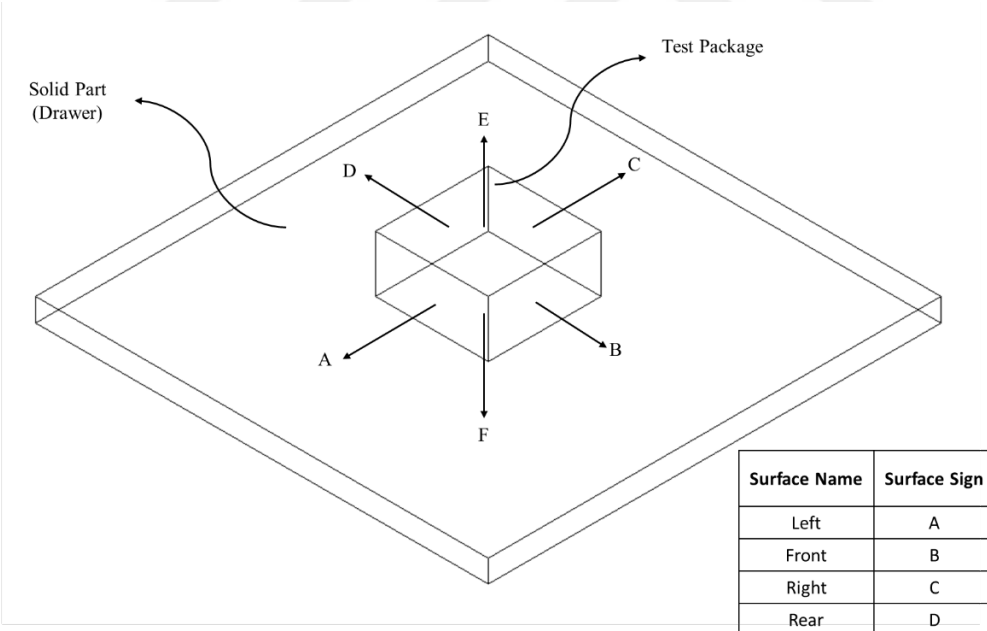

Surface Name	Surface Sign	Heat Transfer Mechanism
Left	A	Convection
Front	B	Convection
Right	C	Convection
Rear	D	Convection
Top	E	Convection
Bottom	F	Conduction

Figure 5.15. The Schematic Illustration of Heat Transfer Mechanism on Test Package Surfaces.

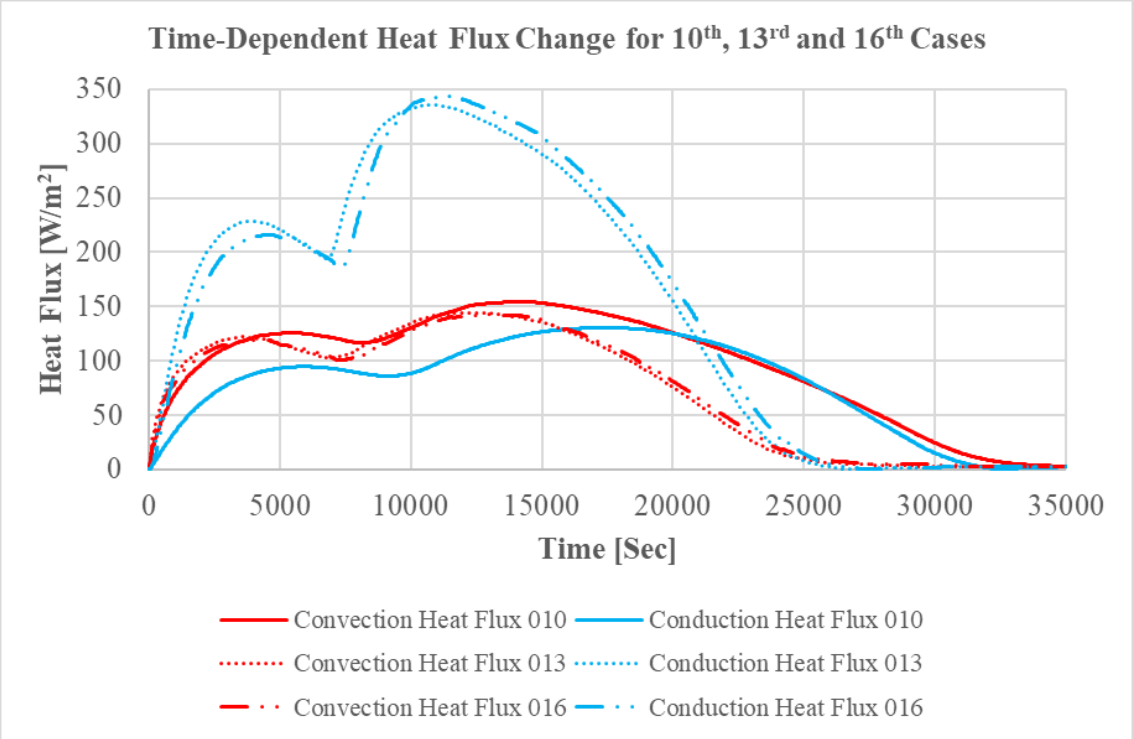

Figure 5.16. Time-Dependent Heat Flux Change for 10th, 13rd and 16th Cases.

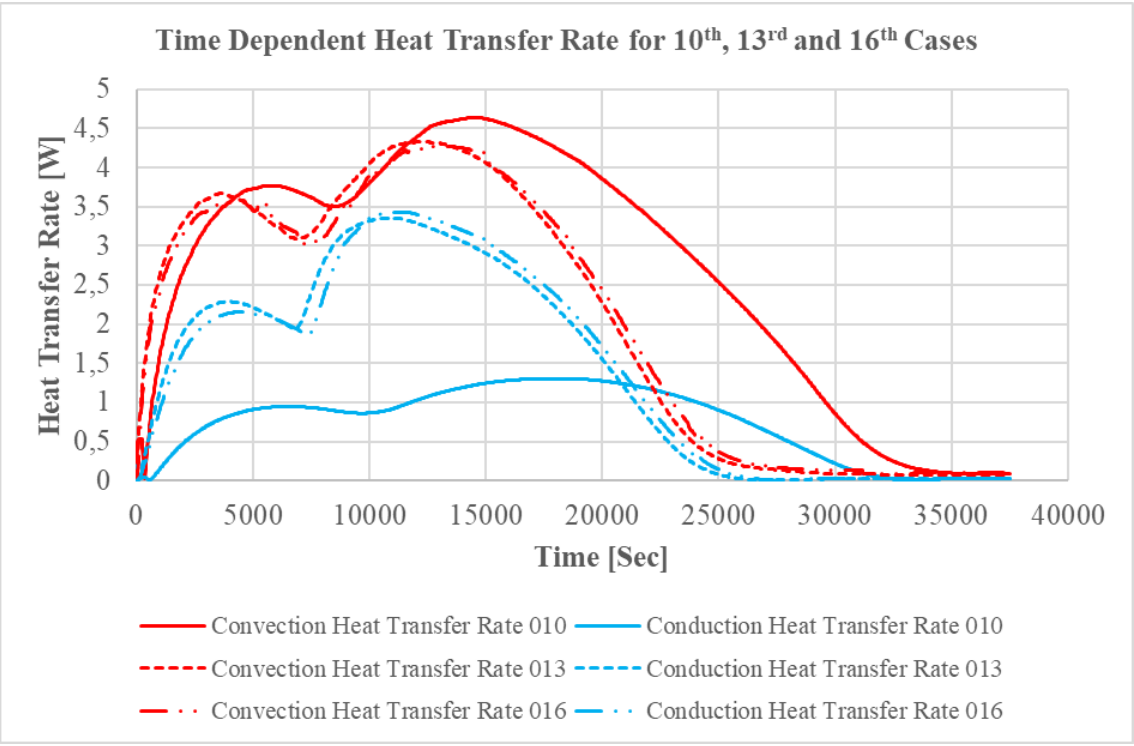

Figure 5.17. Time-Dependent Heat Transfer Rate for 10th, 13rd and 16th Cases.

5.5. The Evaluation of The Simulation of The Inside Air of The Refrigerator

As one of the features that distinguish this study from the other researches is cooling simulation of the refrigerator in addition to freezing of test package, the CFD result of that is examined in this section. First of all, the amount of the air flow rate inside refrigerator obtained from numerical calculation is compared with experimental results obtained by wind tunnel measurement as it is tabulated in Table 4.2. When the measurement uncertainty of wind tunnel and the modeling approach of evaporator, which is to accept fin thickness as 1 mm instead of 0.125 mm in order to generate mesh for fin geometry, are considered, these values can be acceptable.

The second verification is done by means of comparison between experimental temperature measurement and numerical calculation. To do that, the temperature on the division walls, blowing air and suction air is measured while freezing process. To prove that, the CFD results of 8^{th} case, which is preferred to use because its result has never been shown until now, is demonstrated on Figure 5.18 and Figure 5.19. It should be stated that small air gaps on the bottom glass have been closed on the CFD model, so the temperature of the bottom wall is calculated within 4% error bar as it is observed from Figure 5.19. Since this error has no high effect on the phase change calculation and the error bar is in the range of 5%, it was decided that this does not need to be improved.

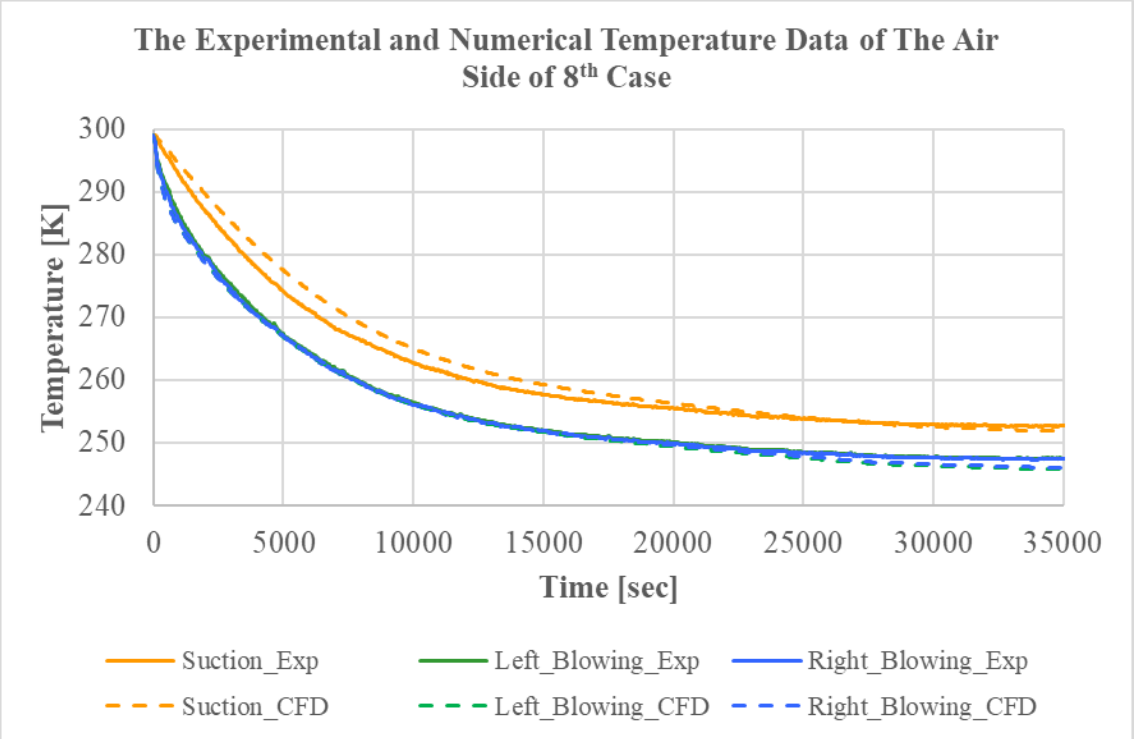

Figure 5.18. The Experimental and Numerical Temperature Data of The Air Side of 8^{th} Case.

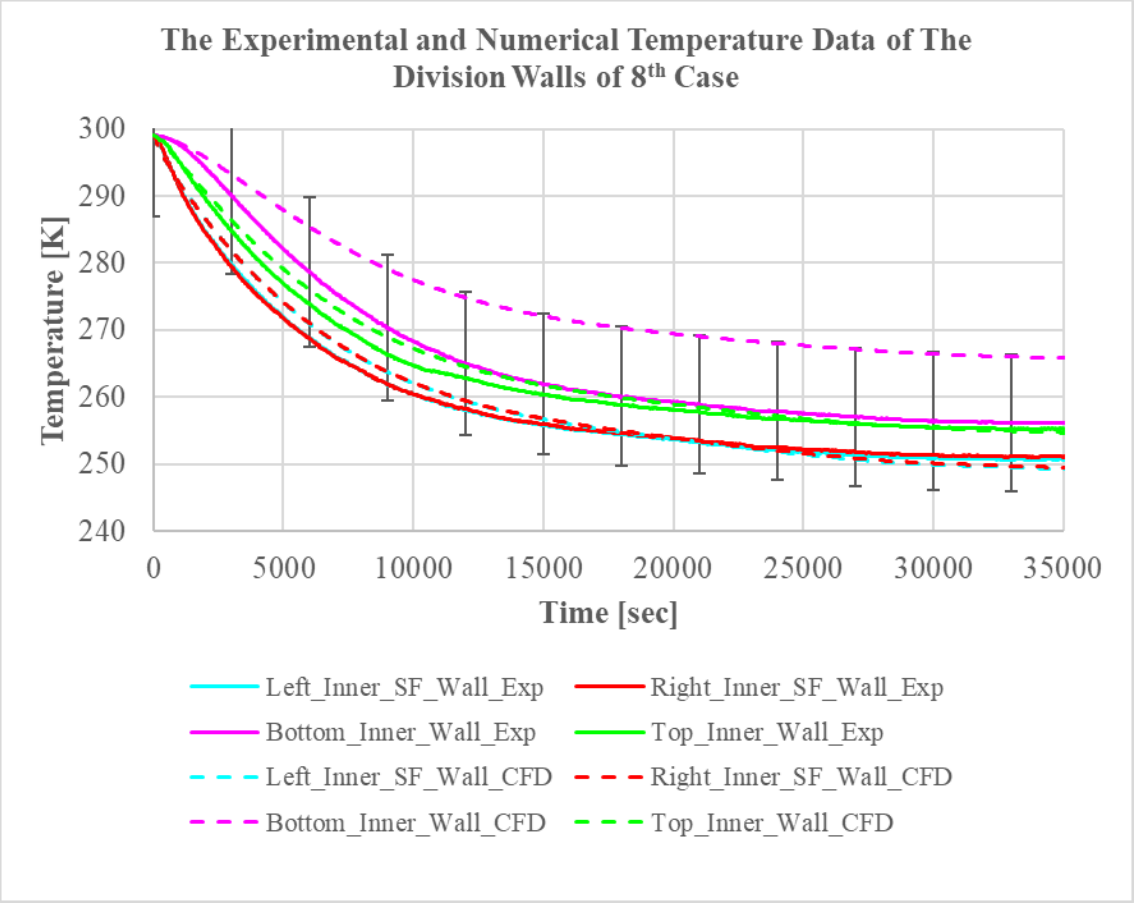

Figure 5.19. The Experimental and Numerical Temperature Data of The Division Walls of 8th Case.

5.6. The Evaluation of The Surface Heat Transfer Coefficient of The Food

In the beginning of the thesis, one novelty of the present work is described as the surface HTC has a great importance on the simulation of the phase change of food. Therefore, the freezing process should be modeled with its ambient instead of using average surface HTC and average ambient air temperature. Tough it is mentioned that this type of simplification could cause fatal error in numerical simulation by some scientist, only few researchers try to get rid of it by including environment in their studies. However, the effect of this inclusion could not be evaluated in detail or demonstrated plainly due to other simplifications such as reducing the problem 2D or ignoring turbulence effect, while the author try to show the influence of the surface HTC without

any simplification except for mass transfer. Thanks to the thin layer wrapped the food, mass transfer is obstructed completely. Therefore in actual fact it is not a simplification, it is a user condition. The spatial and temporal change of the surface HTC of the food are calculated numerically and the results are plotted as in Figure 5.20. This calculation is performed thanks to the transient data of the convective heat transfer rate from each surface, the blowing temperature from the air duct opening, and the area-weighted average wall temperature of the each surface. Additionally, each surface is illustrated in Figure 5.21.

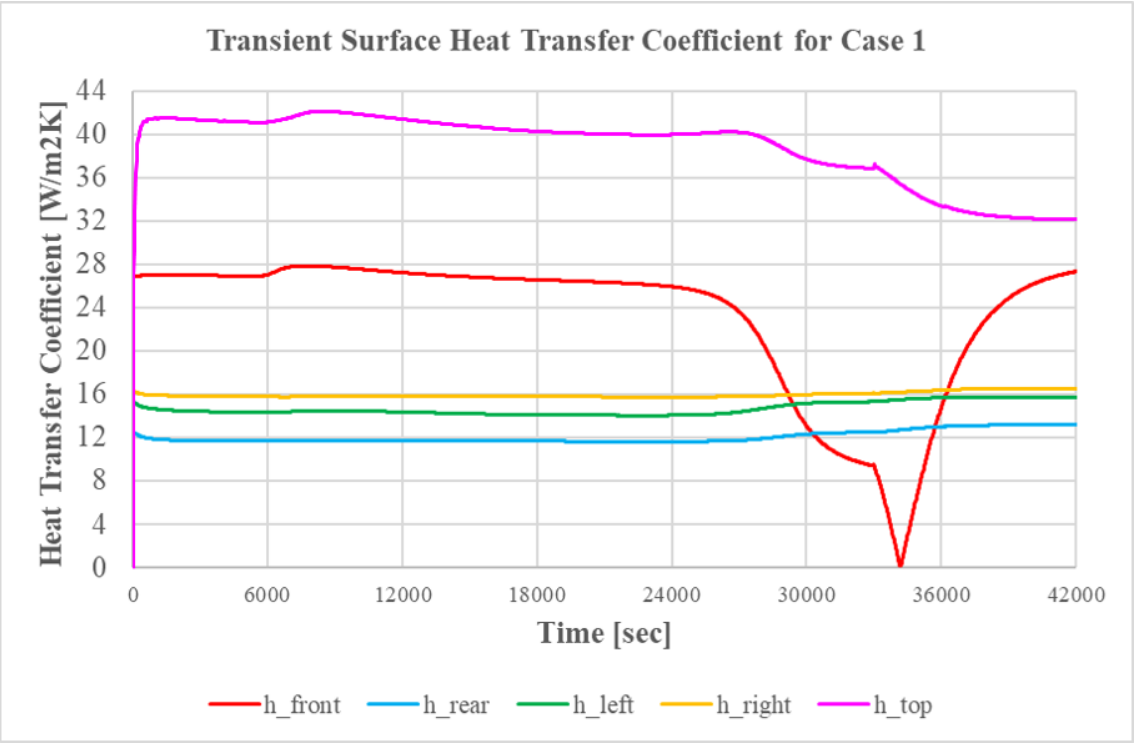

Figure 5.20. The Change in The Surface Heat Transfer Coefficient for 1st Case.

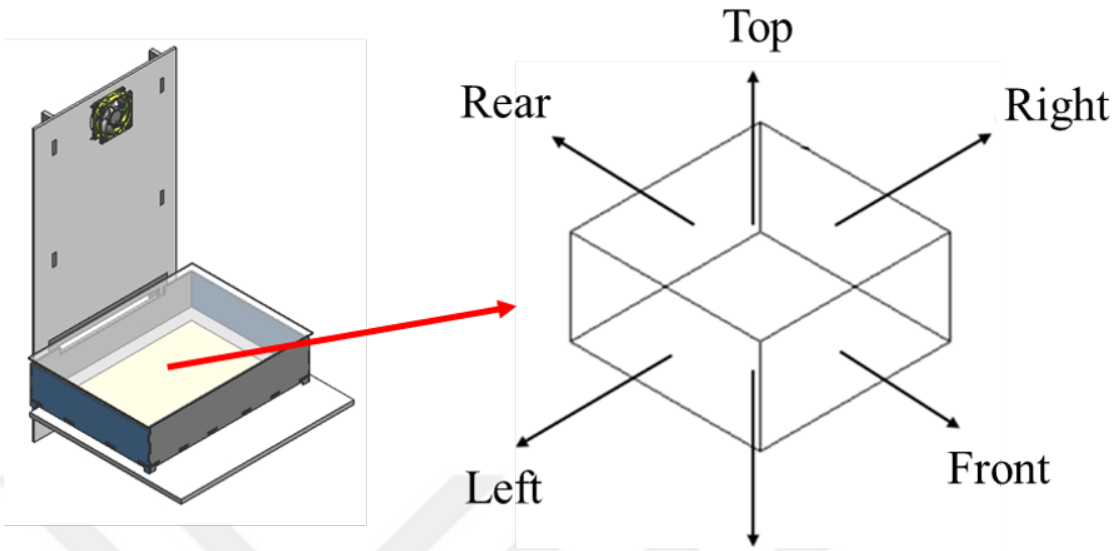

Figure 5.21. The Schematic Illustration of The Test Package Surfaces.

6. CONCLUSION AND FUTURE WORK

6.1. Conclusion

The preservation of food has a great importance for human beings in order to keep them alive since it is not always possible to reach food everywhere. When an excessive increase in population on the world and the result of that increased demand for food are considered, it makes the development of protection techniques inevitable. Therefore, a lot of scientists, researchers and engineers extremely focus on developing new techniques and/or improving available methods in order to keep natural resources and make the environment sustainable. In this study, the author exceedingly has worked on the freezing process of food, which is one of the most conventional methods and at the same time is open to improvement, especially phase change of beef. He has aimed to simulate freezing of beef inside a domestic refrigerator, to verify his simulation results, to determine key factors in freezing of beef and to generate a public knowledge about its simulation and significant parameters and has achieved all of them successfully.

After a wide range survey of the literature has been conducted, the simulation models of a phase change process are compiled neatly and evaluated with their pros and cons. By considering the capability and applicability of them, the apparent specific heat method has been preferred for use in the simulation of freezing of beef in this study since it is relatively simpler, cheaper and easier than the others. The results of the numerical simulation with error values show that this method is able to give an acceptable prediction of the freezing time of beef for both academic study and industrial application.

The effect of the air flow rate or air velocity is one parameter investigated in this study. Considering that the Nusselt correlation is used to determine a convection heat transfer coefficient, the air velocity directly affects the freezing process of the test

package. The present study demonstrates this explicitly. In addition that, the present study depicts that surface HTC plays a crucial role on the accuracy of the modeling solidification or melting process of a material. Therefore, the temporal and spatial change of surface HTC should be added to model.

This study has demonstrated that blowing type for industrial application has a major effect since it influences not only freezing process or quality of beef but also the performance, working characteristic and cooling components of a refrigerator. Therefore, it should be evaluated thoroughly when this type of change is wanted to be made.

The last thing studied in the present work is to reveal the impact of heat transfer by conduction and convection from bottom surface and the other surfaces of the test package to environment on freezing process, respectively. This study has showed that freezing time could be reduced by increasing the amount of heat transferred by conduction. Therefore, it is advised that the optimization between conduction and convection heat transfer from the test package surfaces to environment should be worked in detail in order to design environmentally friendly refrigerators and provide a fridge capable of high-quality freezing of food for customer.

6.2. Future Work

The modeling of a phase transition problem is undoubtedly a complex problem. Therefore, many important attempts to simulate that process numerically have been made in literature. Almost all researchers have tried to broaden the border of the previous attempts and/or to improve the accuracy of a numerical calculation. As in the other studies, the present investigation has areas to be developed. These could be listed as follows:

- By adding the effect of the thin plastic layer on the test package surface, more accurate results could be obtained.
- To simulate a real case, which is modeling the heat and mass transfer from test

package to the refrigerator air, and vice versa, mass transfer could be added to future work.

- To observe how the parameters examined in this study influence freezing or cooling process under a real working condition of a refrigerator, cycling working condition of a refrigerator could be included in the future.
- To simulate the evaporator surface temperature in more realistic manner, compression cycle or evaporation model inside the evaporator pipe could be included in the future.
- To compare the models for phase-change problems, all methods could be applied by choosing one case from this study.

REFERENCES

1. Belman-Flores, J. M., A. Gallegos-Munoz and A. Puente-Delgado, "Analysis of The Temperature Stratification of A No-frost Domestic Refrigerator with Bottom Mount Configuration", *Applied Thermal Engineering*, Vol. 65, No. 1, pp. 299–307, 2014.

2. WHO, F. I. U. W., *Transforming Food Systems for Affordable Healthy Diets*, Tech. rep., Rome, 2020.

3. Food, T. and A. O. of The United Nations, "The Food and Agriculture Organization", `http://www.fao.org/platform-food-loss-waste/en/`, accessed in March 2021.

4. Zhou, G. H., X. L. Xu and Y. Liu, "Preservation Technologies for Fresh Meat: A Review", *Meat Science*, Vol. 86, No. 1, pp. 119–128, 2010.

5. Kaale, L. D., T. M. Eikevik, T. Rustad and K. Kolsaker, "Superchilling of Food: A Review", *Journal of Food Engineering*, Vol. 107, No. 2, pp. 141–146, 2011.

6. Tan, K.-C., W. Ho, J. I. Katz and S.-J. Feng, "A Study of The Occurrence of Supercooling of Water", *American Journal of Physics*, Vol. 84, No. 4, pp. 293–300, 2016.

7. Gholaminejad, A. and R. Hosseini, "A Study of Water Supercooling", *Journal of Electronics Cooling and Thermal Control*, Vol. 3, No. 1, pp. 1–6, 2013.

8. Ramaswamy, H. and M. Marcotte, *Food Processing: Principles and Applications*, CRC Press, Boca Raton, FL, 1 edn., 2005.

9. Bulut, M., O. Bayer, E. Kırtıl and A. Bayındırlı, "Effect of Freezing Rate and Storage On The Texture and Quality Parameters of Strawberry and Green Bean

Frozen in Home Type Freezer", *International Journal of Refrigeration*, Vol. 88, pp. 360–369, 2018.

10. Sun, D.-W., *Handbook of Frozen Food Processing and Packaging*, CRC Press, Boca Raton, Fla, 2 edn., 2012.

11. Anonymous, *Recommendations for The Processing and Handling of Frozen Foods*, Paris:International Institute of Refrigeration, 3 edn., 1986.

12. Ansys, *Fluent 12.0 User's Guide*, 2009.

13. Atlanta: GA: American Society of Heating, R. and A. C. Engineers, *ASHRAE Handbook - Refrigeration*, 2018.

14. Hu, H. and S. A. Argyropoulos, "Mathematical Modelling of Solidification and Melting: A Review", *Modelling and Simulation in Materials Science and Engineering*, Vol. 4, No. 4, p. 371, 1996.

15. Nazzi Ehms, J. H., R. De Césaro Oliveski, L. A. Oliveira Rocha, C. Biserni and M. Garai, "Fixed Grid Numerical Models for Solidification and Melting of Phase Change Materials (PCMs)", *Applied Sciences*, Vol. 9, No. 20, p. 4334, 2019.

16. König-Haagen, A., E. Franquet, E. Pernot and D. Brüggemann, "A Comprehensive Benchmark of Fixed-grid Methods for The Modelling of Melting,", *International Journal of Thermal Sciences*, Vol. 118, pp. 69–103, 2017.

17. Cleland, A. C. and R. L. Earle, "Assessment of Freezing Time Prediction Methods", *Journal of Food Science*, Vol. 49, No. 4, pp. 1034–1042, 1984.

18. Nicolaï, B. M. and J. De Baerdemaeker, "Sensitivity Analysis with respect to the Surface Heat Transfer Coefficient as Applied to Thermal Process Calculations", *Journal of Food Engineering*, Vol. 28, No. 1, pp. 21–33, 1996.

19. Moraga, N. O., L. A. Jauriat and R. A. Lemus-Mondaca, "Heat and Mass Transfer in Conjugate Food Freezing/Air Natural Convection", *International Journal of Refrigeration*, Vol. 35, No. 4, pp. 880–889, 2012.

20. Hoang, D. K., S. J. Lovatt, J. R. Olatunji and J. K. Carsona, "Validated Numerical Model of Heat Transfer in The Forced Air Freezing of Bulk Packed Whole Chickens", *International Journal of Refrigeration*, Vol. 118, pp. 93–103, 2020.

21. Moraga, N. O. and C. H. Salinas, "Numerical Model for Heat and Fluid Flow in Food Freezing", *Numerical Heat Transfer, Part A: Applications*, Vol. 35, No. 1, pp. 75–81, 2017.

22. Moraga, N. O. and E. E. Medina, "Conjugate Forced Convection and Heat Conduction with Freezing of Water Content in A Plate Shaped Food", *International Journal of Heat and Mass Transfer*, Vol. 43, No. 1, pp. 53–67, 2000.

23. Moraga, N. O. and D. R. Rivera, "Advantages in Predicting Conjugate Freezing of Meat in A Domestic Freezer by CFD with Turbulence K- 3D Model and A Local Exergy Destruction Analysis", *International Journal of Refrigeration*, 2021, `https://doi.org/10.1016/j.ijrefrig.2021.02.002`.

24. Hoang, D. K., S. J. Lovatt, J. R. Olatunji and J. K. Carsona, "Experimental Measurement and Numerical Modelling of Cooling Rates of Bulk-packed Chicken Drumsticks During Forced-air Freezing", *International Journal of Refrigeration*, Vol. 114, pp. 165–174, 2020.

25. Hashemi, H. and C. M. Sliepcevich, "A Numerical Method for Solving Two-dimensional Problems of Heat Conduction with Change of Phase", *Chemical Engineering Progress Symposium Series*, Vol. 63, No. 79, pp. 34–41, 1967.

26. Dima, J. B., M. V. Santos, P. J. Baron, A. Califano and N. E. Zaritzky, "Experimental Study and Numerical Modeling of The Freezing Process of Marine Prod-

ucts,", *Food and Bioproducts Processing*, Vol. 92, No. 1, pp. 54–66, 2014.

27. Pham, Q. T., "Freezing Time Formulas for Foods with Low Moisture Content, Low Freezing Point and for Cryogenic Freezing", *Journal of Food Engineering*, Vol. 127, pp. 85–92, 2014.

28. Santos, M. V., V. Vampa, A. Califano and N. Zaritzky, "Numerical Simulations of Chilling and Freezing Processes Applied to Bakery Products in Irregularly 3D Geometries", *Journal of Food Engineering*, Vol. 100, No. 1, pp. 32–42, 2010.

29. Tocci, A. M. and R. H. Mascheroni, "Numerical Models for The Simulation of The Simultaneous Heat and Mass Transfer During Food Freezing and Storage", *International Communications in Heat and Mass Transfer*, Vol. 22, No. 2, pp. 251–260, 1995.

30. Moraga, N. O. and H. G. Barraza, "Predicting Heat Conduction During Solidification of A Food Inside A Freezer due to Natural Convection", *Journal of Food Engineering*, Vol. 56, No. 1, pp. 17–26, 2003.

31. Huan, Z., S. He and Y. Ma, "Numerical Simulation and Analysis for Quick-frozen Food Processing", *Journal of Food Engineering*, Vol. 60, No. 3, pp. 267–273, 2003.

32. Hamdami, N., J. Y. Monteau and A. L. Bail, "Simulation of Coupled Heat and Mass Transfer During Freezing of A Porous Humid Matrix", *International Journal of Refrigeration*, Vol. 27, No. 6, pp. 595–603, 2004.

33. Poirier, D. and M. Salcudean, "On Numerical Methods Used in Mathematical Modeling of Phase Change in Liquid Metals", *Journal of Heat Transfer*, Vol. 110, No. 3, pp. 562–570, 1988.

34. Heim, D. and J. A. Clarke, "Numerical Modelling and Thermal Simulation of PCM–gypsum Composites with ESP-r", *Energy and Buildings*, Vol. 36, No. 8, pp. 795–805, 2004.

35. Yao, W.-A., H.-X. Yao, C. Zuo and X.-F. Hu, "Precise Integration Boundary Element Method for Solving Dual Phase Change Problems Based On The Effective Heat Capacity Model", *Engineering Analysis with Boundary Elements*, Vol. 108, pp. 411–421, 2019.

36. Voller, V. R. and C. R. Swaminathan, "General Source-Based Method For Solidification Phase Change", *Numerical Heat Transfer*, Vol. 19, No. 2, pp. 175–189, 1991.

37. Salcudean, M. and Z. Abdullah, "On The Numerical Modelling of Heat Transfer During Solidification Processes", *International Journal for Numerical Methods in Engineering*, Vol. 25, No. 2, pp. 445–473, 1988.

38. Scheerlinck, N., P. Verboven, K. A. Fikiin, J. De Baerdemaeker and B. M. Nicolaï, "Finite Element Computation Of Unsteady Phase Change Heat Transfer During Freezing Or Thawing Of Food Using A Combined Enthalpy And Kirchhoff Transform Method", *Transactions of the ASAE*, Vol. 44, No. 2, pp. 429–438, 2001.

39. Perussello, C. A., V. C. Mariani and [U+FFFD] C. do Amarante, "Combined Modelling of Thermal Properties and Freezing Process by Convection Applied to Green Beans", *Applied Thermal Engineering*, Vol. 31, No. 14–15, pp. 2894–2901, 2011.

40. Zilio, C., G. Righetti, G. Pernigotto and G. A. Longo, "Analysis of The Freezing Time of Chicken Breast Finite Cylinders", *International Journal of Refrigeration*, Vol. 95, pp. 38–50, 2018.

41. Anderson, B. A., S. Sun, F. Erdogdu and R. P. Singh, "Thawing and Freezing of Selected Meat Products in Household Refrigerators", *International Journal of Refrigeration*, Vol. 27, No. 1, pp. 63–72, 2004.

42. Rolph, W. D. and K. Bathe, "An Efficient Algorithm for Analysis of Nonlinear Heat Transfer with Phase Changes", *International Journal for Numerical Methods*

in Engineering, Vol. 18, No. 1, pp. 119–134, 1982.

43. Dalhuijsen, A. J. and A. Segal, "Comparison of Finite Element Techniques for Solidification Problem", *International Journal for Numerical Methods in Engineering*, Vol. 23, No. 10, pp. 1807–1927, 1986.

44. Pham, Q. T., "Comparison Of General-Purpose Finite-Element Methods For The Stefan Problem", *Numerical Heat Transfer*, Vol. 27, No. 4, pp. 417–435, 1995.

45. Fikiin, K. A., "Generalised Numerical Modelling of Unsteady Heat Transfer During Cooling and Freezing Using An Improved Enthalpy Method and Quasi-one-dimensional Formulation", *International Journal of Refrigeration*, Vol. 19, No. 2, pp. 132–140, 1996.

46. Swaminathan, C. and V. Voller, "A General Enthalpy Method for Modeling Solidification Processes", *Metallurgical Transactions B*, Vol. 23, No. 5, pp. 651–664, 1992.

47. Kiani, H., Z. Zhang and D. W. Sun, "Experimental Analysis and Modeling of Ultrasound Assisted Freezing of Potato Spheres", *Ultrasonics Sonochemistry*, Vol. 26, pp. 321–331, 2015.

48. Galione, P. A., O. Lehmkuhl, J. Rigola and A. Oliva, "Fixed-Grid Modeling of Solid-Liquid Phase Change in Unstructured Meshes Using Explicit Time Schemes", *Numerical Heat Transfer*, Vol. 65, No. 1, pp. 27–52, 2013.

49. Iten, M., S. Liu and A. Shukla, "Experimental Validation of An Air-PCM Storage Unit Comparing The Effective Heat Capacity and Enthalpy Methods through CFD Simulations", *Energy*, Vol. 155, pp. 495–503, 2018.

50. Voller, V. R. and C. Prakash, "A Fixed Grid Numerical Modelling Methodology for Convection-diffusion Mushy Region Phase-change Problems", *International Journal of Heat and Mass Transfer*, Vol. 30, No. 8, pp. 1709–1719, 1987.

51. Shih, T. H., W. W. Liou, A. Shabbir, Z. Yang and J. Zhu, "A New k-[U+03F5] Eddy Viscosity Model for High Reynolds Number Turbulent Flows", *Computers and Fluids*, Vol. 24, No. 3, pp. 227–238, 1995.

52. Douglas, J. J. and J. T. Gallie, "Equation Subject to A Moving Boundary Condition", *Duke Mathematical Journal*, Vol. 22, No. 4, pp. 557–571, 1955.

53. Heitz, W. L. and J. W. Westwater, "Extension of The Numerical Method for Melting and Freezing Problems", *International Journal of Heat and Mass Transfer*, Vol. 13, No. 8, pp. 1371–1375, 1970.

54. Ismail, K. A. and J. R. Henríquez, "Solidification of PCM Inside A Spherical Capsule", *Energy Conversion and Management*, Vol. 41, No. 2, pp. 173–187, 2000.

55. Gupta, R. S. and D. Kumar, "Variable Time Step Methods for One-dimensional Stefan Problem with Mixed Boundary Condition", *International Journal of Heat and Mass Transfer*, Vol. 24, No. 2, pp. 251–259, 1981.

56. Versteeg, H. K. and W. Malalasekera, *An Introduction to Computational Fluid Dynamics: The Finite Volume Method*, Pearson/Prentice Hall, Harlow, 2 edn., 2007.

57. White, F. M., *Fluid Mechanics*, McGraw-Hill, Boston, 4 edn., 1998.

58. Erickson, M. and Y. C. Hung, *Quality in Frozen Food*, Springer, Boston, 1997.

59. Zhao, Y., W. Ji, J. Guo, L. Chen, C. Tian, Y. Wang and J. Wang, "Numerical and Experimental Study On The Quick Freezing Process of The Bayberry", *Food and Bioproducts Processing*, Vol. 119, pp. 98–107, 2020.

APPENDIX A: THERMAL PROPERTIES OF THE TEST PACKAGE

Table A.1. The Apparent Specific Heat of The Test Package.

Temperature (K)	**Apparent Specific Heat (J/kg.K)**	**Temperature (K)**	**Apparent Specific Heat (J/kg.K)**
245.15	400	271.30	26,856.98
250.15	700	271.40	27,950.50
254.65	1,504.95	271.50	29,090.76
262.00	3,900.29	271.60	30,269.52
263.50	4,599.45	271.70	31,463.68
265.00	5,540.31	271.80	32,683.28
265.50	5,921.66	271.90	33,874.24
266.00	6,378.08	272.00	34,911.95
266.50	6,924.81	272.10	35,660.67
267.00	7,574.77	272.21	35,982.71
267.50	8,346.21	272.22	35,986.95
268.00	9,342.68	272.23	35,986.88
268.50	10,649.86	272.30	35,868.69
269.00	12,256.30	272.40	35,259.05
269.25	13,194.72	272.50	34,123.79
269.50	14,230.31	272.75	29,611.86
269.75	15,397.66	273.00	24,079.42
270.00	16,713.32	273.25	17,681.24
270.25	18,203.42	273.50	11,894.61
270.50	19,867.49	273.75	6,636.67
270.75	21,741.96	274.00	3,781.65
270.90	23,007.71	274.20	2,908.58
271.00	23,918.12	287.15	3,153.82
271.10	24,837.78	300.15	3,400.01
271.20	25,839.28		

Table A.2. The Thermal Conductivity of The Test Package.

Temperature (K)	**Thermal Conductivity (W/m.K)**
300.15	0.32526
287.15	0.31037
272.22	0.29111
271.9	0.86277
271.65	0.95717
271.4	1.02496
271.15	1.07611
270.65	1.14847
270.15	1.19757
269.15	1.26090
268.15	1.30106
267.15	1.32970
266.15	1.35180
265.15	1.36986
264.15	1.38527
263.15	1.39886
262.15	1.41114
261.15	1.42249
260.15	1.43313
259.15	1.44324
258.15	1.45295
257.15	1.46236
256.15	1.47152
255.15	1.48051
250.15	1.52396
245.15	1.56675

APPENDIX B: EXPERIMENTAL MEASUREMENT AND NUMERICAL CALCULATION FOR A SAMPLE CASE

The all calculated and measured temperature data of the 1st case is graphed in order to show the reader where the temperature data is obtained from and to set an example for the other cases and to be set an example for the other cases.

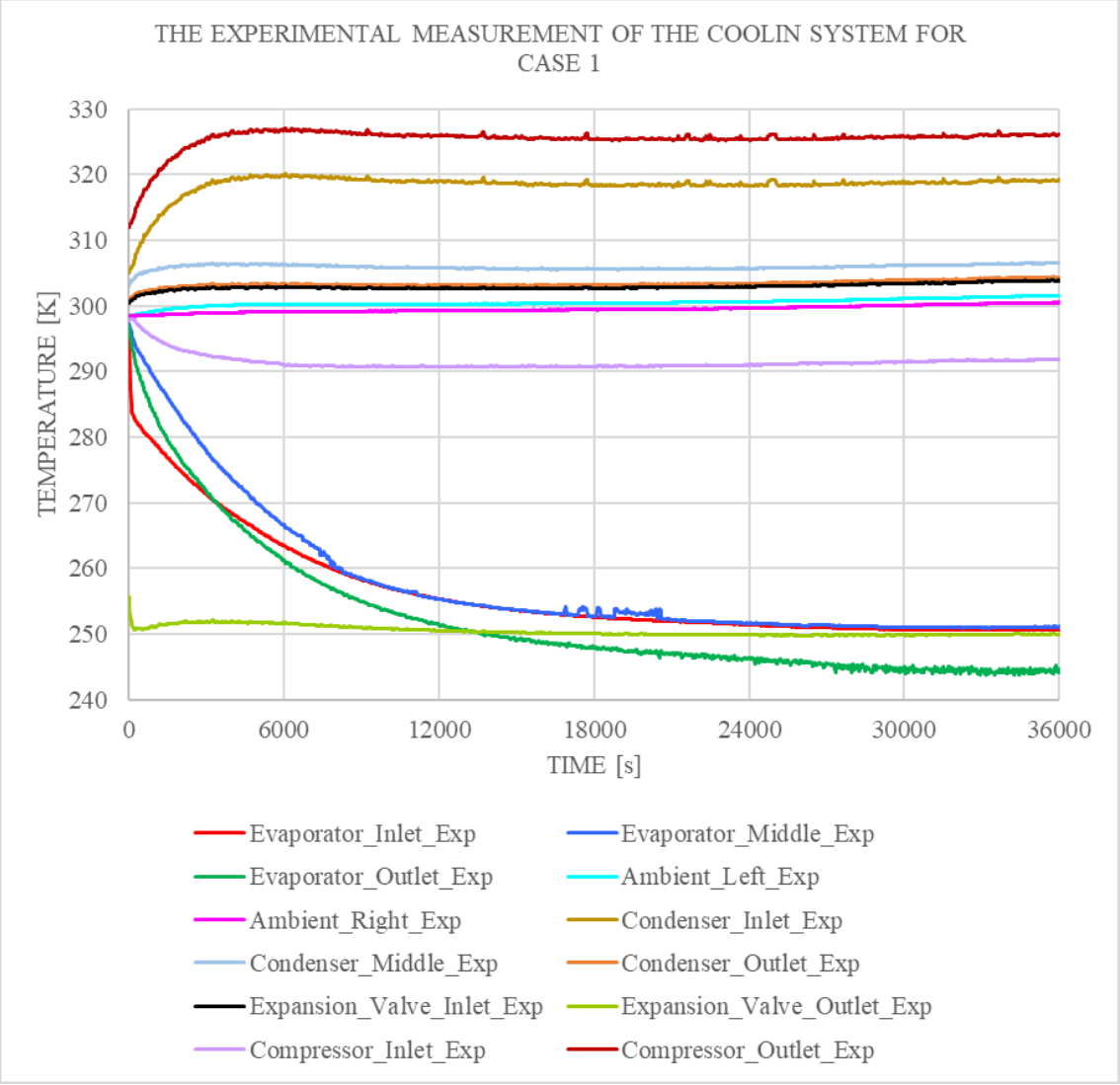

Figure B.1. The Experimental Measurement of The Cooling System for Case 1.

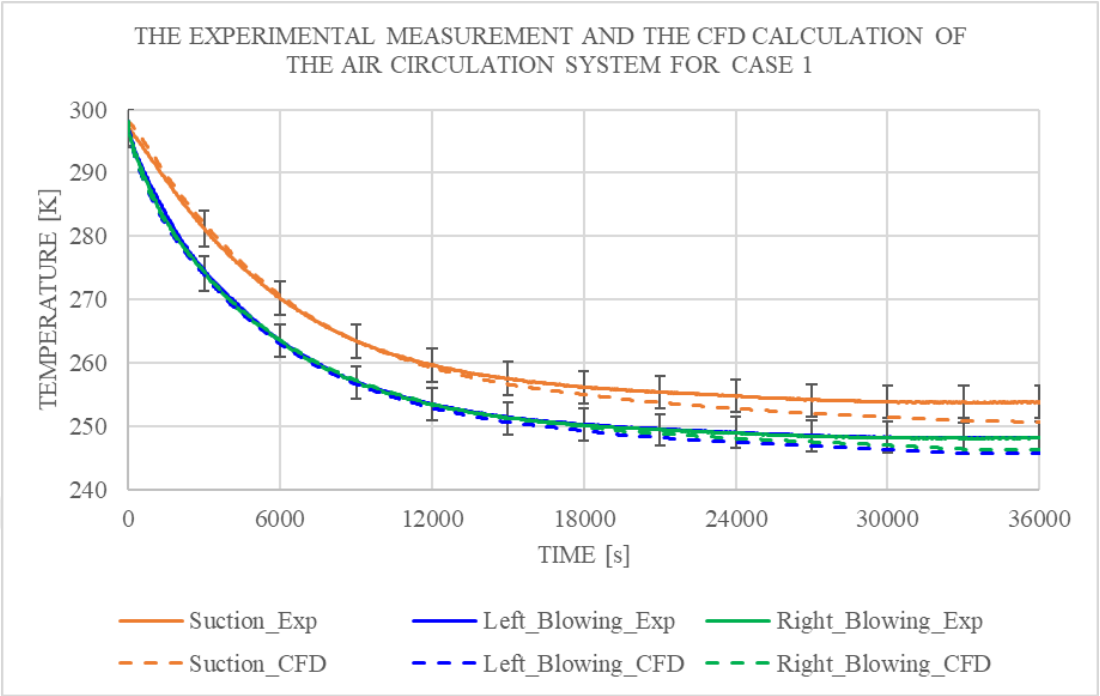

Figure B.2. The Experimental Measurement and The CFD Calculation of The Air Circulation System for Case 1.

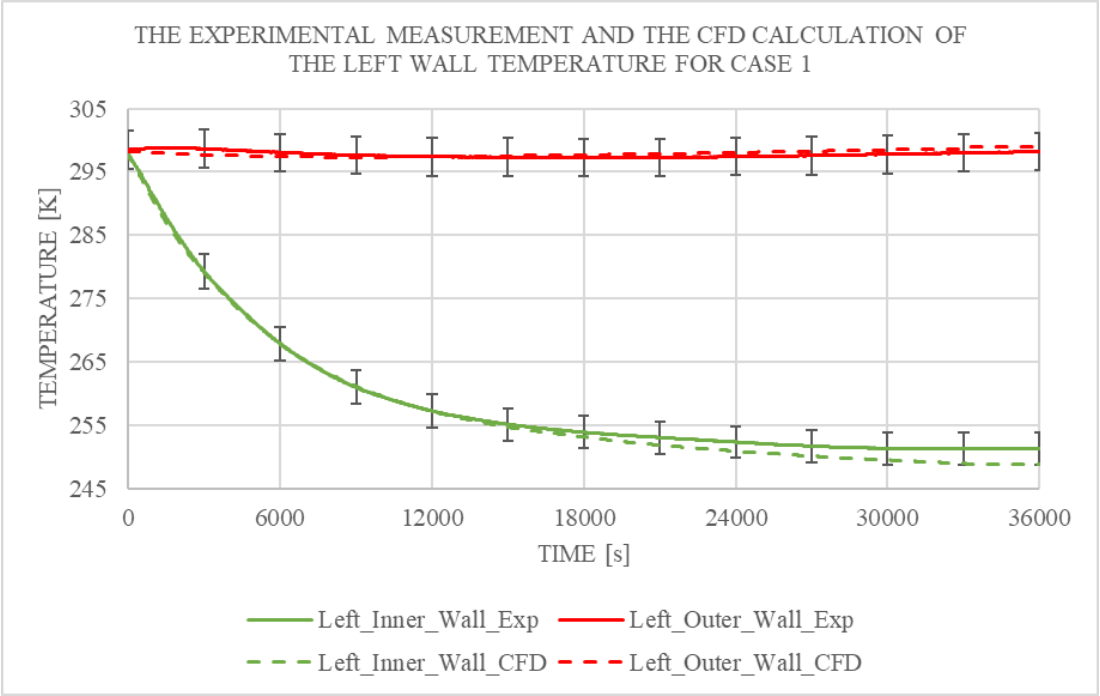

Figure B.3. The Experimental Measurement and The CFD Calculation of The Left Wall Temperature for Case 1.

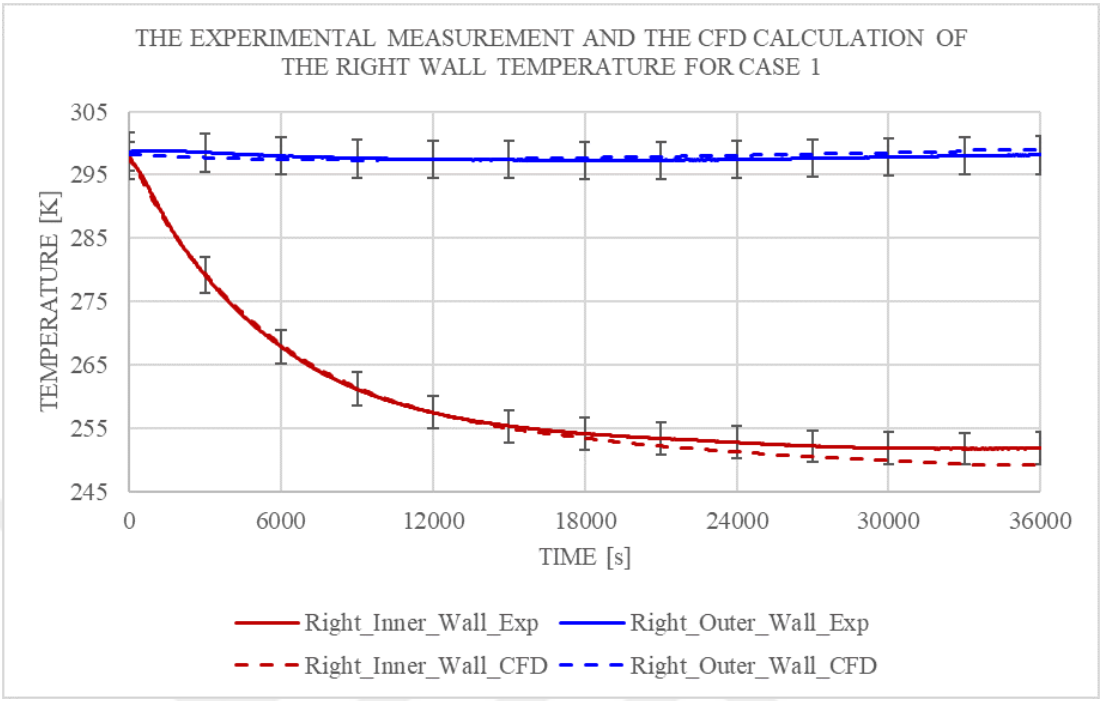

Figure B.4. The Experimental Measurement and The CFD Calculation of The Right Wall Temperature for Case 1.

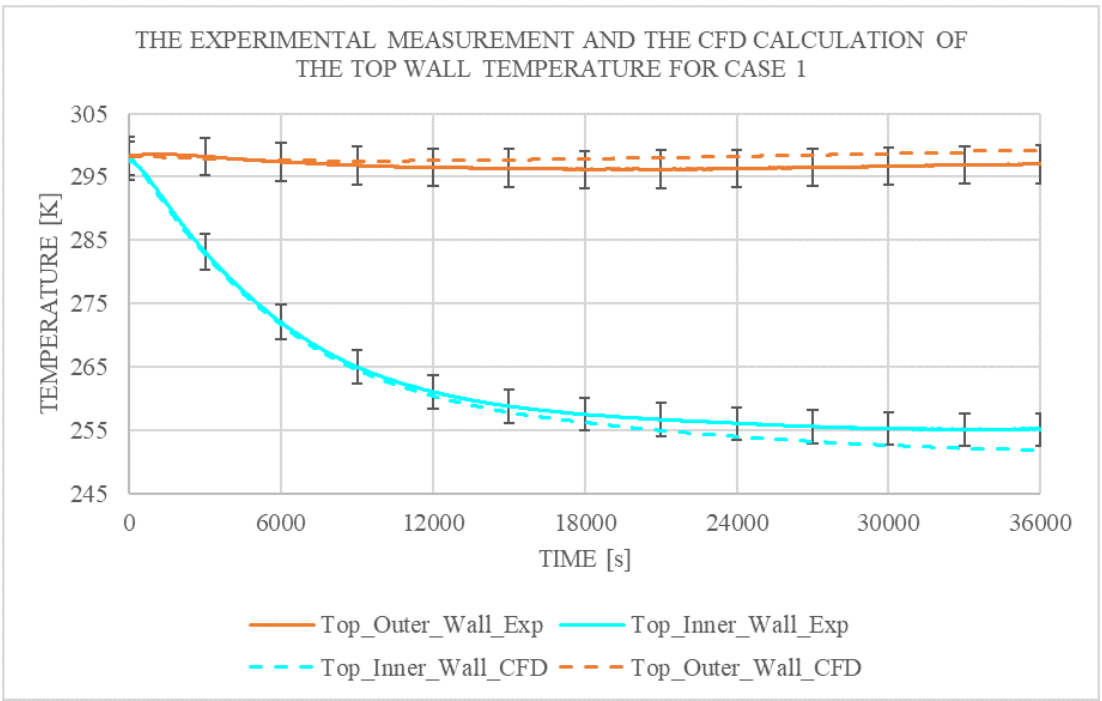

Figure B.5. The Experimental Measurement and The CFD Calculation of The Top Wall Temperature for Case 1.

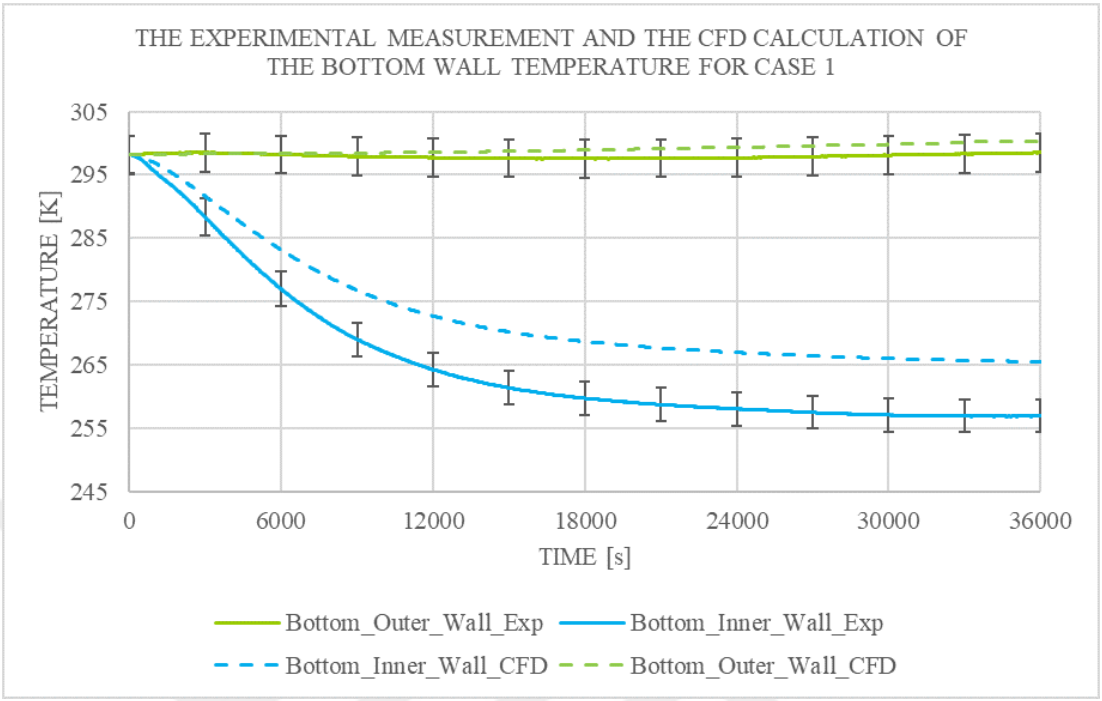

Figure B.6. The Experimental Measurement and The CFD Calculation of The Bottom Wall Temperature for Case 1.

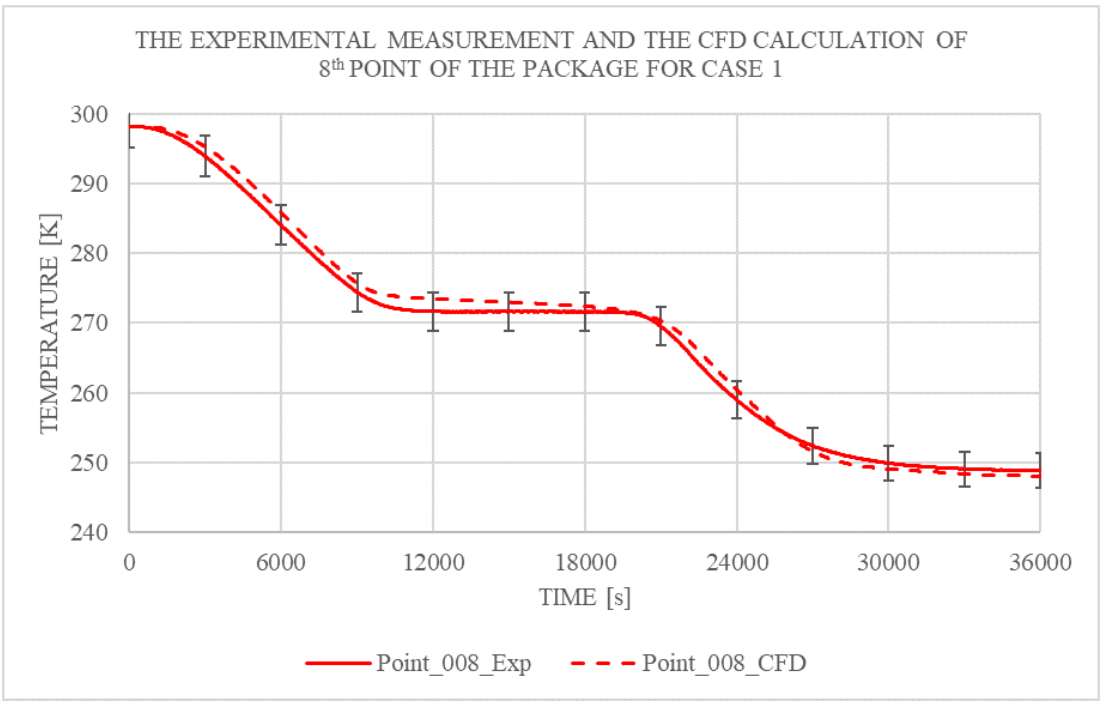

Figure B.7. The Experimental Measurement and The CFD Calculation of 8th Point of The Package for Case 1.

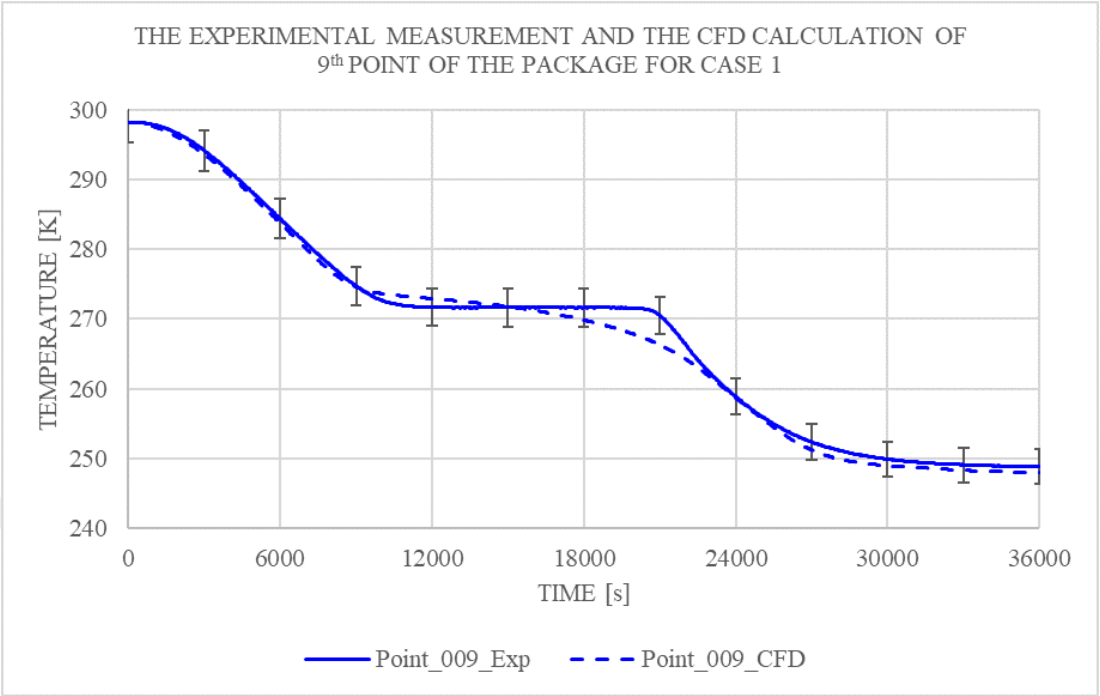

Figure B.8. The Experimental Measurement and The CFD Calculation of 9th Point of The Package for Case 1.

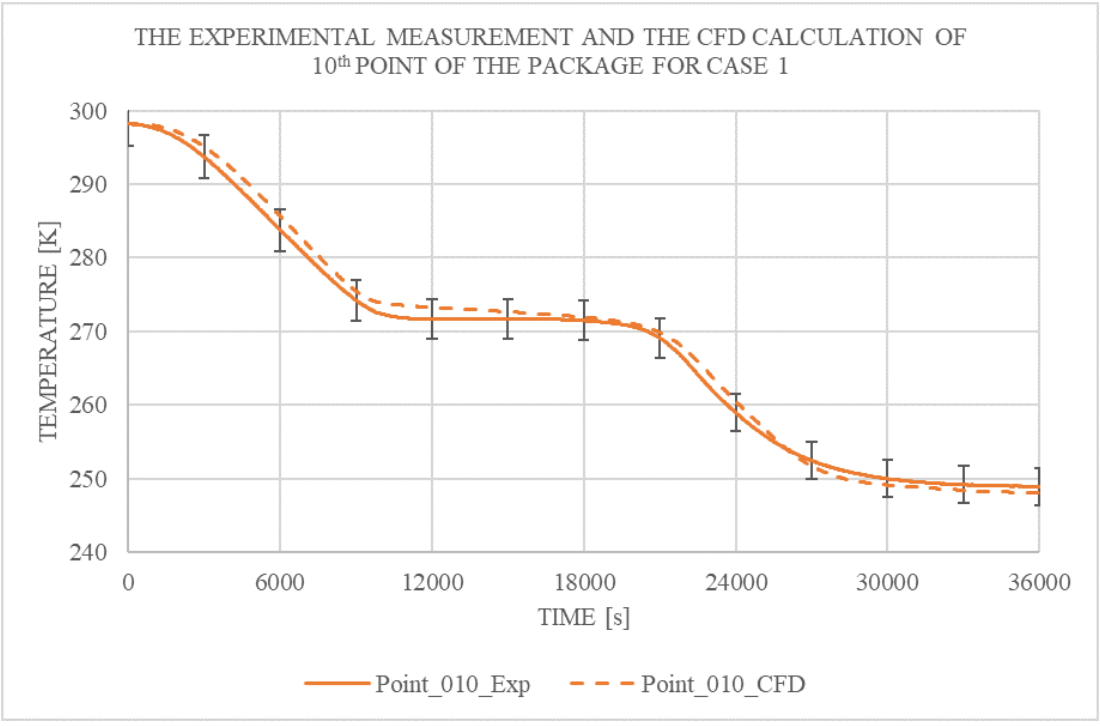

Figure B.9. The Experimental Measurement and The CFD Calculation of 10th Point of The Package for Case 1.

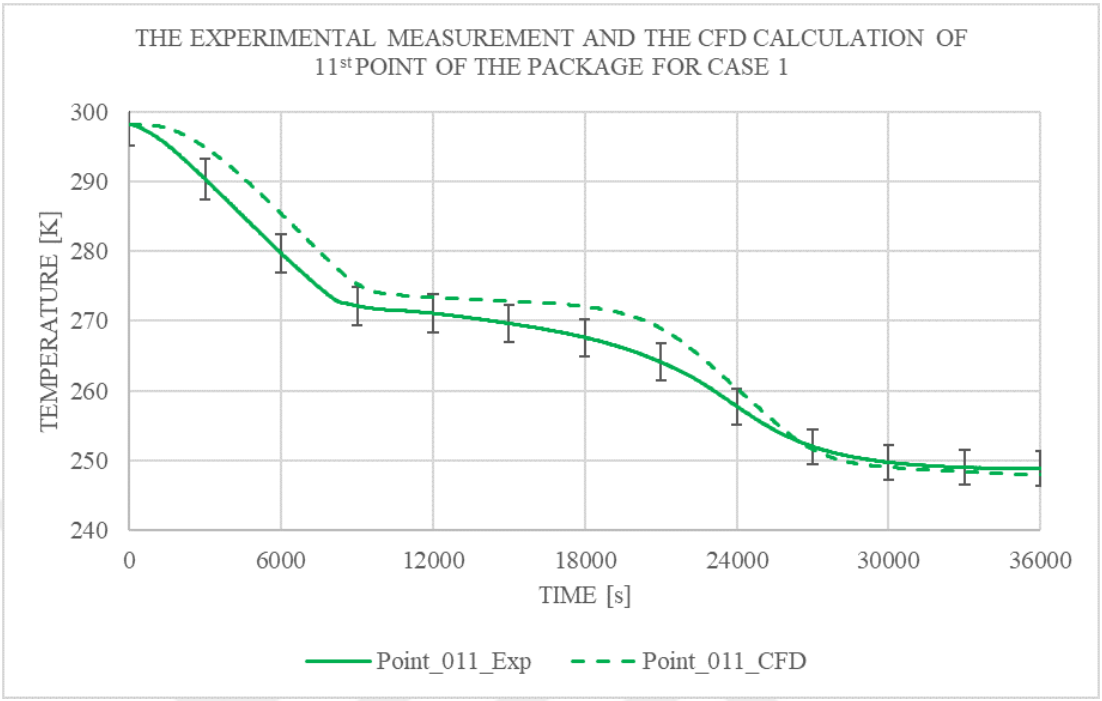

Figure B.10. The Experimental Measurement and The CFD Calculation of 11st Point of The Package for Case 1.

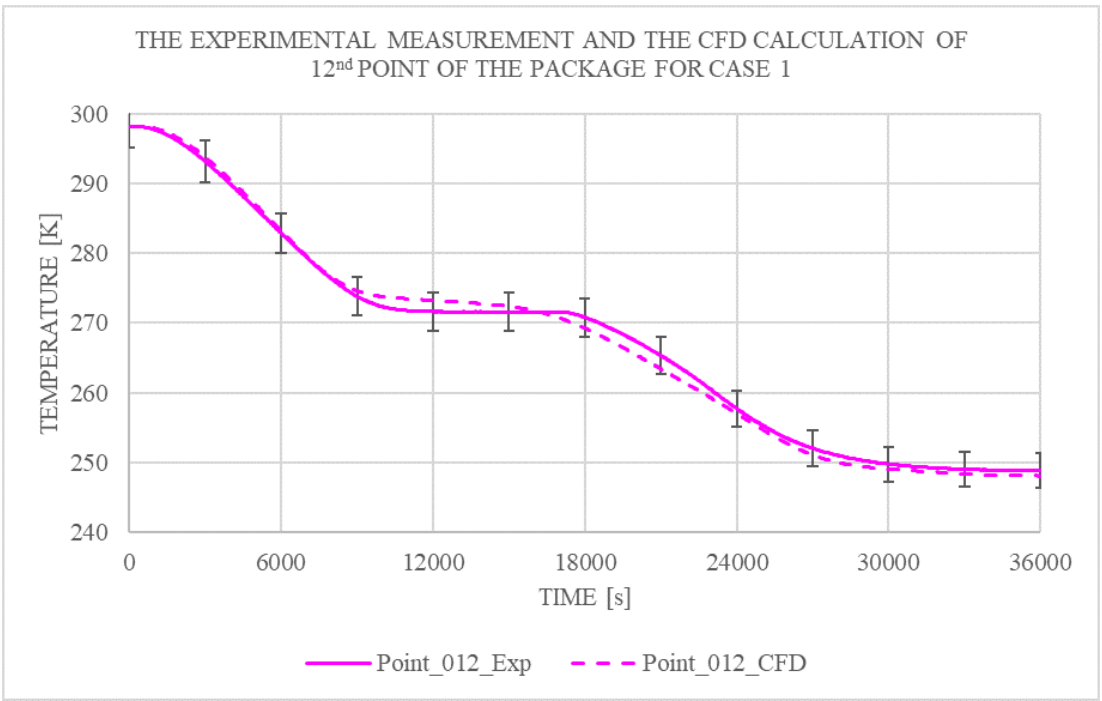

Figure B.11. The Experimental Measurement and The CFD Calculation of 12nd Point of The Package for Case 1.

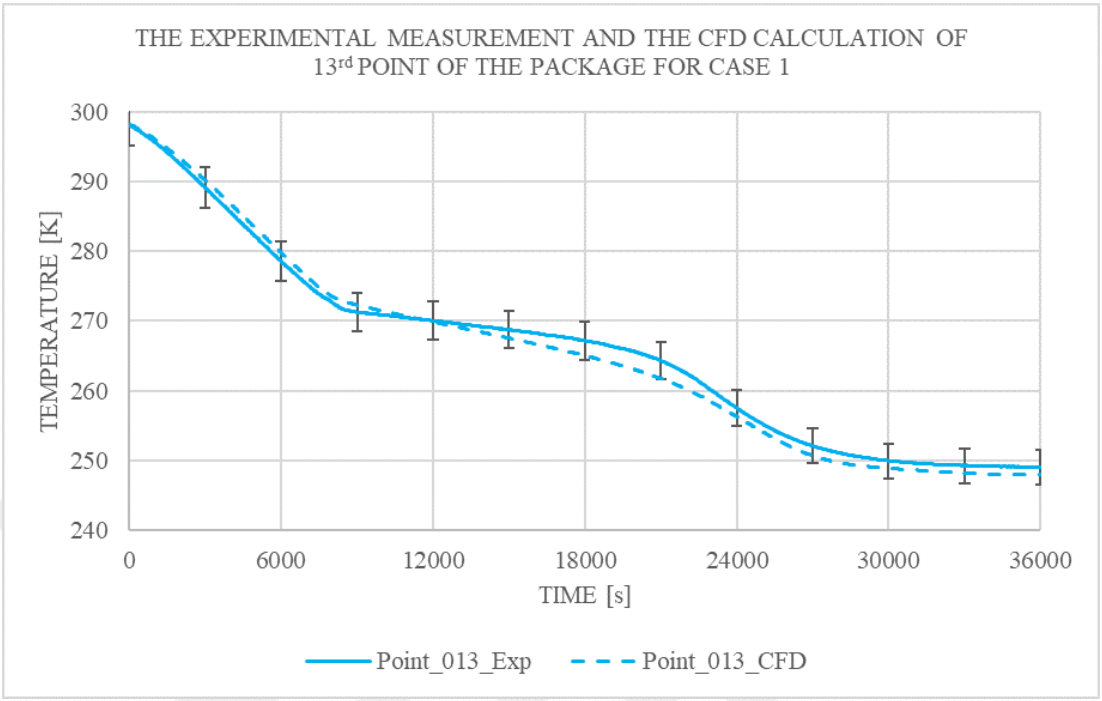

Figure B.12. The Experimental Measurement and The CFD Calculation of 13rd Point of The Package for Case 1.

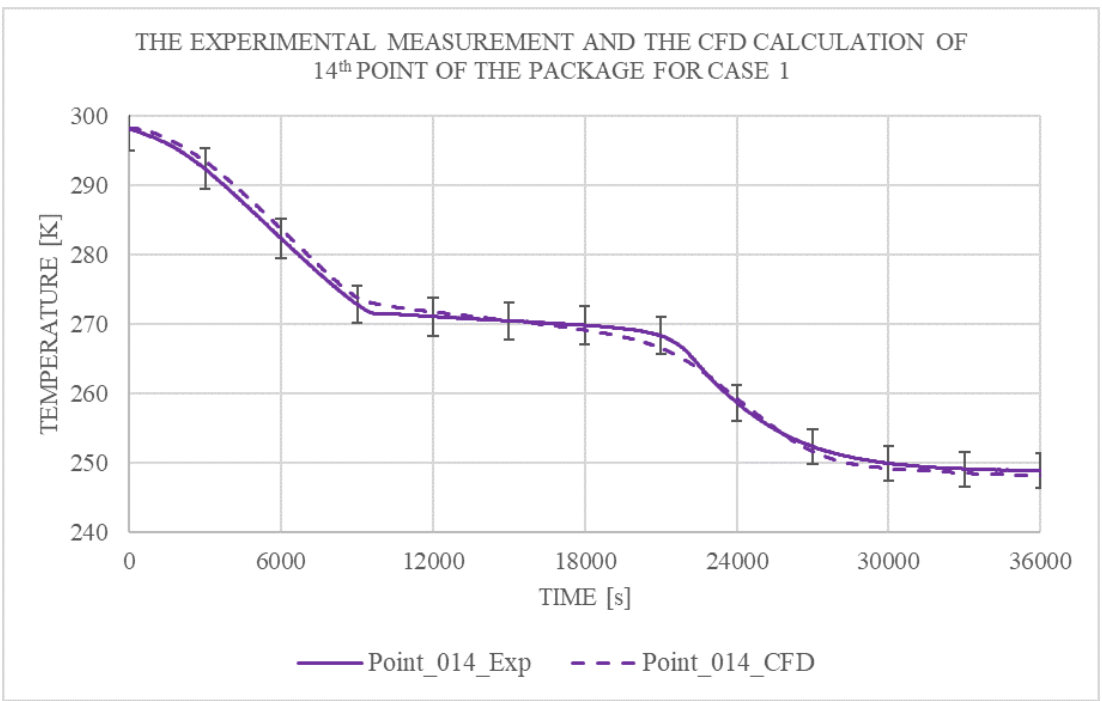

Figure B.13. The Experimental Measurement and The CFD Calculation of 14th Point of The Package for Case 1.

APPENDIX C: UNCERTAINITY ANALYSIS FOR EXPERIMENT SETUP

The result of the uncertainty analysis of an experiment setup is a key factor to determine the quality of the measurement system. In the present study, there are two main types of measurement system which for temperature and flow rate measurement. In this part, how the certainty analysis of them is made is explained.

For thermocouple measurement, the UDAQ system is calibrated by the Calibration Team of Arçelik. The team follows the TS EN ISO/IEC 17025 Calibration Procedure and uses Fluke 5500 A Calibrator as a reference system. After they completes calibration, the uncertainty of thermocouple measurement in calibration is determined according to EA-4/02 M: 2013 Standard. The uncertainty has been calculated for 223.15K to 323.15K.

For flow rate measurement, the uncertainty analysis differs from the previous one in that the former requires some extra calculations due to more than one device used to wind tunnel. To calculate the uncertainty of the wind tunnel, the uncertainty of devices is known as it is tabulated in Table C.1.

Table C.1. The Measurement Range and The Uncertainty of The Measuring Device.

Device	**Measuring Range**	**Uncertainty**
Micromanometer	(-2000) – (+2000) (Pa)	±1.7 (Pa)
Nozzle Coefficient (C)	0.26	±0.012
Nozzle Cross-Section Area (A)	45.6 (cm^2)	±0.005 (cm^2)
Density (ρ)	1.177 (kg/m^3)	±0.002 (kg/m^3)

The volumetric flow rate applied to the system could be written as:

$$\dot{Q} = CA\left[\frac{2\left(\Delta P\right)}{\rho}\right]^{\frac{1}{2}} \tag{C.1}$$

where is volumetric flow rate, C is nozzle coefficient, A is nozzle cross-section area, is pressure drop and is density.

The total measurement uncertainty of volumetric flow rate is expressed by:

$$S_{\dot{Q}} = \left[\left(\frac{\partial \dot{Q}}{\partial C}S_C\right)^2 + \left(\frac{\partial \dot{Q}}{\partial A}S_A\right)^2 + \left(\frac{\partial \dot{Q}}{\partial \Delta P}S_{\Delta P}\right)^2 + \left(\frac{\partial \dot{Q}}{\partial \rho}S_\rho\right)^2\right]^{1/2} \tag{C.2}$$

where S shows the uncertainty of the measurement of a subscript. The relative uncertainty of the wind tunnel for volumetric flow rate measurement is calculated with the equation C.2 and it is shown on Figure C.1.

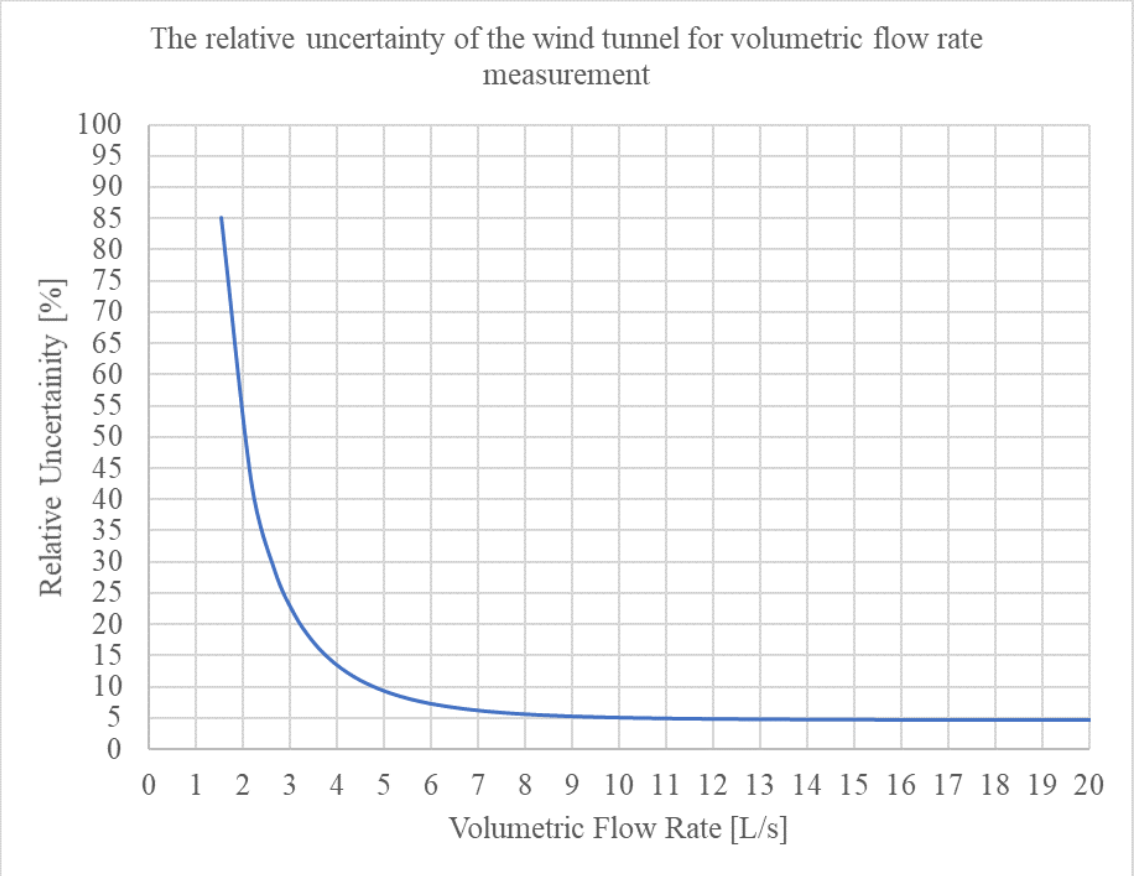

Figure C.1. The Relative Uncertainty of The Wind Tunnel for Volumetric Flow Rate Measurement.

APPENDIX D: The Temperature Distribution in Test Package

Additionally, the time-dependent temperature distribution on the middle plane of the test package for 10th, 13rd and 16th cases is given.

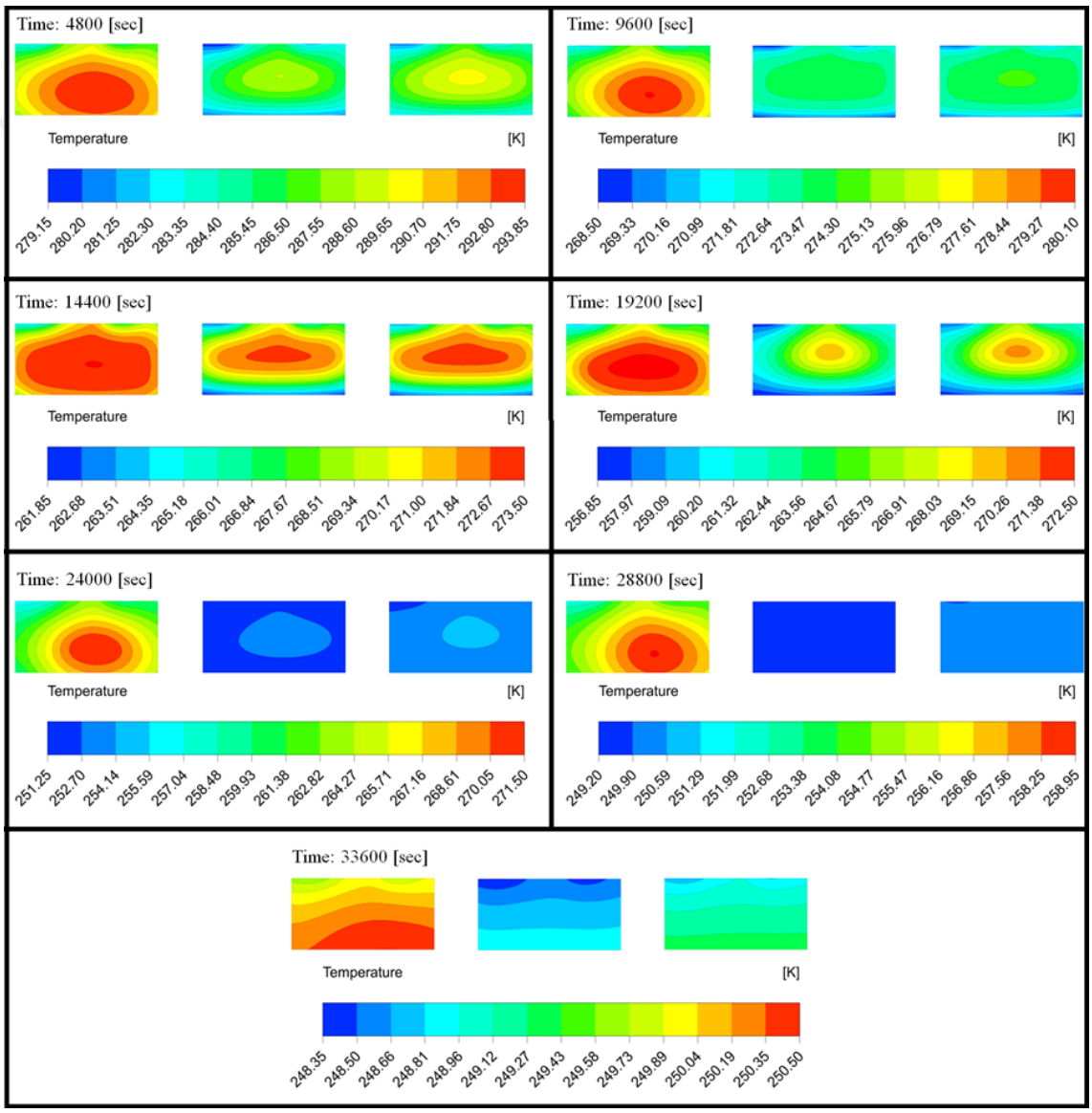

Figure D.1. The Time-dependent Temperature Gradient in The Mid-section of The Test Package for 10th, 13rd and 16th Cases